

Self-Supported Catalysts

Zheng Wang, Gang Chen, and Kuiling Ding*

State Key Laboratory of Organometallic Chemistry, Shanghai Institute of Organic Chemistry, Chinese Academy of Sciences, 354 Fenglin Road, Shanghai 200032, China

Received June 9, 2008

Contents

1. Introduction	322
2. Achiral Self-Supported Catalysts	324
2.1. Hydrogenation	324
2.1.1. Coordination Polymers with Aryldiisocyanide Ligands	324
2.1.2. Poly-Carboxylate Coordination Polymers	326
2.2. Carbon–Carbon Bond-Forming Reactions	327
2.2.1. Poly-N-Ligand Coordination Polymers	327
2.2.2. Polyphenoxide Coordination Polymers	329
2.2.3. Polycarboxylate Coordination Polymers	330
2.2.4. Lanthanide Disulfonate Polymers	332
2.2.5. Palladium Coordination Polymers for Suzuki–Miyaura Coupling	333
2.2.6. Poly-Carbene Coordination Polymers	335
2.3. Oxidation	335
2.3.1. Poly-N-Ligand Coordination Polymers	335
2.3.2. Poly-Carboxylate Polymers	336
2.3.3. Lanthanide Disulfonate Polymers	338
2.4. Polymerization	338
2.5. Ring Opening of Epoxides	340
2.6. Miscellaneous	340
3. Self-Supported Chiral Catalysts	342
3.1. Background	342
3.2. Enantioselective Hydrogenation	344
3.3. Enantioselective Oxidations	347
3.3.1. Enantioselective Epoxidation	347
3.3.2. Enantioselective Sulfoxidation	349
3.4. Asymmetric C–C Bond-Formation Reactions	350
3.4.1. Michael Addition	350
3.4.2. Carbonyl–Ene Reaction	350
3.4.3. Addition of Diethylzinc to Aldehydes	351
3.5. Asymmetric Ring Opening of Epoxide	353
3.6. Miscellaneous	353
4. General Considerations in Self-Supported Catalyst Design	354
5. Concluding Remarks and Outlook	356
6. Abbreviations	356
7. Acknowledgments	357
8. References	357

1. Introduction

Development of practical catalysts for efficient synthesis is of key importance to the chemical industry.^{1,2} While

homogeneous catalysts usually exhibit the advantages of high activity and selectivity in a broad range of synthetic reactions,³ their practical applications remain limited in scope due to catalyst instability and difficulty in catalyst/product separation. Immobilization of a homogeneous catalyst can in principle facilitate its recovery and reuse and therefore is of considerable interest to both academia and industry.^{4–7} Over the past decades a number of approaches^{8,9} have been developed for this purpose, typically including using inert inorganic materials or organic polymers as supports or conducting the reactions in some unconventional media such as ionic liquids or supercritical CO₂ fluid. Although extremely successful, classical immobilization with various prefabricated supports is often plagued by negative effects such as reduced catalytic activity and/or selectivity as a result of the poor accessibility, random anchoring, or disturbed geometry of the active sites in the solid matrix.

In the past decade or so another class of immobilized catalysts has emerged. These catalysts are functional metal–organic assemblies with infinitely extended structures, which are generally constructed by cross-linking of polytopic ligands and metal centers via coordination bonds under relatively mild conditions. The basic notion is to use a ditopic (or polytopic) ligand to connect adjacent metal centers, either of which may carry the information of catalytically active sites, by coordination bonds (Scheme 1). The resulting solids, containing active sites either integrated at metal nodes or located on the backbones, can further be categorized into coordination polymers¹⁰ or organic–inorganic hybrid solids.^{11,12} Depending on the coordination geometry of the metal and the bonding preference of donating atoms as well as the geometry of the bridging ligand, polymeric structures with 1-D chain, 2-D layer, or 3-D network can be generated. As a result of the high dimensionality, the resulting solid with proper functionalities can be insoluble in the conventional reaction media and thus may potentially be useful in heterogeneous catalysis. Owing to the tailorable nature of the building units and the relatively mild synthetic conditions, other catalytically useful properties such as porosity and chirality, etc., can also be incorporated into the resulting polymeric materials. Since such a class of heterogeneous catalysts can be viewed as immobilized homogeneous catalysts without using any external supports, it may be considered as self-supported catalysts in the following context.

The earliest attempts of using coordination polymers for heterogeneous catalysis can be dated back to the 1980s,^{13–16} when Efraty and co-workers tested some noble metal (Rh, Pd, Pt) coordination polymers of diisocyanates for heterogeneous catalytic olefin hydrogenations. Although these early studies have undoubtedly exemplified the prospect of coor-

* To whom correspondence should be addressed. Phone: +86 21-5492-5146. Fax: +86 21-6416-6128. E-mail: kding@mail.sioc.ac.cn.



Zheng Wang was born in Henan Province (China) in 1964. He received his Ph.D. degree from Nanjing University in 2002 under the supervision of Professor Xiaozeng You, working on the synthesis and structural characterization of microporous coordination polymers. After postdoctoral work (2002–2004) with Professor Yonghae Kim at the Korea Advanced Institute of Science and Technology, he joined Shanghai Institute of Organic Chemistry, where he is now an associate professor at State Key Laboratory of Organometallic Chemistry. His current interest concerns transition-metal complex-catalyzed organic reactions.



Kuiling Ding was born in Henan Province (China) in 1966. He received his B.S. degree from Zhengzhou University (1985) and Ph.D. degree from Nanjing University (1990) under the supervision of Professor Yangjie Wu. He became an assistant professor at Zhengzhou University in 1990 and full professor at the same place in 1995. During 1993–1994 he was engaged in postdoctoral research with Professor Teruo Matsuura at Ryukoku University (Japan). In the period from 1997 to 1998 he was a UNESCO research fellow with Professor Koichi Mikami at Tokyo Institute of Technology (Japan). He joined the Shanghai Institute of Organic Chemistry in 1999, where he is currently a professor of chemistry. His research interests include development of new chiral catalysts and methodologies for asymmetric catalysis.



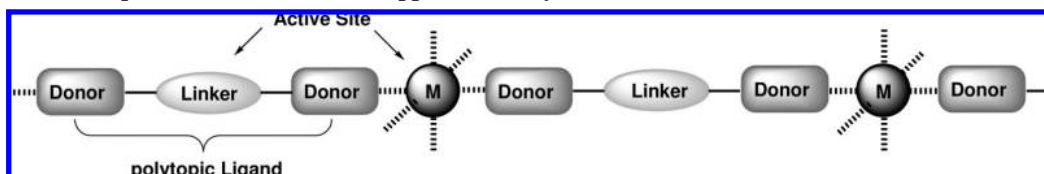
Gang Chen was born in Anhui Province (China) in 1981. He received his B.S. degree in 2003 from the Chemistry & Chemical Engineering Department, Anhui University. He joined Professor Kuiling Ding's group as a Ph.D. student at Shanghai Institute of Organic Chemistry in 2003. His current research interest focuses on the development of new methodologies for asymmetric catalysis.

dination polymers in heterogeneous catalysis of organic reactions, the results were largely ignored for nearly a decade. In retrospect, an important reason might arguably be attributed to the fact that these early reports failed to give much detailed structural information of the catalysts owing to the unavailability of single-crystalline solids. Besides, the relatively poor selectivities of reported procedures may also make them synthetically less attractive. Since the 1990s there has been a surge of research interest in the synthesis and structure elucidation of coordination polymers, resulting in the dis-

covery of numerous crystalline metal–organic frameworks with microporous structures.^{10,17–20} This structural feature inspired many researchers to further investigate the zeolite-like application potentials of such polymers, mostly in fields such as gas sorption and storage but to a relatively lesser degree in heterogeneous catalysis. From the perspective of heterogeneous catalysis, this class of solid materials has obvious similarities both in structure and in composition as well as in catalytic function and therefore will be discussed collectively in this review under the title of self-supported catalysts with a focus on their structures and catalytic performances. Given the great chemical and structural diversity as well as the multidisciplinary nature of the research activities, it is not surprising to see that there are several terms currently in use for describing this type of catalyst, including coordination polymers, metal–organic frameworks (MOF), coordination networks, hybrid inorganic–organic frameworks, and hybrid metal–organic solids, etc. Some of these terms will still be used here for the sake of coherence with their original descriptions.

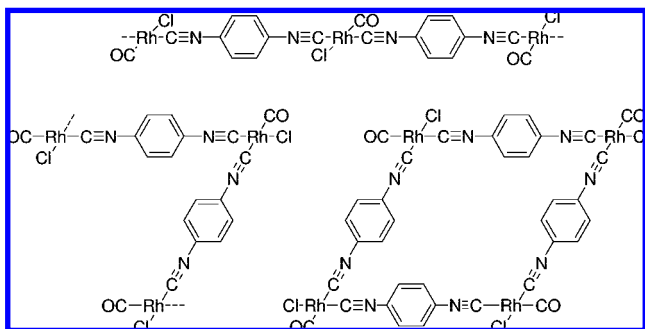
The application of coordination polymers as heterogeneous catalysts has been partially covered in several elegant reviews,^{19,21–23} but a comprehensive overview of the research field is still missing. Some salient features of this class of catalysts will be discussed in the ensuing parts. Wherever applicable, we will attempt to touch on catalysis-relevant issues such as catalyst preparation, porosity, stability, solubility, development and accessibility of the catalytic sites,

Scheme 1. Schematic Representation of the Self-Supported Catalysts^a



^a M = metal centers. Donor = donating atoms. The catalytically active sites can be either located at the metal centers or incorporated into the linker moieties of the polytopic ligands.

Scheme 2. Proposed Patterns for the Structural Units in $[\text{RhCl}(\text{CO})((\text{CN})_2\text{C}_6\text{H}_4)]_n$ (1)



catalytic activity and selectivity, as well as catalyst recovery and reuse, etc., with an effort to identify and summarize some of the structural and chemical factors which may be important for future development. The review will cover both achiral and chiral self-supported catalysts with the case studies being organized according to reaction types. With respect to the structure presentation of the polymeric catalyst solids, in most cases we will adopt empirical formulas as simplified representations since accurate depiction of an extended crystal structure would necessarily require considerable space. Unfortunately in some cases this may cause a sacrifice in clarity since catalytically important issues such as the presence or absence of pores and the geometric arrangement of active sites in the solid catalysts would be hard to understand without the help of multiple structural diagrams. In such a case, the reader is referred to the original publication for a better structure understanding.

2. Achiral Self-Supported Catalysts

2.1. Hydrogenation

2.1.1. Coordination Polymers with Aryldiisocyanide Ligands

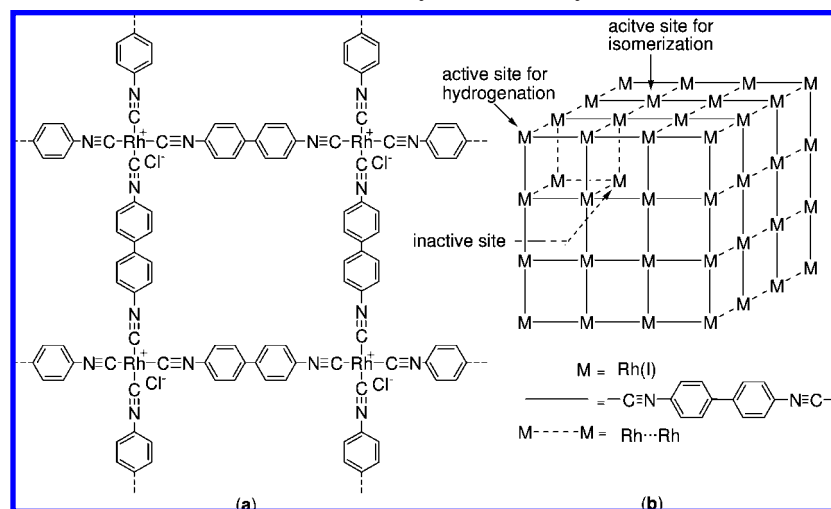
During the 1980s Efraty and Feinstein-Jaffe and their co-workers reported the heterogeneous catalytic activity of a class of organometallic polymers with aryldiisocyanide linkages in the hydrogenation of a variety of alkenes and alkynes (*vide infra*).^{13–16} Isocyanide ligands have bonding properties analogous to carbon monoxide in terms of their σ -donation and π^* -acceptor capabilities and are versatile in bonding with d^8 transition metals such as Rh(I), Pd(II), and Pt(II) or d^6 transition elements, e.g., Ru(II) and Rh(III). Moreover, the isocyanide–metal bond is approximately linear, which might facilitate structural control in polymerization with rigid aryldiisocyanide ligands.

The first example of a self-supported catalyst can be traced back to 1982, when Efraty and Feinstein reported that the rhodium coordination polymer $[\text{RhCl}(\text{CO})(1,4\text{-(CN)}_2\text{C}_6\text{H}_4)]_n$ (**1**) was effective for the heterogeneous catalysis of hydrogenation and isomerization of 1-hexene.¹³ Polymer **1** was prepared by reaction of $[\text{Rh}(\text{CO})_2\text{Cl}]_2$ with two equivalents of a ditopic ligand 1,4-diiisocyanobenzene, which was expected to form stereochemically rigid linear linkages between the rhodium nuclei. Although the exact nature of the polymer remained unknown, the authors proposed several possible extended structures featuring either regular or irregular intrachain Rh \cdots Rh interactions of units such as a linear polymer, a nonlinear polymer, or a tetranuclear cyclic oligomer, as shown in Scheme 2. It was believed that

catalytic sites can be developed in the solid matrix of **1** by photolytic dissociation of the carbonyl ligand and breaking of the weak Rh \cdots Rh interactions. This is to make sure vacant sites on Rh nuclei are available for reactant coordination and activation. Hydrogenation of 1-hexene was tested as the model reaction, performed using a suspension of **1** (loading of Rh ca. 0.86 mol %) in benzene under 0.5 atm of hydrogen at 25 °C. Both the hydrogenation product *n*-hexane and the isomerization products *trans*- and *cis*-2-hexenes were obtained in varying relative amounts under either photolytic (350 nm) or dark conditions. A comparison between the reaction profiles indicated that photoirradiation can assist in the catalytic initiation process. Remarkably, active catalytic sites were shown to be present only in the insoluble solid matrix, and no leaching of the metal or the diisocyanide into the reaction solution was detected. According to the authors, the active catalyst matrix can be recycled without an appreciable loss in activity provided it is kept under inert atmosphere. This may infer the durability of the catalyst in this system; however, the detailed performance in catalyst reuse was not reported. Although the involved mechanism was not very clear, the study has exemplified the feasibility of using insoluble coordination polymers for heterogeneous catalysis.

In a subsequent work, Feinstein-Jaffe and Efraty further examined the catalytic activity of the coordination polymer $[\text{Rh}(\text{diisocyanobiphenyl})_2^+\text{Cl}^- \cdot 2.53\text{H}_2\text{O}]_n$ (**2**) (Scheme 3) in the hydrogenation of 1-hexene.¹⁶ Powder X-ray analysis of **2** revealed an organized tetragonal system with a stacked layer structure and columnar metal chains (Scheme 3) with an intermetallic distance of 3.4 Å in the chains. It was believed that the peripherally exposed (001) faces in **2** should be of particular interest for heterogeneous catalysis since they may provide as many as three vacant surface sites per metal for oxidative addition of hydrogen and coordination of the alkene substrate. According to the authors these vacant 001 surface sites can be produced either by labilization of the terminating ligands or by rupture of weak interchain Rh(I) \cdots Rh(I) interactions. Hydrogenation and isomerization of 1-hexene was performed in the presence of a catalytic amount of the suspended **2** in methanol under 2 atm of H₂ at ambient temperature. Although the catalysis was demonstrated to be heterogeneous in nature, the somewhat sluggish reaction rate led the authors to conclude that only a small percentage of the Rh nuclei in the polymeric matrix are effective in catalysis. Most probably, these active sites are located at the outer surface of (001) faces, while those interior rhodium atoms are less or completely inactive. Later on, Lawrence, Sermon, and Feinstein-Jaffe further examined the catalytic activity of the hexagonal and tetragonal modifications of Rh(I) bis-4,4'-diiisocyanobiphenyl chloride polymers in olefin hydrogenations and proposed a simple model to account for the observed catalytic activity.²⁴ In this model (Scheme 3b) three distinct types of Rh sites, located on the internal face, external face, or edge of the (001) face, can be identified in the polymer matrix and have been proposed to be responsible for hydrogenation and isomerization or inactive in the olefin hydrogenations, respectively. Intuitively, these three types of metal sites should play different roles in catalysis. Cooperative effects between adjacent rhodium sites in the polymers are also thought to be likely in cyclohexene hydrogenations, but just how this might happen is still unclear.

Scheme 3. Schematic Representation of the Tetragonal Coordination Polymer [Rh(4,4'-diisocyanobiphenyl)₂⁺Cl⁻·2.53H₂O]_n (2) (a), and the Proposed Model of Different Active Sites in the Polymer for Catalysis (b)

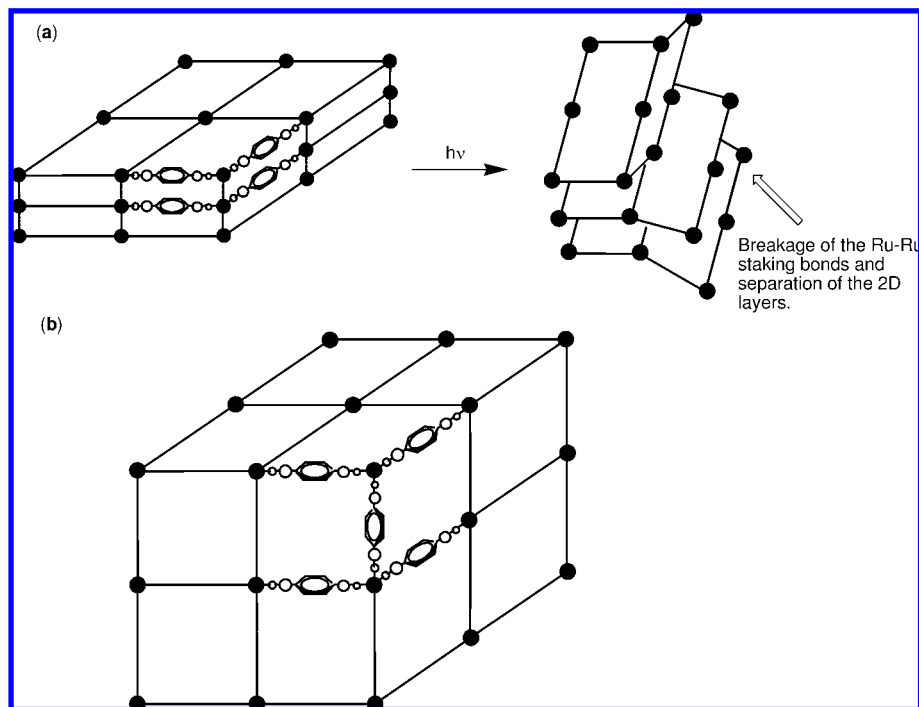


The 4,4'-diisocyanobiphenyl coordination polymers of palladium and platinum were found to be also effective in the heterogeneous catalysis of the hydrogenation of alkenes and alkynes, as reported by Efraty and co-workers during the 1980s.^{14,15} The zerovalent metal coordination polymers with approximate compositions [M(4,4'-diisocyanobiphenyl)_x·yH₂O]_n (**3**) (M = Pd, $x = 1.82 \pm 0.12$ and $y = 1-3$; M = Pt, $x = 1.25 \pm 0.12$ and $y = 0-2$) were prepared in toluene as insoluble polycrystalline precipitates. Characterization by means of elemental analyses, IR, solid-state UV spectra, X-ray photoelectron spectra, thermal gravimetric analyses, as well as powder X-ray diffraction suggested that the structures of these polymers appear to be similar, consisting of [M(4,4'-diisocyanobiphenyl)]_n chains cross-linked by bridging 4,4'-diisocyanobiphenyl ligands to a more or less degree. The Pd(0) and Pt(0) coordination polymers **3** were evaluated for catalysis of hydrogenation of a variety of alkenes and alkynes. Although the observed activities and selectivities vary significantly from case to case, the catalyses were confirmed to be heterogeneous as the filtrates of the mixtures during the reaction courses did not show any further catalytic activities. Moreover, neither metal leaching nor catalyst degradation was observed under the experimental conditions. According to the authors, the catalysts may be recycled without any apparent loss in their catalytic activity, but no details on catalyst reuse were reported. Interestingly, the prehydrogenated catalysts were found to be more active than those of the untreated catalysts, suggesting that the as-synthesized coordination polymers may act as catalyst precursors in the hydrogenation reactions.

In the diisocyanide coordination polymers of Rh(I) discussed above^{13,16,24} a noteworthy structural feature is the stacking of two-dimensional layers through direct metal–metal interactions along the third direction. In contrast, the d⁶ transition metals such as Ru(II) can exhibit an octahedral coordination geometry and thus may result in a three-dimensional coordination polymer on reaction with a aryl-diisocyanide ligand. Such a structural modification may have some consequences in the catalytic behavior of the resulting coordination polymers. With this in mind, Tannenbaum examined the heterogeneous catalysis of Ru(II) coordination polymers with 1,4-diisocyanobenzene in the hydrogenation of 1-hexene and found that the catalytic reactivity of the Ru(II) coordination polymers is indeed correlated to the

existence or absence of the metal–metal stacking interactions in their structures.²⁵ Treatment of 1,4-diisocyanobenzene with RuCl₂(CO)₂(EtOH)₂ or RuCl₂(CO)₃(EtOH) led to the isolation of two distinct polymeric complexes with empirical formulas [Ru(1,4-diisocyanobenzene)_{4/2}²⁺(2Cl)₂²⁻]_n (**4a**) and [Ru(1,4-diisocyanobenzene)_{6/2}²⁺(2Cl)₂²⁻]_n (**4b**) (Scheme 4). Structural characterization of the coordination polymers **4a,b** using FT-IR, elemental analyses, UV–vis diffuse reflectance spectra, as well as X-ray powder diffraction (XRPD) analyses indicated that they adopt different structures. Polymer **4a** has a three-dimensional network analogous to the above-discussed complexes between Rh(I) and diisocyanobenzene ligands, constructed from stacking of ruthenium-containing two-dimensional complexes, with Ru–Ru interactions (intermetallic distance of 3.25 Å) along the z direction (Scheme 4a). In contrast, polymer **4b** adopts a three-dimensional cubic structure with all the Ru atoms cross-linked by the 1,4-diisocyanobenzene ligands in the three directions (Scheme 4b). The author envisaged that such structural features could have strong implications in the catalytic behavior of the resulting polymers, e.g., cleavage of the layers in polymer **4a** by breaking the weak Ru–Ru interactions can create the unsaturation of coordination at Ru centers necessary for interaction with substrate and therefore function as a catalyst. In contrast, the coordination sites of Ru centers in 3D polymer **4b** are totally blocked by the bridging diisocyanide ligands and unavailable for substrate activation, rendering it incapable of acting as a catalyst. Indeed, polymer **4a** was found to be an effective catalyst in the hydrogenation reaction of 1-hexene, albeit the chemoselectivity is unsatisfactory as evidenced by formation of hydrogenation and isomerization products. Conversely, polymer **4b** did not exhibit any noteworthy catalytic activity, which seems to be consistent with its assigned structure. A significant induction period (approximately 2 h) was observed in **4a** catalyzed hydrogenation of 1-hexene, suggesting that polymer **4a** in its original form may not be the actual active catalyst. Some structural modification of **4a** to form electron-deficient ruthenium sites, e.g., by cleavage of layers of the polymer through intercalation of the organic compound, seems to occur prior to catalysis. The induction period was drastically reduced by irradiation of the reaction mixture with 350-nm UV light prior to and during the reaction,²⁶ indicating that the energy of irradiation is sufficient to break the Ru–Ru stacking bonds

Scheme 4. Schematic Descriptions of Three-Dimensional Tetragonal Network Structure of Polymer 4a with Stacking Ru–Ru Bonds in the z Axis and Its Activation by UV Irradiation (a), and Three-Dimensional Cubic Network Structure of Polymer 4b with Ru Centers Cross-Linked in All Three Directions (b)^a



^a Reprinted from ref 25. Copyright 1994 American Chemical Society.

and sustain the interlayer separation (Scheme 4a). Catalysis was believed to be heterogeneous, but neither the leaching of Ru nor the possible reuse of the catalyst was reported.

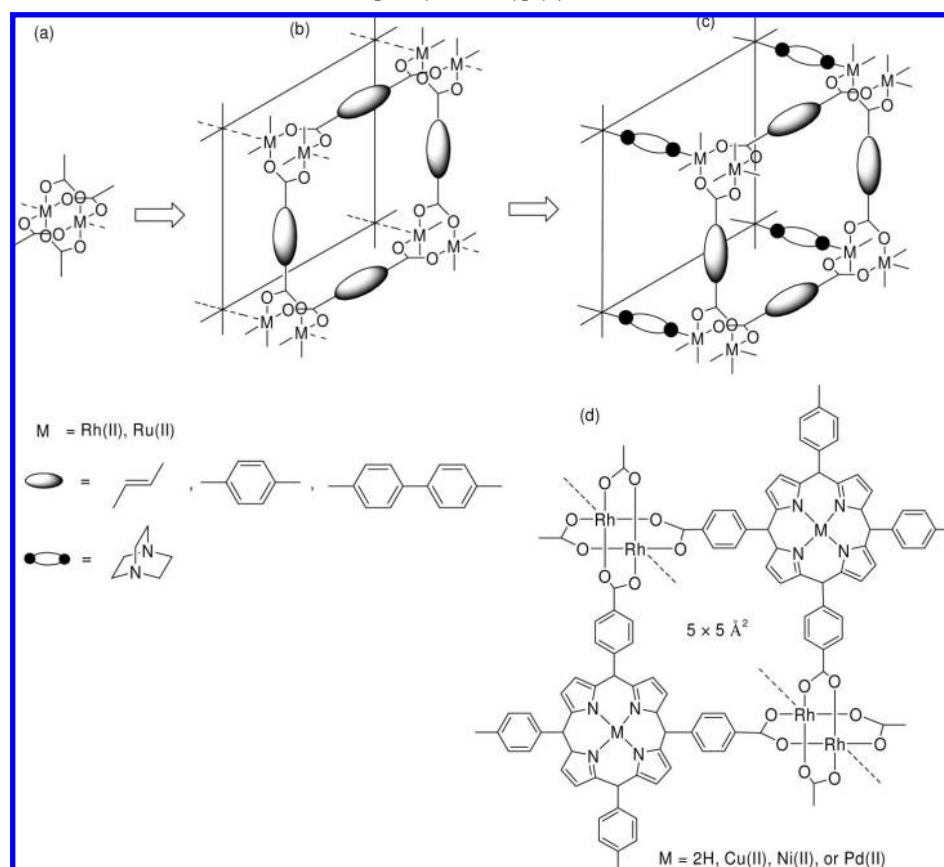
2.1.2. Poly-Carboxylate Coordination Polymers

In a series of reports Mori and co-workers demonstrated the heterogeneous catalytic activities of a variety of rhodium and ruthenium coordination polymers with polycarboxylic acids, including rhodium dicarboxylates $[\text{Rh}_2(\text{trans-O}_2\text{C-C}_6\text{H}_4\text{-CO}_2)_2]_n$ (Rh terephthalate) and $[\text{Rh}_2(p\text{-O}_2\text{C-C}_6\text{H}_4\text{-CO}_2)_2]_n$ (Rh fumarate),²⁷ ruthenium dicarboxylates $[\text{Ru}_2(p\text{-O}_2\text{C-C}_6\text{H}_4\text{-CO}_2)_2]_n$, $[\text{Ru}_2(p\text{-O}_2\text{C-C}_6\text{H}_4\text{-CO}_2)_2]_n$, $[\text{Ru}_2(p\text{-O}_2\text{C-C}_6\text{H}_4\text{-CO}_2)_2(\text{DABCO})]_n$ (DABCO = 1,4-diazabicyclo[2,2,2]octane), and $[\text{Ru}_2(p\text{-O}_2\text{C-C}_6\text{H}_4\text{-C}_6\text{H}_4\text{-CO}_2)_2(\text{DABCO})]_n$,²⁸ and a rhodium tetracarboxylate, rhodium(II) 4,4',4'',4'''-(21*H*,23*H*-porphine-5,10,15,20-tetrayl)tetrakisbenzoate,²⁹ in the hydrogenation reaction of small olefins (ethylene, propene, and butene). These coordination polymers were typically synthesized in a one-pot fashion from simple metal salts and the corresponding dicarboxylic acids. Although the precise structural details of these solid compounds were not very clear, characterization with a combination of techniques such as elemental analysis, IR, magnetic susceptibility measurement, BET surface area determination, and XRPD, etc., indicated that these polymers have common structural units (Scheme 5a–c) featuring dinuclear metal centers linked to each other in a paddle-wheel pattern (Scheme 5a) by the bridging dicarboxylates to form 2-dimensional extended arrays (Scheme 5b). For the coordination polymers containing DABCO, the 2-D metal dicarboxylate layers are further pillared up by the bridging DABCOs to form 3-D structures (Scheme 5c). The Rh fumarate and terephthalate polymers were shown to be very active for the catalytic hydrogenation of ethylene, propene, and butene at $-18\text{ }^\circ\text{C}$ and for H–D exchanges between the $\text{H}_2\text{-D}_2$ couple or two propene

molecules ($\text{C}_3\text{H}_6\text{-C}_3\text{D}_6$) even at $-73\text{ }^\circ\text{C}$.^{27,29} Similar dinuclear ruthenium(II,II) dicarboxylate polymers mentioned above were also shown to be effective catalysts for the hydrogenation of ethylene with varying degrees of activities.²⁸ In the case of the rhodium polymer of porphyrin tetracarboxylate, which acts as a four connector to link the Rh centers, high activities for the hydrogenation of ethene and propene have also been reported.²⁹ The results of these studies have recently been reviewed by Mori and co-workers³⁰ and thus will not be further discussed herein.

Mori and co-workers also reported that several rhodium(II) carboxylate polymers containing metalloporphyrin units in their structures, $[\text{Rh}_2(\text{MTCPP})]$ ($\text{M} = \text{Cu}^{2+}, \text{Ni}^{2+}, \text{Pd}^{2+}$) ($\text{H}_2\text{TCPP} = 4,4',4'',4'''$ -(21*H*,23*H*-porphine-5,10,15,20-tetrayl)tetrakis benzoic acid) (Scheme 5d), were also efficient heterogeneous catalysts for the hydrogenation of small olefins at approximately $-73\text{ }^\circ\text{C}$.^{31,32} These compounds were synthesized by ligand-exchange reactions of rhodium acetate with MTCPP. Structural characterization using elemental analysis, FT-IR, DR-UV–vis, XRPD, BET, and thermal analyses suggested that these complexes possess carboxylate-bridged dinuclear rhodium(II) sites interconnected by metal [Cu(II), Ni(II), or Pd(II)] porphyrin units to form polymers with uniform micropores of ca. 5.0 Å (Scheme 5d). These bimetallic polymers were tested as heterogeneous catalysts in the hydrogenation of ethene, propene, and 1-butene. Remarkably, kinetic studies revealed that a synergistic effect between the two types of metal centers was operative in the catalysis with these bimetallic coordination polymers. It was shown that activation of the hydrogen molecule occurred exclusively at the dinuclear rhodium sites, while the metal centers at the porphyrin ring can enrich the olefin concentration in the micropores by coordination and as a result facilitated intramolecular transfer of hydrogen. It is conceivable that with the advantages of design at the molecular level

Scheme 5. Schematic Descriptions of the Paddle-Wheel Pattern in the Coordination Geometries of the Dinuclear Rhodium and Ruthenium Carboxylate Complexes (a), Deduced Two-Dimensional Structures of Dinuclear Rhodium or Ruthenium Dicarboxylate Coordination Polymers (b), Proposed Three-Dimensional Structures of Dinuclear Metal Dicarboxylates Bridged by DABCO (c), and Deduced Molecular Structure of $[\text{Rh}_2(\text{MTCPP})]$ (d)



coordination polymers may comprise a viable route to the synthesis of multimetallic heterogeneous catalysts where cooperative effects between adjacent active sites are beneficial for catalysis.

2.2. Carbon–Carbon Bond-Forming Reactions

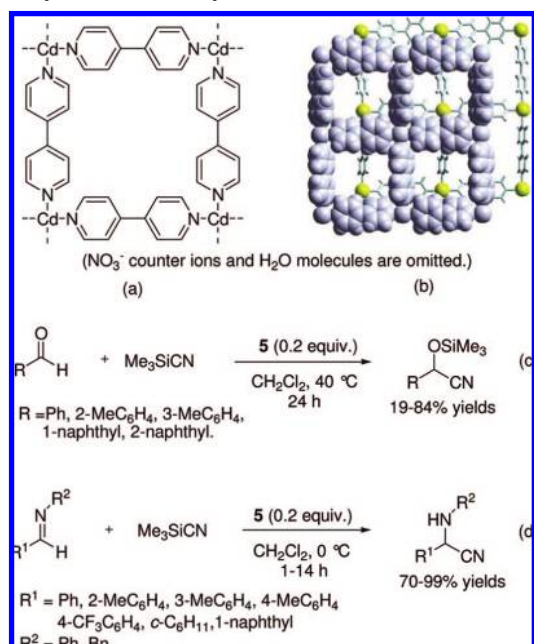
2.2.1. Poly-*N*-Ligand Coordination Polymers

The first example on the use of a crystalline coordination network material as a zeolite-like heterogeneous catalyst in organic reaction was reported by Fujita and co-workers in 1994.³³ The coordination polymer $\{[\text{Cd}(\text{bpy})_2(\text{H}_2\text{O})_2](\text{NO}_3)_2 \cdot \text{H}_2\text{O}\}_n$ (bpy = 4,4'-bipyridine) (**5**) was easily obtained as colorless crystals by treatment of $\text{Cd}(\text{NO}_3)_2$ with 4,4'-bipyridine in H_2O – EtOH at ambient temperature. Although the crystal structure of this polymer had not been fully solved then, low-quality diffraction data showed that the alignment of $\text{Cd}(\text{II})$ and 4,4'-bpy in **5** consists of a layered array of infinite square networks (Scheme 6a). This coordination network was used as a heterogeneous Lewis-acidic catalyst for the cyanosilylation of aldehydes (Scheme 6c). Treatment of benzaldehyde with cyanotrimethylsilane in a CH_2Cl_2 suspension of powdered **5** at 40 °C for 24 h gave 2-(trimethylsilyloxy)phenylacetonitrile in 77% yield. Control experiments using powdered $\text{Cd}(\text{NO}_3)_2$ or 4,4'-bpy alone or the supernatant from a CH_2Cl_2 suspension of the coordination polymer led to no reaction, thus confirming the heterogeneous nature of the catalysis. As in zeolites, interesting shape and/or size selectivity was observed in reactions of the several tested aldehyde substrates. For example, the yield for

cyanosilylation of 2-tolualdehyde is significantly higher than that of 3-tolualdehyde. In addition, 1- and 2-naphthaldehyde were good substrates to give the products in 62% and 84% yields, respectively; the bulkier 9-anthraldehyde was hardly reacted. These shape specificities were tentatively ascribed by the authors to the cavity size of the network. Similar shape specificity was also observed in the clathration of substituted aromatics; while *o*-dibromobenzene and *o*-dichlorobenzene were clathrated in the cavity efficiently, their meta and para isomers were not included. Although a detailed mechanism of this reaction remained unclear, this landmark work demonstrated convincingly for the first time that crystalline coordination polymer with a regular structure can be employed as a zeolite-mimic heterogeneous catalyst for selective organic reactions.

In a subsequent paper, Fujita and co-workers reported the X-ray crystallographic study of the coordination polymer **5**.³⁴ In this compound the $\text{Cd}(\text{II})$ atom has a hexacoordinate environment with pyridyl groups of four bpy ligands at the equatorial positions and two water molecules at the apical positions. The 2D square grid layer is cationic with nitrate counteranions existing in the grid and water molecules being enclathrated between the layers. The grid layers stack on each other in such a way that each $\text{Cd}(\text{II})$ center is located ca. 4.8 Å above the square cavity of the next layer (Scheme 6b). With these results in hand, Ohmori and Fujita further examined the catalytic performance of the same infinite grid complex **5** for cyanosilylation of imines (Scheme 6d).³⁵ The cyanosilylation of (*E*)-*N*-benzylideneaniline ($\text{R}_1 = \text{R}_2 = \text{Ph}$) proceeds efficiently in a CH_2Cl_2 suspension of powdered **5**

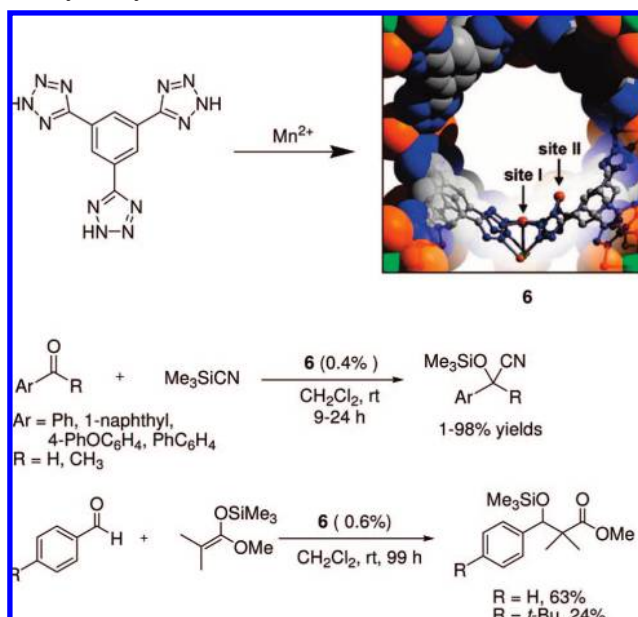
Scheme 6. Schematic Representation of Coordination Polymer $\{[\text{Cd}(\text{4,4}'\text{-bpy})_2(\text{H}_2\text{O})_2](\text{NO}_3)_2 \cdot \text{H}_2\text{O}\}_n$ (5**) (a) and Its Three-Dimensional Structure Showing the Geometrical Relationship between the Two Adjacent Layers (b) as well as Application of **5** in the Heterogeneous Catalysis of Cyanosilylation of Aldehydes (c) and Imines (d)^a**



^a Scheme 6b was reproduced by permission from ref 35 <http://dx.doi.org/10.1039/b406114b> The Royal Society of Chemistry.

(0.2 equiv relative to the imine) at 0 °C, affording the corresponding α -amino nitrile in 98% isolated yield in 1 h. The heterogeneous nature of the catalysis was furthermore confirmed by the inactivity of the supernatant in the cyanosilylation of (*E*)-*N*-[4-(trifluoromethyl)benzylidene]aniline (R₁ = 4-CF₃C₆H₄, R₂ = Ph). The imine cyanosilylation reaction was suggested to be surface promoted since the complex did not take up a detectable amount of imines into the channels when crystals of **5** were immersed in CH₂Cl₂ solution of the imines. In such a case, only the fraction of Cd(II) sites that are located on the external surface of the solid would be effective for catalysis. Even so, the catalytic activity of **5** is remarkably high. Considering the structural feature of the solid, the authors believed that the staggered stacking of the layers should facilitate substrate coordination to the Cd(II) center once it was accommodated in the hydrophobic square cavity of the upper layer. Competing experiments revealed that the cyanosilylation activity of (*E*)-*N*-benzylideneaniline is much higher than that of benzaldehyde, indicating that the heterogeneous reaction should involve selective activation of imino nitrogen by the weak Lewis-acidic Cd(II) center. With regard to this observed reactivity difference between the heterogeneous cyanosilylation of (*E*)-*N*-benzylideneaniline and benzaldehyde, a plausible explanation would be that the as-synthesized polymer **5**, with the Cd(II) centers being coordinatively saturated by the bpy and water ligands, can only act as a catalyst precursor for the reactions. The axially coordinated water molecules on the Cd(II) sites of the solid might be labile enough, which have to be replaced by the substrates before initiation of the catalytic cycles. Provided the coordination ability toward Cd(II) follows the sequence imine > water > benzaldehyde, the observed higher activity of imine toward nucleophilic attack should be understandable.

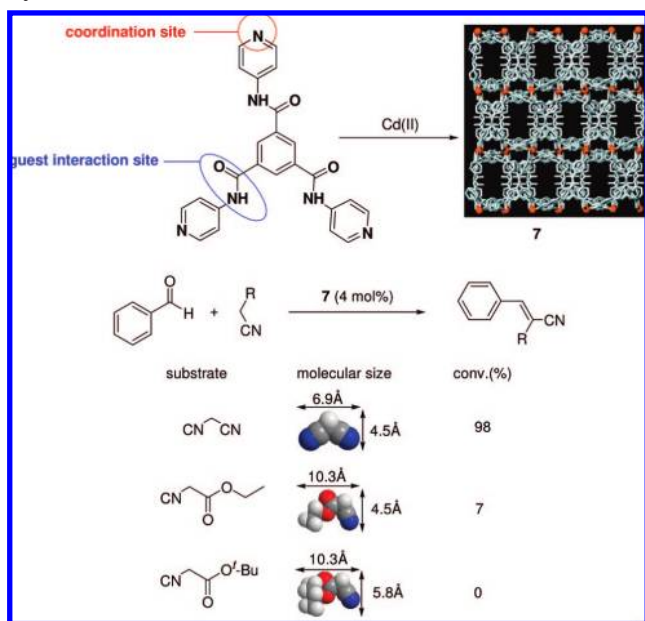
Scheme 7. Cyanosilylation and Mukaiyama–Aldol Reactions Catalyzed by $\text{Mn}_3[(\text{Mn}_4\text{Cl})_3(\text{BTT})_8(\text{CH}_3\text{OH})_{10}]_2$ (6**)^a**



^a The figure of **6** was reprinted from ref 36. Copyright 2008 American Chemical Society.

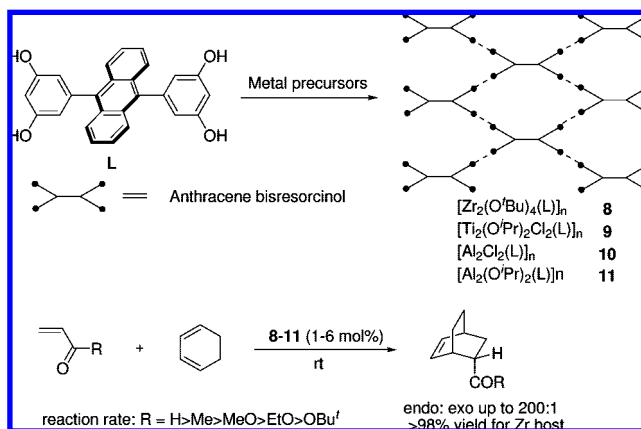
The synthetic utility of the catalyst **5** has been further extended to a variety of imines, including both aromatic and aliphatic substrates. In many cases, the α -aminonitrile products were isolated nearly quantitatively by simple filtration of the heterogeneous catalyst. The authors concluded that incorporation of catalytic active metal centers in network complexes could provide a new strategy for designing solid catalyst at the molecular level.

Amicroporous MOF with a composition $\text{Mn}_3[(\text{Mn}_4\text{Cl})_3(\text{BTT})_8(\text{CH}_3\text{OH})_{10}]_2$ (**6**) (H₃BTT = 1,3,5-benzenetristetrazol-5-yl) was recently reported by Long and co-workers to be an efficient heterogeneous catalyst for the cyanosilylation of aromatic aldehydes and ketones as well as the Mukaiyama–aldol reaction (Scheme 7).³⁶ X-ray crystallographic analysis revealed that the coordination polymer adopts a sodalite-type structure with a cubic network of 7 and 10 Å pores. Remarkably, two types of coordinatively unsaturated Mn(II) sites (sites I and II) were identified with high concentrations on the internal pore surfaces in the polymer, and both are well exposed to interact with guest molecules that enter the framework pores. Site I is five coordinate with one chloride and four bridging tetrazolate ligands, while site II is only two coordinate by two tetrazolate ligands, and therefore, both metal sites are coordinatively unsaturated and may serve as potent Lewis acids. Treatment of selected aldehydes or ketones with cyanotrimethylsilane in the presence of **6** leads to rapid conversion to the corresponding cyanosilylated products. A pronounced size selectivity consistent with the pore dimensions was observed in the reactions. While conversions of 98% and 90% were obtained for benzaldehyde and 1-naphthaldehyde, respectively, larger carbonyl substrates (4-PhOC₆H₄CHO, 4-PhC₆H₄CHO, or acetophenone) only gave much lower yields (18–28%), presumably caused by their inability to diffuse through the pores of the catalyst. The Mukaiyama–aldol reactions between the selected aldehydes with silyl enolates were also found to proceed in a size-selective fashion, attesting to the heterogeneity of the reaction. With respect to the possible recovery and reuse of this catalyst, no data has been reported yet.

Scheme 8. Knoevenagel Condensation Reaction Catalyzed by 7^a

^a Reprinted from ref 37. Copyright 2007 American Chemical Society.

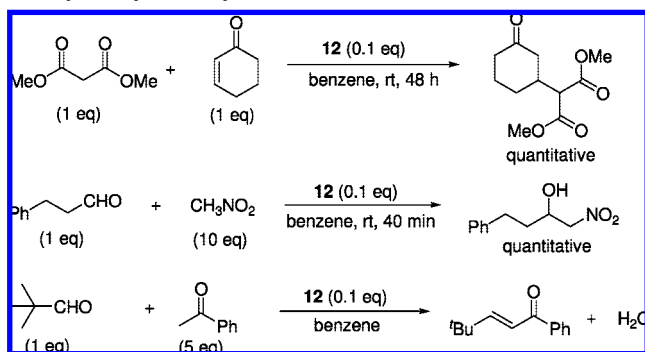
Kitagawa and co-workers reported a 3D porous coordination polymer functionalized with amide groups for the heterogeneous catalysis of the Knoevenagel condensation reaction.³⁷ Upon treatment of $\text{Cd}(\text{NO}_3)_2 \cdot 4\text{H}_2\text{O}$ with 1,3,5-benzene tricarboxylic acid tris[*N*-(4-pyridyl)amide] (4-btapa), a three-connector ligand containing three pyridyl groups as coordination sites and three amide groups as guest interaction sites, a crystalline coordination polymer with the empirical formula $\{[\text{Cd}(4\text{-btapa})_2(\text{NO}_3)_2] \cdot 6\text{H}_2\text{O} \cdot 2\text{DMF}\}_n$ (DMF = *N,N'*-dimethylformamide) (**7**) was obtained (Scheme 8). An X-ray crystallographic study indicated that **7** adopts a 3D porous structure with a channel size of $4.7 \times 7.3 \text{ \AA}^2$ and channel surfaces being functionalized with highly ordered amide groups. The polymer was shown to selectively accommodate certain guest molecules and believed to act as a base to heterogeneously catalyze the Knoevenagel condensation reaction of benzaldehyde with several active methylene compounds (Scheme 8). Interestingly, the selectivity is found to be dependent on the relative size of the reactants and the pore window of the host. For example, the malononitrile was a good substrate with 98% conversion of the starting material, whereas the bulkier substrate ethyl cyanoacetate or cyano-acetic acid *tert*-butyl ester only reacted negligibly. This guest selectivity suggests that the reaction occurs inside the channels rather than on the surface of the solid. In this case the Cd centers are saturated by coordination with the pyridyl groups and act only as structural nodes in the material, while the amide groups on the tunnel walls act as active sites. ¹H NMR and IR studies of **7** treated with active methylene substrates indicate that only the smallest molecule, malononitrile, is selectively adsorbed and activated in the channels of **7**, which is consistent with the observed reactivity of the methylene substrates (Scheme 8). The heterogeneity and recyclability of the polymer in the Knoevenagel condensation of benzaldehyde and malononitrile were also confirmed. The polymer complex was easily isolated from the reaction suspension by filtration and can be reused without loss of activity, albeit without details reported.

Scheme 9. Diels–Alder Reaction Catalyzed by Lewis-Acidic Anthracene Bisresorcinol–Metal Coordination Polymers 8–11

2.2.2. Polyphenoxide Coordination Polymers

A couple of polyphenoxide coordination polymers have been examined as heterogeneous Lewis-acidic catalysts for organic transformations. Aoyama and co-workers demonstrated that coordination polymers with formulas of $[\text{Zr}_2(\text{O}^i\text{Bu})_4(\text{L})_n]$ (**8**),³⁸ $[\text{Ti}_2(\text{O}^i\text{Pr})_2\text{Cl}_2(\text{L})_n]$ (**9**),³⁹ $[\text{Al}_2\text{Cl}_2(\text{L})_n]$ (**10**), or $[\text{Al}_2(\text{O}^i\text{Pr})_2(\text{L})_n]$ (**11**) (L = anthracene bisresorcinol derivative)⁴⁰ were efficient heterogeneous Lewis-acidic catalysts in the Diels–Alder reaction of 1,3-cyclohexadiene with a variety of dienophiles (Scheme 9). The polymers were easily prepared in high yields by condensation reactions of 10-bis(3,5-dihydroxyphenyl)anthracene, an X-shaped tetraol, with the appropriate Zr(IV), Ti(IV), or Al(III) salt precursors under mild conditions. Although the exact structures of these powder solids were unknown owing to their amorphous nature, they were shown to be highly porous and have vacant coordination sites on the metal centers available for interaction with the guest molecules. In the heterogeneous catalysis of Diels–Alder reaction of acrolein with 1,3-cyclohexadiene, these polymers exhibited activities higher than their corresponding homogeneous counterparts with high stereoselectivities (endo/exo ratios typically >99/1 for Ti or Al and >95/5 for Zr). The catalysts were readily separated from the product by filtration or decantation and reused several times without significant deactivation. The insoluble Zr polymeric catalyst can even be packed in a column³⁸ with reactant mixture being introduced as a mobile phase at one end and the product being collected at the other end of the flow system. Importantly, the authors noted that the efficient solid-state catalysis in the case of the $[\text{Al}_2\text{Cl}_2(\text{L})_n]$ host (**10**) is based on the combination of two types of vacancies present in the solid, i.e., the space vacancy and coordinative unsaturation as revealed by ²⁷Al MAS NMR spectroscopy.⁴⁰

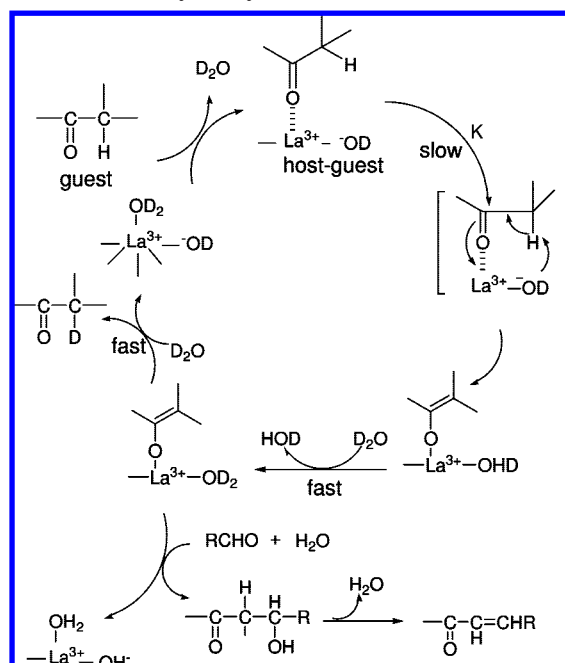
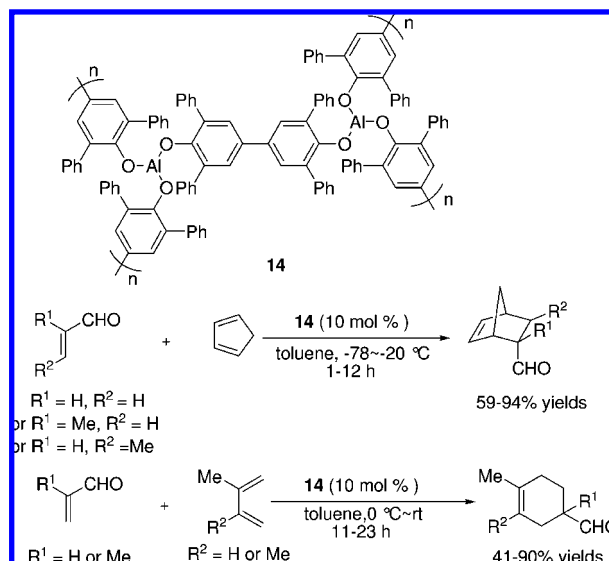
Aoyama further demonstrated that incorporation of a different type of metal center such as La^{3+} ions into the anthracenebisresorcinol coordination network may result in a dramatic change in catalytic properties to give a catalyst which is effective for typical base-catalyzed reactions.⁴¹ Treatment of anthracenebisresorcinol with $\text{La}(\text{O}^i\text{Pr})_3$ in THF led to formation of an amorphous La coordination polymer with the empirical formula $[\text{L}^{4-} \cdot 1.5\text{THF} \cdot 2(\text{LaOH}) \cdot 4\text{H}_2\text{O}]$ (**12**) (L = anthracenebisresorcinol), which is insoluble in all common solvents. On the basis of some spectroscopic evidence the polymer was deduced to be comprised of the polyphenoxide anion and hydroxylanthanum dication with $\text{O}^- \cdots [\text{LaOH}]^{2+} \cdots \text{O}^-$ bridges. The La(III) polyphenoxide

Scheme 10. Michael, Nitroaldol, and Aldol Reactions Catalyzed by La Polymer 12

complex was shown to catalyze Michael, nitroaldol, and aldol reactions with varying degrees of efficiencies (Scheme 10). In the former two reactions the products were obtained in nearly quantitative yields. Catalysis was demonstrated to be heterogeneous since the reactions did not proceed further in the supernatant liquid when the catalyst was removed from solution. Furthermore, the La polymer can be easily recovered without leaching into the organic phase and was reported to be reusable. Although the exact mechanisms for the reactions are not clear, the authors proposed that the La polymer may play a dual role in catalysis. It was presumed that the La polymer might be bifunctional for catalysis, i.e., the La(III)-coordinated anionic ligands could have acted as Brønsted bases to promote enolization of the Michael/aldol donors, while the metal centers may have functioned as Lewis acids to contribute to the reactivity.

Aoyama and co-workers further reported that $[L^{4-} \cdot 2(\text{LaOH})^{2+} \cdot 6\text{H}_2\text{O}]$ (**13**) ($L = \text{anthracenebis(resorcinol)}$), another microporous La-anthracenebis(resorcinol) coordination polymer obtained by aqueous workup of **12**, possesses catalytic activity for ketone enolization and aldol reactions in pure water at neutral pH.⁴² In marked contrast to simple La(III) alkoxides and aryloxides, La(III)-network **13** was shown to be stable against hydrolytic decomposition. In the presence of the La polymer, cyclohexanone in D_2O was shown to undergo facile deuterium incorporation at the α positions of the carbonyl group to give 2,2,6,6-tetradeuterated ketone. Mechanically, the H/D exchange was caused by a reversible enolization of the ketone, a process completely catalyzed by the La polymer. Kinetic study of the process revealed a Michaelis–Menten-type behavior, which led the authors to propose a mechanism featuring reversible substrate binding to **13**, which functions as an enzyme mimic for ketone enolization (Scheme 11). Herein the metal-ligated OD^- anion acts as the base, while the La(III) center cooperates in the enolization as a Lewis acid. The authors further showed that the aldol reactions occurred concomitantly with dehydration, which took place catalytically in the presence of an aldehyde (furfural or benzaldehyde) as an enolate acceptor.

Yamamoto and co-workers reported the synthesis and catalytic applications of an aluminum coordination polymer with a bisphenol.⁴³ The aluminum trisphenoxide polymer **14** was prepared as an insoluble solid by treatment of the biphenol in toluene with a hexane solution of Me_3Al and used as an efficient catalyst for the Diels–Alder reaction of a variety of acrolein derivatives, affording the corresponding adducts in moderate to excellent yields (40–99%) (Scheme 12). Particularly, in the reaction of acrolein with cyclopentadiene polymer **14** was recovered quantitatively by simple

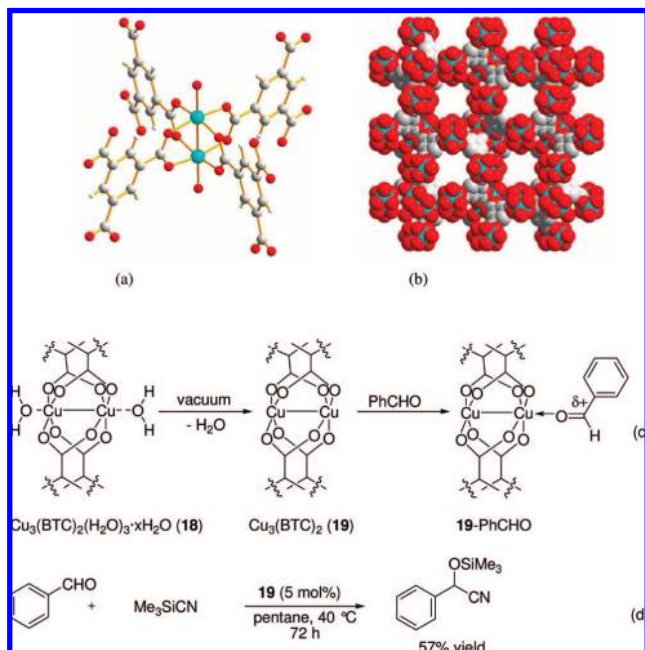
Scheme 11. Proposed Mechanism for Reversible Enolization of the Ketone Catalyzed by 13**Scheme 12. Diels–Alder Reactions Catalyzed by Aluminum Trisphenoxide Polymer 14**

filtration and reused for seven cycles without a decrease in activity. However, irregularities in the yields can be observed for consecutive runs.

2.2.3. Polycarboxylate Coordination Polymers

Several studies have shown that metal coordination polymers constructed from polycarboxylate ligands can be used as heterogeneous achiral catalysts to promote C–C bond-forming reactions. The di- and polycarboxylic acids have been extensively used as building blocks for construction of various porous coordination polymer architectures,⁴⁴ wherein the polycarboxylates can adopt versatile coordination modes with various metal ions. Many of the resulting polymers are crystalline in morphology and neutral in framework charge and can exhibit catalytically useful properties such as microporosity and thermal stability.

Scheme 13. Structure of the Dimeric Cu(II) Tetracarboxylate unit in **18 (a), Space-Filling Structure of **18** Viewed Along the 001 Direction (turquoise, red, and gray represent Cu, O, and C atoms, respectively) (b), Schematic Representation of Dehydration of **18** for Benzaldehyde Activation (c), Cyanosilylation of Benzaldehyde Catalyzed by **19** (d)**



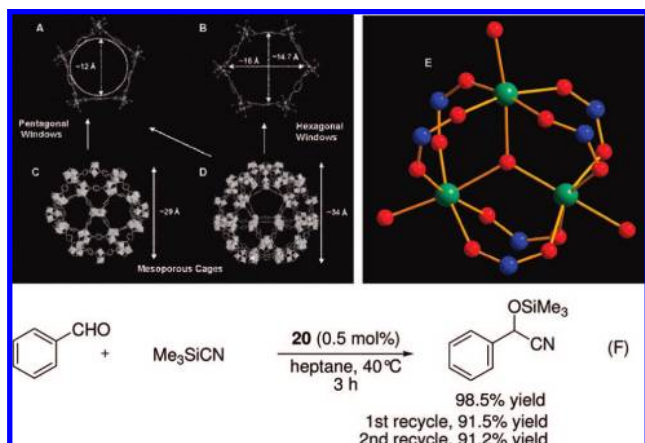
Ruiz-Valero and co-workers reported preliminary results on studies of the catalytic properties of several rare-earth metal succinate coordination polymers, $[\text{Sc}_2(\text{OOCCH}_2\text{H}_4\text{COO})_{2.5}(\text{OH})]$ (**15**), $[\text{Y}_2(\text{OOCCH}_2\text{H}_4\text{COO})_3(\text{H}_2\text{O})_2] \cdot \text{H}_2\text{O}$ (**16**), and $[\text{La}_2(\text{OOCCH}_2\text{H}_4\text{COO})_3(\text{H}_2\text{O})_2] \cdot \text{H}_2\text{O}$ (**17**) [where $(\text{OOCCH}_2\text{H}_4\text{COO})^{2-} = \text{succinate}$].^{45,46} These lanthanide coordination polymers were obtained as single crystals via hydrothermal chemistry. X-ray crystallographic analyses indicated that the scandium polymer **15** has a more compact structure, while the frameworks of **16** and **17** have channels large enough to enclathrate guest water molecules. With regard to the catalytic properties, the Sc polymer **15** was reported to be an effective and reusable heterogeneous catalyst for the Friedel–Crafts acylation reaction of anisole with acetic anhydride. Furthermore, all three lanthanide polymers were found to be effective as Lewis acid catalysts for acetalization of benzaldehyde and phenyl acetaldehyde with trimethyl orthoformate at 60–70 °C. However, the heterogeneous nature of the latter catalysis case may have to be rigorously confirmed since catalyst leaching into the solution might be possible at elevated temperatures.

Kaskel and co-workers carried out a critical study on the catalytic properties of the desolvated porous MOF compound $[\text{Cu}_3(\text{BTC})_2(\text{H}_2\text{O})_3 \cdot x\text{H}_2\text{O}]_n$ (**18**) (BTC = benzene-1,3,5-tricarboxylate) in the cyanosilylation of benzaldehyde (Scheme 13).⁴⁷ The synthesis and characterization of copper carboxylate coordination polymer **18** was first reported by Williams and co-workers in 1999.⁴⁸ X-ray crystallographic structural analysis revealed that **18** is highly porous, comprised of dimeric copper(II) crossed-linked in a paddle-wheel pattern by tetracarboxylate units from the BTC ligands (Scheme 13a) to form a three-dimensional system of channels with a pore size of 1 nm and an accessible porosity of about 40% in the solid (Scheme 13b). The terminal axial water ligands (Scheme 13a) are directed from the Cu atoms to the interior

of the nanopores (Scheme 13b). Importantly, it was shown that the tunnel walls of this compound are chemically modifiable since these water ligands are labile enough to allow for their replacement by pyridines or removal by thermal treatment under vacuum without loss of structural integrity. Thus, it is conceivable that the substrate with adequate Lewis basicity might also undergo similar ligand exchanges on the metal sites or directly bond to the coordinatively unsaturated metal sites, resulting in activation of the substrate toward nucleophilic attack. In Kaskel's report, thermal treatment of **18** under vacuum gave rise to $\text{Cu}_3(\text{BTC})_2$ (**19**) with coordination vacancy at Cu(II) sites, which allows easy access of substrate to the copper sites (Scheme 13c). Chemisorption of benzaldehyde on the unsaturated Cu(II) sites of **19** results in the activation of its carbonyl group toward nucleophilic attack. On reaction with trimethylsilyl cyanide in nonpolar solvents such as pentane, for which filtration tests have demonstrated the heterogeneous nature of the reaction mechanism, the cyanosilylation products were obtained in reasonable yield (57%) with a high selectivity. However, the catalytic performance of the system was shown to be sensitive to the reaction parameters, exhibiting a remarkable solvent and temperature effect on catalysis. For example, coordinating solvent such as THF was found to inhibit the reaction, presumably by blocking the Lewis-acidic sites of the catalyst, while CH_2Cl_2 or relatively high reaction temperatures (80 °C) caused decomposition of the catalyst.

Very recently, Kaskel and co-workers demonstrated that a chromium carboxylate-based MOF, $[\text{Cr}_3\text{X}(\text{BDC})_3\text{O}(\text{H}_2\text{O})_2]_n$ (**20**; X = F, OH; BDC = benzene-1,4-dicarboxylate), can function as a highly active heterogeneous catalyst for the cyanosilylation of benzaldehyde.⁴⁹ Synthesis and characterization of MOF **20** was first reported by Férey and co-workers in 2005.⁵⁰ The solid was shown to be extraordinarily porous having a very high specific surface area ($S_{\text{Langmuir}} \approx 5900 \text{ m}^2 \cdot \text{g}^{-1}$) and a hierarchy of extra-large pore sizes ($\sim 30\text{--}34 \text{ \AA}$). The pores and pore windows (12–16 Å) are big enough to allow for easy access of even large reactant molecules to diffuse into the pores, and also large product molecules can move out of the network (Scheme 14A–D). The chromium ions in **20** have a pseudo-octahedral coordination, five sites of which are occupied by the $\mu_3\text{-O}$ atom in the middle of the chromium trimers and four oxygen atoms derived from the carboxylate groups of the terephthalate linkers, while the sixth coordination site around each chromium is held by a water molecule, a fluorine atom, or a hydroxyl group (Scheme 14E). Since the framework of **20** is thermally stable up to 275 °C, the axially coordinated water molecules can be easily removed in vacuum and at elevated temperature, leaving behind the Lewis-acidic chromium sites accessible for potential reactants. Therefore, MOF **20** was activated in vacuum at 120 °C overnight prior to submission for catalysis. The catalytic activity of **20** was evaluated using the cyanosilylation of benzaldehyde as a test reaction (Scheme 14F).⁴⁹ Compared to $\text{Cu}_3(\text{BTC})_2$ (**19**), **20** exhibited a much higher activity. Under a catalyst loading of only 0.5 mol % the product was obtained in a yield of 98.5% in 3 h. Catalysis was confirmed to be heterogeneous by a filtration experiment. A recycling test in the cyanosilylation of benzaldehyde indicated that catalyst **20** can be reused three times with a slightly reduced activity. Given these results, it seems worthwhile to extend the catalysis further to more challenging substrates. In addition, **20** was demonstrated to

Scheme 14. Structures of Pores and Pore Windows in Chromium-Based MOF 20: Ball-and-Stick View and Free Dimensions (Å) of the Pentagonal and Hexagonal Windows (A and B); Ball-and-Stick View of the Two Cages (C and D); Coordination Sphere around Chromium (E) (chromium octahedra, oxygen, fluorine, and carbon atoms are given in green, red, red, and blue, respectively); (F) Cyanosilylation of Benzaldehyde Catalyzed by 20^a



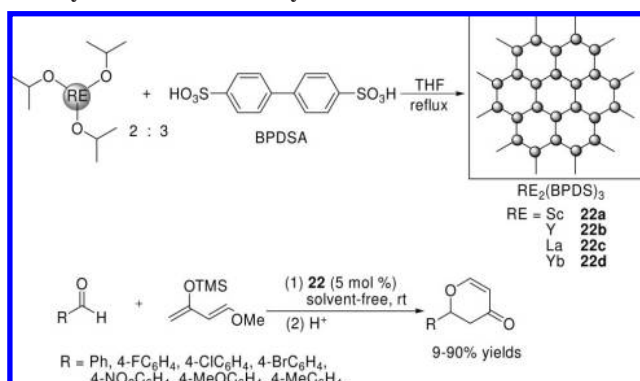
^a Scheme 14A–D is reprinted with permission from ref 50. Copyright 2008 AAAS.

be a suitable support for palladium immobilization by which the resulting composite showed a better catalytic performance in the hydrogenation of styrene and cyclooctene than some commercial supported palladium catalysts.

Serre and co-workers reported the heterogeneous catalytic properties of a hybrid inorganic–organic iron(III) carboxylate solid with the structural formula $[\text{Fe}^{\text{III}}_3\text{O}(\text{H}_2\text{O})_2 \cdot \text{F} \cdot (\text{BTC})_2 \cdot n\text{H}_2\text{O}]$ ($n \approx 14.5$) (**21**) for the Friedel–Crafts benzylation of benzene with benzyl chloride.⁵¹ The solid was prepared as a polycrystalline powder under hydrothermal conditions and found to adopt a zeolite architecture with large pores (free apertures of ca. 25 and 29 Å) accessible through microporous windows (ca. 5.5 and 8.6 Å) by synchrotron X-ray powder diffraction technique. Liquid-phase benzylation of benzene with benzyl chloride in the presence of **21** at 70 °C showed high activity and selectivity, quickly giving diphenylmethane in nearly 100% selectivity with 100% benzyl chloride conversion (reaction time approximately 10 min including a short induction period of 5 min). The observed high benzylation activity of **21** was tentatively ascribed by the authors to the redox property of trivalent iron species, which were assumed to play a significant role in activating both reactants. However, the exact mechanism of such an interaction still remains to be clarified.

The alkylation of aromatics is a reaction of considerable industrial interest and can be catalyzed by medium- and large-pore acidic zeolites, which usually favor formation of less bulky *para*-alkylation products. Farrusseng and co-workers reported a highly regioselective *para*-alkylation of aromatic compounds using the isorecticular MOF compounds $\text{Zn}_4\text{O}(\text{BDC})_3$ (IRMOF-1) and $\text{Zn}_4\text{O}(\text{NDC})_3$ (NDC = 2,6-naphthalenedicarboxylate) (IRMOF-8), originally developed by Yaghi et al.⁵² as acid catalysts.⁵³ The zinc carboxylate IRMOFs employed in this study were synthesized by a modified procedure to result in an IRMOF-1 sample occluded with a minor amount of zinc hydroxide nanoclusters [with a global composition of $\text{Zn}_4\text{O}(\text{BDC}) \cdot 2\text{H}_2\text{O} + \text{Zn}(\text{OH})_2$]. IRMOF-1 and IRMOF-8 have channel window sizes of 7.8

Scheme 15. Schematic Representation of the Lanthanide Disulfonate Coordination Polymers 22a–d and Their Application as Catalysts in Hetero-Diels–Alder Reaction of Aldehydes with Danishefsky’s Diene

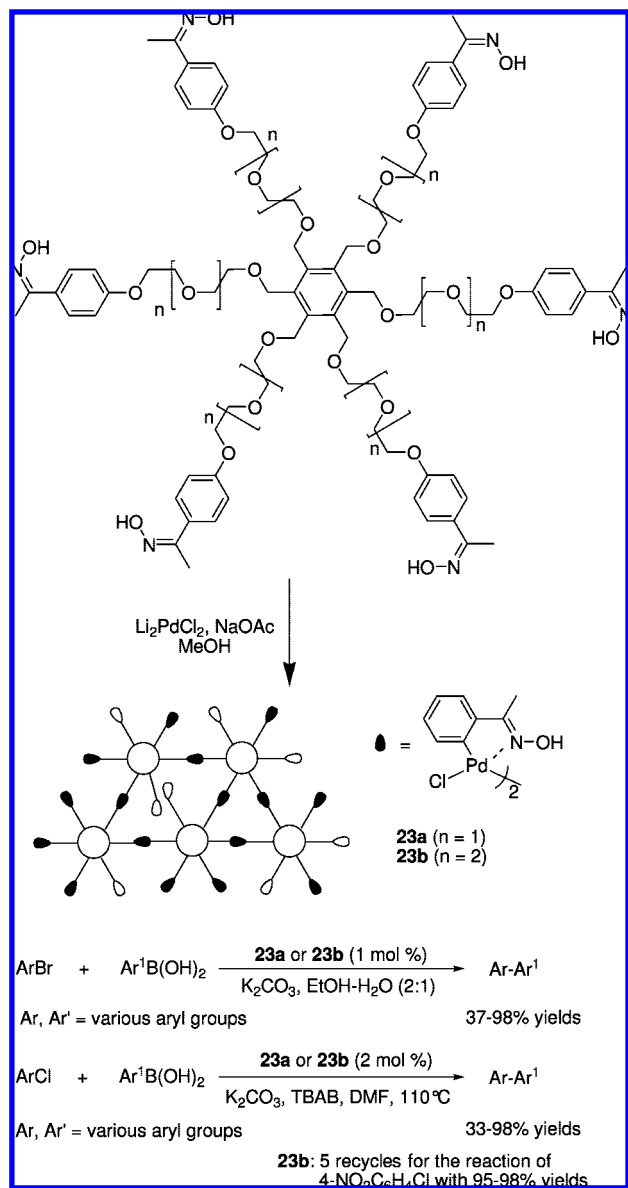


and 9.2 Å, respectively, which are slightly larger than that of the acidic form of beta zeolite (H-BEA, 6.1 Å), and were tested in the alkylation of toluene and biphenyl with *tert*-butylchloride using H-BEA, AlCl_3 , and ZnCl_2 as reference catalysts. Under the reaction conditions the IRMOFs were as active as H-BEA and AlCl_3 but exhibited a remarkably superior shape selectivity toward the less bulky *para* products. For example, in the alkylation of biphenyl, regioselectivities for 4-*tert*-butylbiphenyl of 96% and 95% in conversions from 60% to 80% were achieved with IRMOF-1 and IRMOF-8, respectively, much higher than those of H-BEA or AlCl_3 (55% or 51%, respectively). Besides, only traces of the dialkylated products (1–2%) were detected using the IRMOFs as the catalysts, which also compare favorably with the values (11–23%) obtained using reference catalysts. Catalysis using IRMOF-1 was confirmed to be heterogeneous, and the IRMOFs were reusable after filtration. However, the exact nature of the active site is still unknown.

2.2.4. Lanthanide Disulfonate Polymers

Several lanthanide disulfonate coordination polymers were reported by Inanaga and co-workers to be effective and recyclable heterogeneous catalysts for the hetero-Diels–Alder reaction of aldehydes with Danishefsky’s diene under solvent-free conditions (Scheme 15).⁵⁴ Refluxing the THF solution of biphenyl-4,4'-disulfonic acid (H_2 -BPDS) with the lanthanide metal salts $\text{M}(\text{O}^i\text{Pr})_3$ ($\text{M} = \text{Sc}, \text{Y}, \text{La}, \text{or Yb}$) followed by simple workup led to the isolation of amorphous polymers with assigned formulas of $[\text{M}_2(\text{BPDS})_3]_n$ (**22a–d**). Although the exact structure of these solids remained unknown, all of them were found to be active catalysts for the hetero-Diels–Alder reaction of Danishefsky’s diene with benzaldehyde. Among the four lanthanide catalysts **22a** turned out to be optimal in terms of the activity, affording the adduct in 90% yield at room temperature in 48 h under a catalyst loading of 5 mol %. Further extension of the scandium polymer catalysis to a couple of substituted benzaldehydes was also successful, affording the corresponding dihydropyranone derivatives in good yields under solvent-free conditions. Remarkably, it was found that the scandium catalyst is stable in air and reusable in the hetero-Diels–Alder reaction of Danishefsky’s diene with benzaldehyde, affording the product in nearly constant yields (83–81%) during three repeated runs. Furthermore, essentially no metal leaching was detected in the third run. However, the activation mechanism is not clear so far.

Scheme 16. Suzuki–Miyaura Coupling Reactions Catalyzed by Self-Supported Star-Shaped Oxime–Palladacycle Catalysts **23a,b**



2.2.5. Palladium Coordination Polymers for Suzuki–Miyaura Coupling

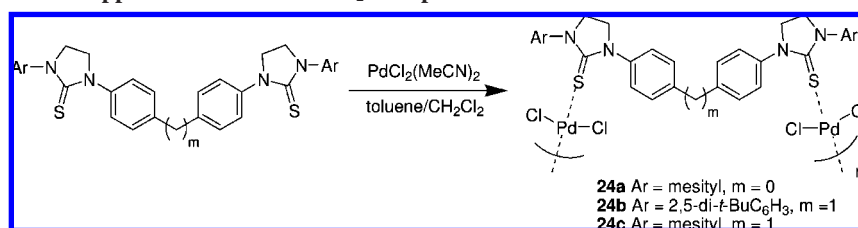
Two self-supported oxime–palladacycle catalysts were shown by Chen and Deng and co-workers to be effective heterogeneous catalysts for the Suzuki–Miyaura coupling of aryl bromides and chlorides.⁵⁵ Treatment of the star-shaped oxime-based ligands and lithium tetrachloropalladate in methanol led to isolation of **23a,b**, which were obtained as amorphous micrometer solid particles (Scheme 16), for which their approximate compositions were assigned on the basis of the ICP analyses of Pd, elemental analysis, and IR results. Solids **23a,b** were tested as catalysts (1 mol % loading) for the Suzuki–Miyaura coupling reactions of a variety of aryl bromides with aryl boronic acids, performed under aerobic conditions in EtOH/H₂O (2:1) at ambient temperature with K₂CO₃ as the base (Scheme 16). Good to excellent yields were obtained in most cases, and the activities of the catalysts were found to be comparable to that of their monomeric counterpart. For the reaction involving more challenging substrates such as aryl chlorides, moderate to excellent yields

of the coupling products were obtained for the activated aryl chlorides. Although independent tests suggested that reactions involving aryl chlorides may not be completely heterogeneous in nature, this seems not to be fatal to the reusability of the catalysts. For example, in the coupling reaction of *p*-nitrochlorobenzene and phenylboronic acid catalyst **23b** could be reused at least 5 times with only a minor decrease in the isolated product yields (98–95%) in slightly prolonged reaction periods (100–130 min). However, in such a case some degree of metal leaching would cause a complication in the product purification procedure.

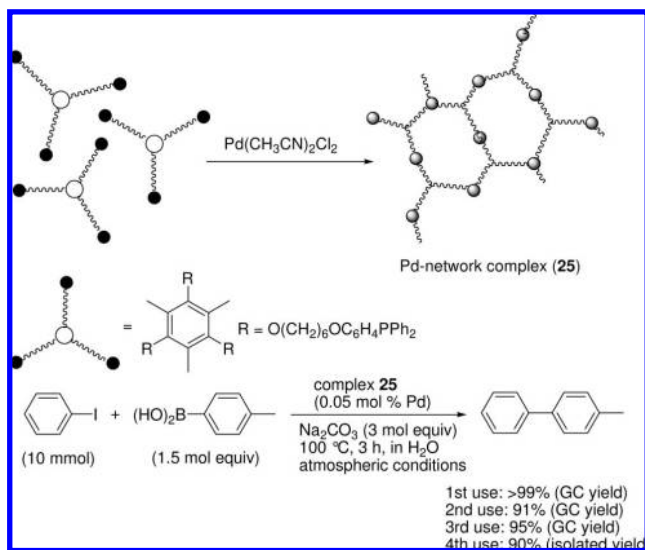
Several assembled thiourea–palladium complexes were further demonstrated by Chen and co-workers to be highly air stable and recyclable self-supported catalysts for the Suzuki–Miyaura coupling reaction of aryl bromides and aryl boronic acids in neat water under aerobic conditions.⁵⁶ The self-supported complexes (**24a–c**) were easily generated by simple treatment of PdCl₂(MeCN)₂ with the bis-thiourea ligands in toluene/dichloromethane at 40 °C (Scheme 17). After removal of the solvent, **24a–c** were isolated as amorphous particles insoluble in water and some organic solvents but soluble in dichloromethane and chloroform. The activities of **24a–c** (1–0.01 mol % loading based on Pd) were subsequently tested for catalysis of Suzuki–Miyaura coupling reactions in neat water, and the products were obtained in good to excellent yields (72–99%) for a wide range of combinations of activated aryl bromides and aryl boronic acids. After completion of the reaction, the catalyst could be recovered by diethyl ether addition followed by filtration. Reuse of **24a** for the Suzuki reaction of 3-nitro-bromobenzene and phenylboronic acid was remarkably successful. According to the report, the recycling experiments were conducted under aerobic conditions under a catalyst loading of 0.2 mol % (based on Pd), and the product was still obtained quantitatively in 1 h even after six runs. Furthermore, ICP analysis of the filtrate from the reaction mixture indicated that palladium leaching was less than 2 ppm for each run, suggesting that the self-supported Pd complexes were quite robust in the reaction system.

Uozumi and co-workers reported a Pd–trisphosphine coordination polymer as an efficient and reusable catalyst for Suzuki–Miyaura reaction under aerobic conditions in water.⁵⁷ A self-assembly process of PdCl₂(CH₃CN)₂ with a C₃-trisphosphine bearing flexible alkyl-chain tethers led to formation of a gel-like Pd complex (**25**), presumably comprised of palladium species and the ligands cross-linked to each other through Pd–P coordinating bonding (Scheme 18). The complex was found to be insoluble in water and several types of organic solvents and subsequently examined as a heterogeneous catalyst for the Suzuki–Miyaura cross-coupling reaction in water. High yields of the coupling products were obtained for a variety of combinations of aryl bromides or iodides with arylboronic acids. The catalyst was successfully reused in the Suzuki–Miyaura reaction of iodobenzene with 4-tolylboronic acid for four cycles without significant loss of catalytic activity (90–99% yields), but potential leaching of the Pd during the recycles has not been reported.

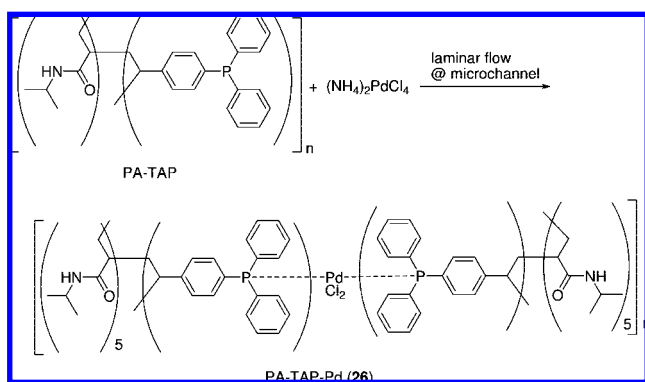
Uozumi and co-workers reported the use of a palladium complex polymer membrane self-assembled inside a micro-channel reactor for efficient catalysis of Suzuki–Miyaura coupling of aryl iodides with arylboronic acids.⁵⁸ Counter-current introduction of an ethyl acetate solution of poly-(acrylamide)-triarylphosphine and an aqueous solution of

Scheme 17. Synthesis of Self-Supported Thiourea–PdCl₂ Complexes 24a–c

Scheme 18. Pd–Trisphosphine Coordination Polymer 25 for the Suzuki–Miyaura Coupling Reaction



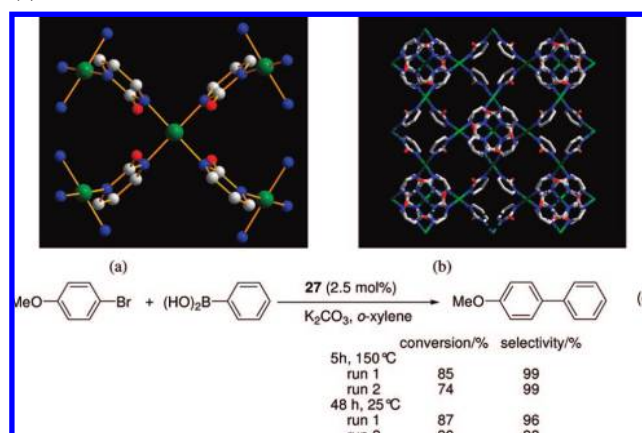
Scheme 19. Formation of the Metallo-Cross-Linked PA-TAP–Pd Polymer 26 for the Suzuki–Miyaura Coupling Reaction



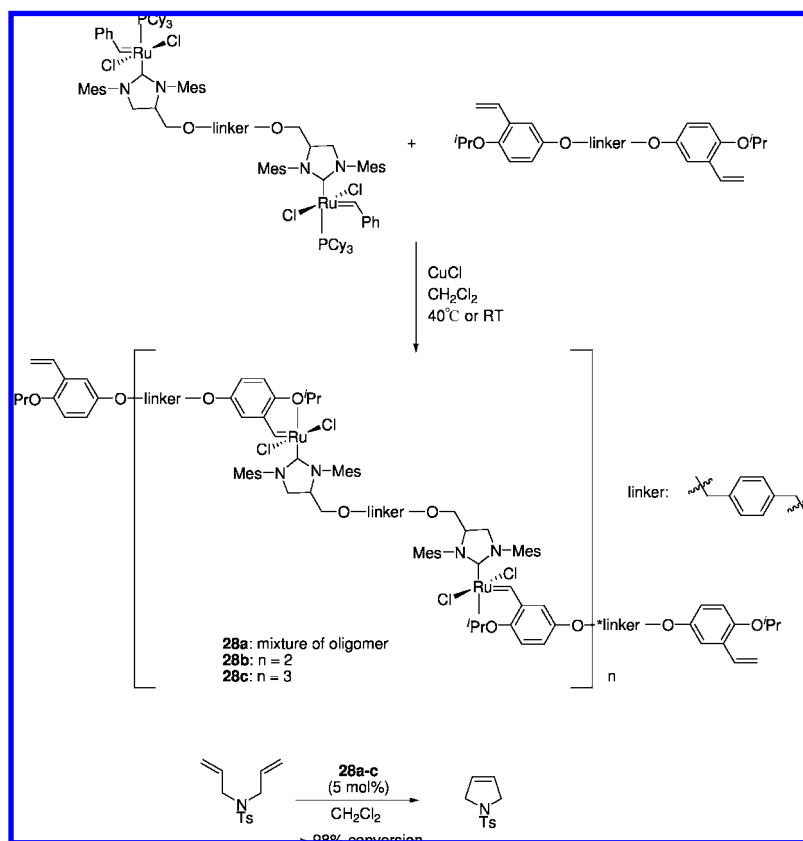
(NH₄)₂PdCl₄ into a Y-shaped microchannel reactor led to spontaneous formation of the palladium-complex membrane, poly(acrylamide)-triarylphosphine palladium (PA-TAP–Pd) (26), by palladium cross-linking of the phosphine-bearing moieties (Scheme 19). The PA-TAP–Pd membrane inside the microchannels was used to catalyze the Suzuki–Miyaura reaction of various combinations of aryl iodides and arylboronic acids under microflow conditions, leading to instantaneous and nearly quantitative production of biaryl compounds within short residence time (4 s) in the channels. Compared to the conventional flask reaction system, the self-assembling formation of polymeric metal complexes inside a microchannel reactor might be advantageous for performing a catalytic reaction involving multiple intermolecular steps.

Corma and Garcia et al. reported that the palladium-containing coordination polymer [Pd(2-pymo)₂]_n (27; 2-pymo = 2-hydroxypyrimidinolate) can act as an active and a

reusable heterogeneous catalyst for Suzuki–Miyaura C–C coupling (Scheme 20).⁵⁹ Synthesis and characterization of 27 was first reported by Navarro et al.⁶⁰ It was found that the microporous polymer is structurally related to the sodalite-type frameworks with Pd(II) sites being located in well-defined framework positions which are accessible to guest molecules through the tunnels and micropores (main pore size 8.8 Å in diameter). Corma and co-worker envisaged that catalysis with 27 might be achieved by expansion of the Pd coordination sphere while keeping the framework structure intact. The Suzuki–Miyaura cross coupling between phenylboronic acid and 4-bromoanisole was performed in the presence of 2.5 mol % 27 in *o*-xylene at high temperature (150 °C) for prolonged periods (5 h). Remarkably, evidence showed that such a drastic condition did not cause any appreciable change in the structural integrity of the catalyst, thus ensuring its further reuse without significant diminution of the activity and selectivity. The catalyst was also active and reusable for the same reaction at room temperature, albeit a longer reaction time is needed. Mechanistic understanding from homogeneous catalysis study suggested that a reversible change from tetracoordination for Pd(II) to dicoordination for Pd(0) can occur during catalysis. If the mechanism is ever applicable to this case, however, it seems surprising that the integrity of the solid framework structure was not broken after catalysis. It was thus speculated that the solid can tolerate a certain number of faults in the crystal during the catalytic cycle. Additionally, coordination polymer 27 was also found to be effective as a heterogeneous catalyst for olefin hydrogenation and alcohol oxidation.⁵⁹ Remarkable shape selectivity was observed in olefin hydrogenation, e.g., 1-octene was selectively converted using 27 as the catalyst, whereas the bulkier cyclododecene was not hydrogenated

Scheme 20. Coordination Environment of MOF 27 (a), 3D Structure of 27 Viewed Along the z Direction (b),^a and Suzuki–Miyaura Coupling Reaction Catalyzed by MOF 27 (c)

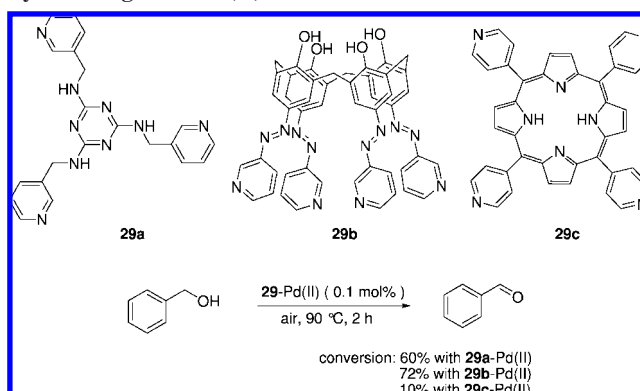
^a Hydrogen atoms omitted for clarity. Green, blue, red, and gray represent Pd, N, O, and C, respectively.

Scheme 21. Self-Supported Oligomeric Grubbs/Hoveyda-Type Ru–Carbene Complexes as Recoverable Catalysts for the RCM Reaction


at all under identical conditions. For the aerobic oxidation of cinnamyl alcohol, complete conversion with 74% selectivity to cinnamylaldehyde was realized with **27** using air as the oxidant under atmospheric pressure.

2.2.6. Poly-Carbene Coordination Polymers

Lee and co-workers reported a type of self-supported oligomeric Grubbs/Hoveyda-type Ru–carbene complex as a recoverable catalyst for ring-closing metathesis (RCM).⁶¹ As shown in Scheme 21, the coupling between the dimeric Ru–carbene complex and isopropoxybenzylidene in the presence of CuCl in CH_2Cl_2 at 40°C afforded an inseparable mixture of oligomeric Ru complexes **28a**, which was precipitated from ethyl acetate as a brown solid. Similar reactions at room temperature provided two oligomeric Ru–carbene complexes **28b** ($n = 2$) and **28c** ($n = 3$) as the major products. The Ru complexes **28** were found to be soluble in halogenated solvents but insoluble in ethyl acetate or toluene; thus, it seems to be possible to conduct the RCM homogeneously using oligomeric Ru complexes **28** in CH_2Cl_2 and recover the catalysts heterogeneously by precipitation with a poor solvent. For the RCM of *N,N*-bisallyl *p*-toluene sulfonamide catalyzed by Ru complexes **28** the observed activities were comparable to that of their homogeneous counterpart. All three oligomeric mixtures of Ru complexes can be recovered heterogeneously by precipitation using ethyl acetate, but the catalytic activities decreased upon reuse. ICP-AES analysis after the first run with **28a** revealed some amount of Ru (16 ppm, ca. 1.13%) has been leached into the ethyl acetate layer.

Scheme 22. Aerobic Oxidation of Benzyl Alcohol Catalyzed by Metallogels 29-Pd(II)


2.3. Oxidation

2.3.1. Poly-*N*-Ligand Coordination Polymers

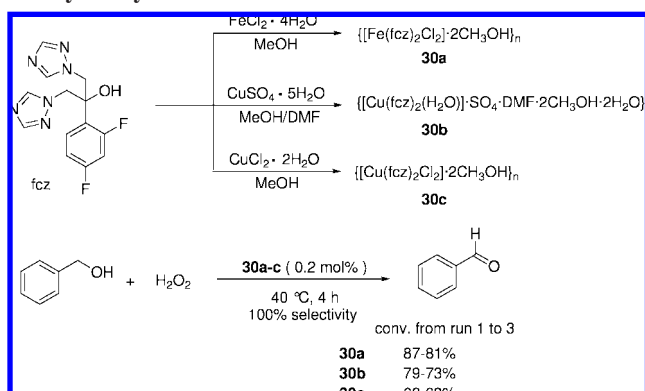
Xu and co-workers reported an example of using coordination polymer metallogels for catalysis of aerobic oxidation of benzyl alcohol (Scheme 22).⁶² Addition of a Pd(II) salt to a solution of polypyridine ligands **29a–c** in DMSO led to generation of the corresponding metallogels **29/Pd(II)** for which the precise structures were unknown. Apart from the stability in water and most organic solvents, these metallogels were shown to be capable of uptaking organic molecules such as DMSO from solution. Such a feature was believed to facilitate the transfer of reactants to the metal sites in the networks of the metallogels; thus, it might be useful for catalysis. In the tested oxidation of benzyl alcohol with oxygen in air the metallogel prepared from ligand **29b** exhibited the optimal result, affording benzaldehyde with a

catalytic turnover about 1.5 times that of Pd(OAc)₂. No palladium black was observed at the end of the reaction, implying the stability of the metallogel catalyst under the reaction conditions. The catalyst was reused with a lower turnover in the second run.

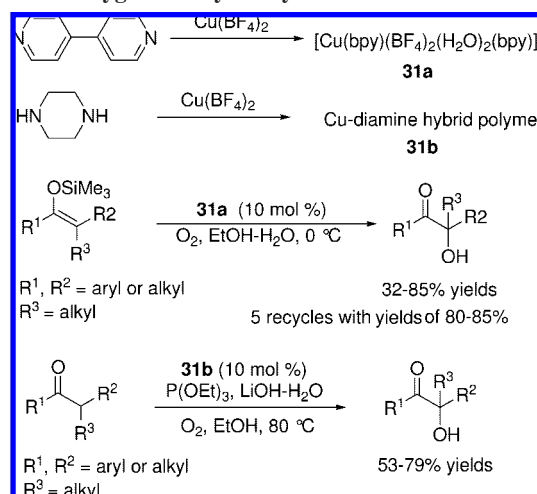
Hou and co-workers investigated the catalytic oxidation of benzyl alcohol by H₂O₂ with three coordination polymers, {[Fe(fc_z)₂Cl₂]·2CH₃OH}_n (**30a**), {[Cu(fc_z)₂(H₂O)]·SO₄·DMF·2CH₃OH·2H₂O}_n (**30b**), and {[Cu(fc_z)₂Cl₂]·2CH₃OH}_n (**30c**) {fc_z = 1-(2,4-difluorophenyl)-1,1-bis[(1*H*-1,2,4-triazol-1-yl)methyl]ethanol}.⁶³ The polymers were synthesized as crystalline solids, and their structures were characterized by X-ray single-crystal diffractions. All polymers were shown to be effective for selective oxidation of benzyl alcohol with 30% aqueous H₂O₂, affording benzaldehyde in moderate to good yields and excellent chemoselectivity (Scheme 23). However, it is worth noting that the catalytic reactions are not completely heterogeneous since control experiments have shown that the filtrates of the catalysts accounted for 10–15% of the total reactivity. These results suggest that the catalysts may have partially been dissolved in the reaction system, but the dominant catalyst species is still the heterogeneous catalyst. It is not clear whether metal leaching or catalyst degradation would occur under prolonged standing of the reaction mixture at the reaction temperature (40 °C). Remarkly, all three polymers were reused for three runs with only minor deterioration (ca. 7%) in benzyl alcohol conversions.

Arai and Yanagisawa et al. investigated the catalytic synthesis of α-hydroxy ketones using a Cu(II)-containing coordination polymer, [Cu(bpy)(BF₄)₂(H₂O)₂(bpy)]_n (**31a**).⁶⁴ With a catalyst loading of 10 mol %, a variety of selected silyl enolates were smoothly oxidized with molecular oxygen to provide the corresponding α-hydroxy carbonyl compounds in moderate to high yields (Scheme 24). The heterogeneous catalyst **31a** was readily isolated from the mixture by centrifugation after completion of the reaction, and the recovered catalyst could be reused in the transformation of the trimethylsilyl enolate of 2-methyl-1-tetralone for five cycles without significant loss of catalytic activity. Very recently, Arai and Yanagisawa further utilized the hybrid polymer **31a** to encapsulate magnetic nanobeads by an in situ self-assembling approach.⁶⁵ The hybrid polymer beads were utilized as catalysts for oxidation of silyl enolates, providing the corresponding α-hydroxy carbonyl compounds in high yields. Upon completion of the reaction the catalyst can readily be recovered by magnetic separation. The recovered catalysts could be used several times with a slight decrease of activity (92–84%).

Scheme 23. Oxidation of Benzyl Alcohol with Aqueous H₂O₂ Catalyzed by 30a–c



Scheme 24. Oxidation of Silyl Enolates and Ketones with Molecular Oxygen Catalyzed by 31

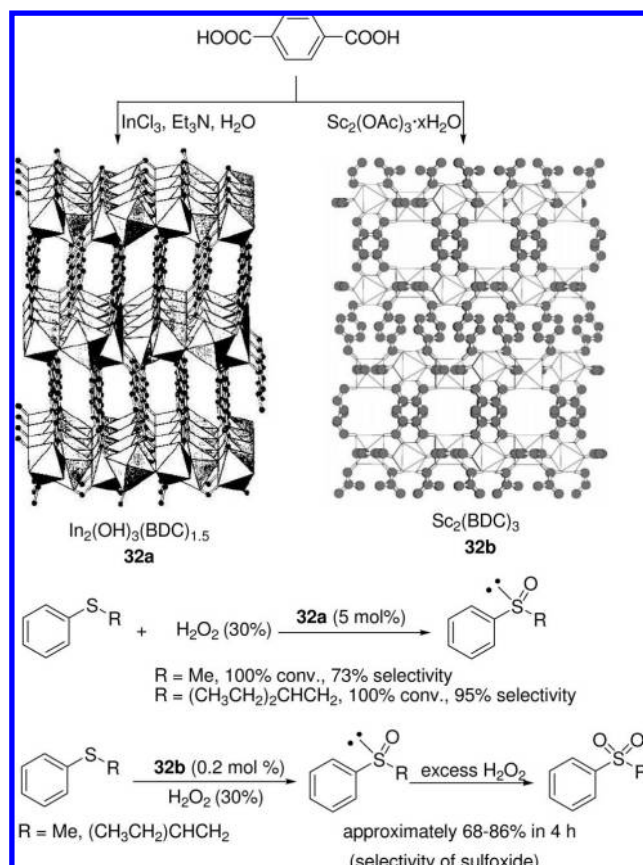


Arai and Yanagisawa et al. also improved the oxidation chemistry using ketones instead of their trimethylsilyl enolates as the substrates (Scheme 24).⁶⁶ Several types of Cu–diamine hybrid polymers were tested as heterogeneous catalysts for direct α-hydroxylation of ketones under strong basic conditions (LiOH). A Cu–piperazine coordination polymer **31b** was the most efficient catalyst, which can tolerate the basic conditions, and gave a series of α-hydroxy aryl ketones in moderate to good yields. The catalyst was recovered in 81% yield by centrifugation after completion of the reaction and reused for the second run with some decrease in efficiency (yield from 79% to 68%).

2.3.2. Poly-Carboxylate Polymers

Monge and co-workers found that In₂(OH)₃(BDC)_{1.5} (**32a**), a crystalline inorganic–organic hybrid polymer obtained under hydrothermal conditions from reaction of InCl₃ and 1,4-benzendicarboxylic acid, was an active heterogeneous catalyst for oxidation of alkylphenylsulfides (Scheme 25).⁶⁷ The 3-dimensional structure of the polymer **32a**, as established by single-crystal X-ray diffraction analysis, can be viewed as having been generated from 2-dimensional InO₆ vertex-sharing octahedral layers that are cross-linked by the dicarboxylate anions (Scheme 25). Oxidation of methylphenylsulfide and (2-ethylbutyl)phenylsulfide was performed in the presence of 5 mol % **32a** as the catalyst in acetonitrile with hydrogen peroxide as the oxidant (Scheme 25). Quantitative conversions of the sulfides were attained in 3–6 h, and the selectivities to the sulfoxides were determined to be 73% and 95%, respectively. According to the report the catalyst can be recycled in successive runs by a simple filtration, but detailed information on catalyst reuse was unavailable. Polymer **32a** has also been reported to be an effective heterogeneous catalyst (0.1 mol % loading) for the hydrogenation reduction of nitroaromatics such as nitrobenzene and 2-methyl-1-nitronaphthalene,⁶⁷ affording the corresponding products in high yields with turnover frequencies of 489 and 385 min⁻¹, respectively. A heterolytic hydrogen cleavage was hypothesized to be involved in the catalytic hydrogenation reaction, but a mechanistic understanding is still unavailable. The pores in **32a** were found to be too small to allow access of a reactant molecule; thus, both the sulfoxidation and hydrogenation catalyses should have taken place on the surface.

Scheme 25. Views of the 3D Structures of $\text{In}_2(\text{OH})_3(\text{BDC})_{1.5}$ (**32a**) and $\text{Sc}_2(\text{BDC})_3$ (**32b**) as well as Their Application in the Catalysis of Alkylphenylsulfide Oxidation^a

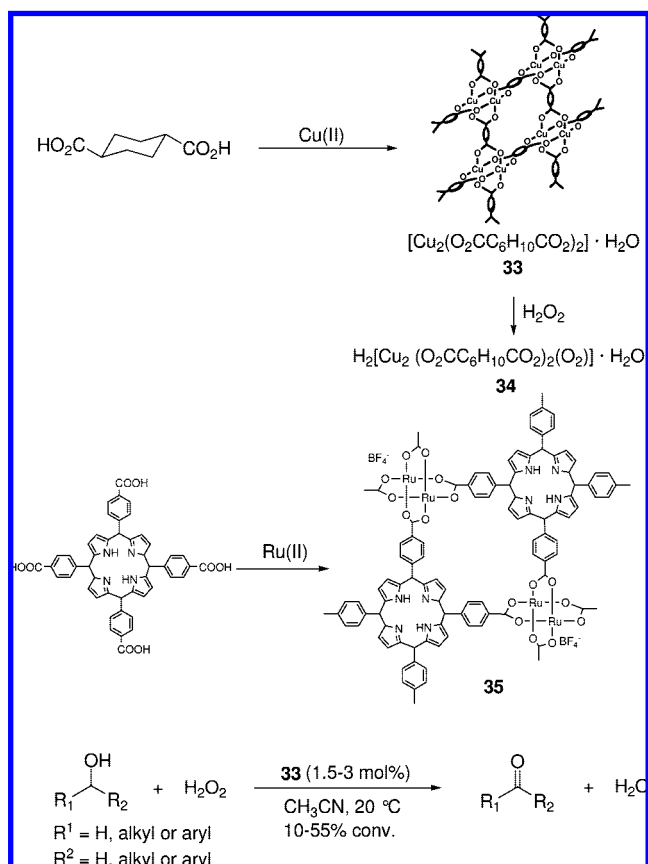


^a Figure of **32a** and **32b** were reprinted from refs 67 and 68. Copyrights 2002 and 2005, respectively, American Chemical Society.

Monge and Ruiz-Valero and co-workers showed that the coordination polymer $[\text{Sc}_2(\text{BDC})_3]$ (**32b**) was also effective as a heterogeneous catalyst in the oxidation of sulfides.⁶⁸ The polymer was synthesized under hydrothermal conditions and crystallographically characterized to have empty nanochannels in its structure (Scheme 25). Kinetic profile studies indicated that **32b** is catalytically active but moderately selective for the oxidation of methyl phenyl sulfide, affording ca. 87% conversion of the sulfide with varying degrees of chemoselectivity (ca. 68–86%) toward the sulfoxide in 4 h. Catalysis was confirmed to be heterogeneous since the supernatant liquid phase after removal of the solid catalyst was shown to be inactive. According to the report, a 1 mol % loading of **32b** could be reused in the reaction at least four times without loss of either activity or selectivity. As a comparison, Ruiz-Valero and co-workers also examined the catalytic activities of the aforementioned lanthanide dicarboxylates **15–17** in the same sulfoxidation reaction.⁴⁶ Chemoselectivities of ca. 90% toward the sulfoxide can be reached for **15–17**, provided that the reactions are stopped at 70% sulfide conversion. The problem of overoxidation to sulfone seems to be persistent at higher conversions, and the nature of the active sites in the catalysts remains unclear.

Mori and co-workers reported the application of a two-dimensional microporous copper carboxylate coordination polymer, $[\text{Cu}_2(\text{O}_2\text{CC}_6\text{H}_{10}\text{CO}_2)_2] \cdot \text{H}_2\text{O}$ (**33**) $[(\text{O}_2\text{CC}_6\text{H}_{10}\text{CO}_2)^{2-} = \text{trans-1,4-cyclohexanedicarboxylate}]$, as a reusable heterogeneous catalyst for highly selective oxidations of alcohols to the corresponding ketones or aldehydes with hydrogen

Scheme 26. Selective Oxidations of Alcohols Catalyzed by **33** or **35**



peroxide (Scheme 26).^{69,70} The compound was found to bear the typical paddle-wheel structural units of the copper carboxylates and possess micropores. In the oxidation of several primary or secondary alcohols with H_2O_2 , **33** exhibited a moderate reactivity at 20 °C with turnover frequencies in the range from ca. 0.04 to 11.7 h^{-1} but was remarkably selective in the transformation toward aldehydes or ketones (99% after 1 h). The filtrate of the mixture of **33** and an excess of H_2O_2 in acetonitrile stirred for 3 days was found to be completely inactive for the oxidation of 2-propanol. Furthermore, no copper species was detected in the filtrate of the catalytic reaction system (<0.02 ppm). These observations indicated that catalysis was truly heterogeneous. Probably the most interesting finding in this study might be ascribed to the isolation and characterization of an active intermediate in the catalysis, the green-colored peroxo copper(II) coordination polymer $\text{H}_2[\text{Cu}_2(\text{O}_2\text{CC}_6\text{H}_{10}\text{CO}_2)_2(\text{O}_2)] \cdot \text{H}_2\text{O}$ (**34**) (Scheme 26). This polymeric peroxo intermediate **34** was isolated by treatment of **33** with an excess amount of hydrogen peroxide and amply characterized by elemental analysis, FT-IR, TG/DTA, magnetic susceptibility, ESR, DR-uv, XRPD, resonance Raman, BET surface area, pore size distribution, and gas occlusion measurements. XRPD analysis revealed that **34** has a structure similar to that of **33** with the exception that the two-dimensional $[\text{Cu}_2(\text{O}_2\text{CC}_6\text{H}_{10}\text{CO}_2)]$ layers were bridged by the peroxo groups via a μ -1,2-*trans*-Cu(1)-OO-Cu(2) species in **34**. It was found that **34** has a pore size similar to that of **33** (4.9 Å in diameter) and is thermally stable up to 132.8 °C in the solid state. Remarkably, NMR tube reaction of 2-propanol with **34** in the absence of H_2O_2 led to formation of acetone, suggesting **34** is an active species for the heterogeneous catalysis. It was noteworthy that according to the report the polymer peroxo

complex **34** should represent the first example of well-characterized active copper peroxo intermediate in heterogeneous oxidation catalysis.

Mori and co-workers further showed that a three-dimensional microporous ruthenium(II,III) polymeric complex, $[\text{Ru}_2(\text{II,III})(\text{H}_2\text{TCPP})]\text{BF}_4$ (**35**), was an effective heterogeneous catalyst for aerobic oxidation of alcohols.^{70,71} The coordination polymer was characterized by elemental analysis, TG/DTA, magnetic susceptibility, FT-IR, diffuse reflectance UV-vis spectroscopy, ESR, X-ray powder diffraction, BET analysis, and nitrogen and oxygen adsorption measurements. On the basis of these results a structural model featuring the dinuclear Ru(II)–Ru(III) moieties bridged in a paddle-wheel pattern by the tetra-carboxylate ligand was proposed for **35** (Scheme 26). No metallation at the center of porphyrin ring was observed as evidenced by the UV-vis spectrum. Gas sorption measurement showed **35** is a microporous compound having an effective pore size of 4.8 Å and a BET surface area of 427 m²/g (Ar). Under an ambient pressure of dioxygen or air at room temperature **35** was shown to catalyze the heterogeneous oxidation of several primary or secondary alcohols with moderate activity (turnover frequencies approximately ranging from 0.04 to 0.8 h⁻¹) and excellent selectivity to the corresponding aldehydes or ketones (95–99%). In contrast, neither the nonporous ruthenium(II,III) fumarate nor the porous **33** exhibited catalytic activities under the otherwise identical conditions. ESR measurement suggested that the reaction pathway might involve formation of Ru–oxygen radical intermediate, presumably as a result of the high affinity of diruthenium(II,III) sites toward molecular oxygen. Furthermore, **35** was shown to be reusable at least two times in the oxidation of 2-propanol without a change of the catalytic activity.

A rare example of a 3D Tb coordination polymer with a complicated formula, $\{\text{Tb}(\text{bpdo})_2[\text{V}_6\text{O}_{13}\{(\text{OCH}_2)_3\text{C}(\text{NH}_2\text{C}-\text{H}_2\text{C}_6\text{H}_4-4-\text{CO}_2)\}\{(\text{OCH}_2)_3\text{C}(\text{NHCH}_2\text{C}_6\text{H}_4-4-\text{CO}_2)\}_2]\} \cdot 1.5\text{DMF} \cdot 3.0\text{EG}$ (**36**) (bpdo = 4,4'-bipyridyl-*N,N'*-dioxide and EG = ethylene glycol), was reported by Han and Hill to be effective for the heterogeneous catalysis of aerobic oxidation of PrSH to PrSSPr and oxidation tetrahydrothiophene to tetrahydrothiophene oxide by *tert*-butylhydroperoxide.⁷² **36** was prepared by self-assembly of Tb(III) ions with 4,4'-bis(pyridine-*N*-oxide) (bpdo) and $[\text{V}_6\text{O}_{13}\{(\text{OCH}_2)_3\text{C}(\text{NHC}-\text{H}_2\text{C}_6\text{H}_4-4-\text{CO}_2)\}_2]^{4+}$, a redox-active bis(triester)–hexavanadate moiety bearing two carboxylates as terminal groups. An X-ray crystallographic study revealed that **36** has a three-dimensional coordination network structure, constructed by pillaring the two-dimensional layers of Tb(III) centers and bpdo units by the triester–trivanadate units. CO₂ gas adsorption measurement indicated that **36** has accessible pores, which probably can uptake some guest molecules for catalytic reactions. **36** was shown to catalyze the oxidation of the environmentally odorous PrSH to the nonodorous disulfide PrSSPr using only ambient air as the oxidant albeit with a modest turnover of 18.5 in 30 days. Catalysis was demonstrated to be heterogeneous as the supernatant showed no catalytic activity. According to the report **36** can be recovered and reused without loss of catalytic activity. On the basis of some kinetic study results a mechanism was hypothesized involving a rate-limiting bimolecular reaction primarily on the outer surface of the particles between PrSH and the V₆ units in **36** and reoxidation of the reduced V₆ units by O₂/air.

Baca and co-workers described the synthesis and characterization of two coordination polymers, $\{[\text{Cu}(\text{Pht})(\text{Im})_2] \cdot 1.5\text{H}_2\text{O}\}_n$ and $[\text{Co}(\text{Pht})(\text{Im})_2]_n$ (Pht²⁻ = dianion of *o*-phthalic acid; Im = imidazole), as well as a preliminary study on their application as catalysts in oxidation of cyclohexene with H₂O₂.⁷³ Under aerobic conditions at ambient temperature multiple oxidation products were obtained with the major one being 2-cyclohexen-1-one accompanied by appreciable amounts of 2-cyclohexen-1-ol. However, the nature of the catalysis remained unclear.

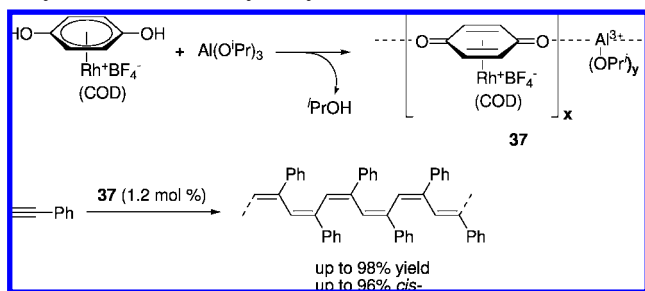
2.3.3. Lanthanide Disulfonate Polymers

Monge and co-workers reported the synthesis, characterization, and catalytic properties of a family of lanthanide disulfonate polymers, $[\text{Ln}(\text{OH})(\text{NDS})(\text{H}_2\text{O})]_n$ (where Ln = La, Pr, and Nd; NDS = 1,5-naphthalenedisulfonate).⁷⁴ The polymers were found to be effective catalysts for oxidation of linalool to hydroxy ethers with an activity comparable to that of microporous bifunctional titanium aluminosilicates, but further information on the heterogeneous nature or reusability of the catalyst was not available.

2.4. Polymerization

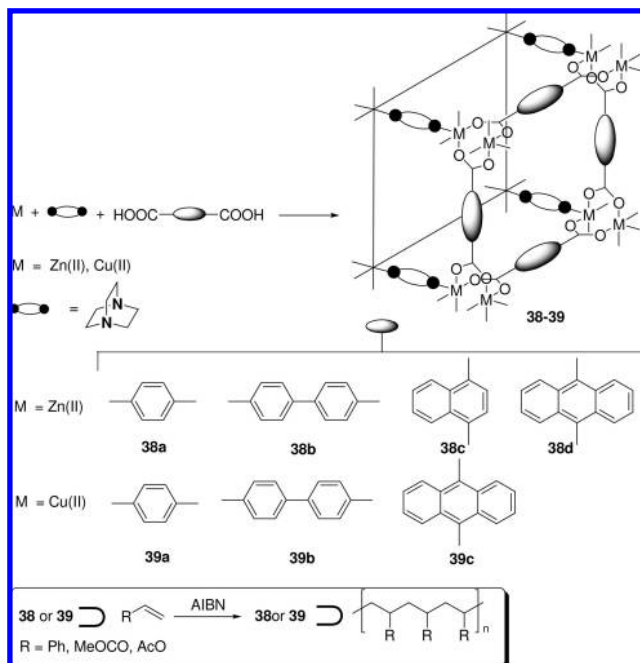
Several examples of polymerization reactions promoted with the self-supported catalysts have been reported. Tanski and Wolczanski investigated a variety of Ti aryldioxy coordination polymers as self-immobilized Ziegler–Natta catalysts in the polymerization of ethene and propene with methylalumoxane (MAO) as the cocatalyst.⁷⁵ The titanium aryldioxy polymers were synthesized as crystalline solids by reactions of Ti(O^{*i*}Pr)₄ with the aryldioxides in pyridine or its derivatives and found to adopt a general formula of $[\text{Ti}(\text{OArO})_2(\text{py})_2]$ (Ar = 1,4-C₆H₄-, 2,7-naphthyl, 4,4'-biphenyl; py = pyridine and 4-Me- or 4-Ph-pyridine). X-ray crystallographic studies revealed that these Ti coordination polymers comprise of one-, two-, or three-dimensional network structures wherein the Ti centers are cross-linked to each other to varying degrees by the bridging aryldioxy ligands. In the assessment of these metal organic networks for ethylene and propylene polymerization activity each of the titanium coordination polymers was slurried in toluene and activated with a large excess of MAO (Al/Ti = 1000) at room temperature under 5 atm of ethylene or propylene gas. The titanium aryldioxy polymers were found to be mediocre Ziegler–Natta catalysts, generating polydisperse linear polyethylene and atactic polypropylene in poor to mediocre activities. The data were consistent with the presence of numerous sites of variable activity in the catalytic systems, presumably generated by an extensive but nonuniform degradation of the coordination polymers. According to the authors, reactions that do not require decomposition of the coordination polymer networks may be more suitable to be investigated from the viewpoint of potential catalysis.

Son and Sweigart et al. reported the synthesis of a nanosized self-supported rhodium quinonoid catalyst and demonstrated its high activity in the stereoselective polymerization of phenylacetylene.⁷⁶ Treatment of $[(\eta^6-1,4\text{-hydroquinone})\text{Rh}(\text{COD})]^+$ with an equimolar amount of Al(O^{*i*}Pr)₃ in THF immediately afforded an insoluble yellow solid, which was characterized as nanosized spheric particles (**37**) wherein the $[(\eta^6-1,4\text{-hydroquinone})\text{Rh}(\text{COD})]^+$ moieties are bridged by Al³⁺ species via μ₂-O bonding (Scheme 27). It was noted that during the self-supporting process the Rh

Scheme 27. Self-Supported Rhodium Nanocatalyst **37 for Polymerization of Phenylacetylene**


unit has undergone a formal change in charge from +1 to -1. Interestingly, slight modifications in reaction conditions such as the reaction volume can lead to a change in average particle sizes (from 340 to 537 nm) and their distributions, which are important properties that influence the activity and ease of separation of nanosized heterogeneous catalysts. The self-supported organometallic nanoparticles **37** demonstrated excellent catalytic activity in the polymerization of phenylacetylene, affording much longer polyphenylacetylene (PPA) than did their homogeneous counterpart, $[(\eta^6\text{-}1,4\text{-hydroquinone})\text{Rh}(\text{COD})]^+$. Furthermore, **37** were also found to be much more stereoselective than their homogeneous counterpart, selectively affording *cis*-PPA (up to 96%) as compared favorably with the mixture of *cis*- and *trans*-PPA (59:41) obtained with the latter. It was speculated that stereoselective nature of the catalysis is a property that results from the heterogenization process, but the mechanism of such an evolution remains unclear. The heterogeneous self-supported catalyst was recovered from the reaction mixture by centrifugation and gave a 94% yield of PPA in the second run.

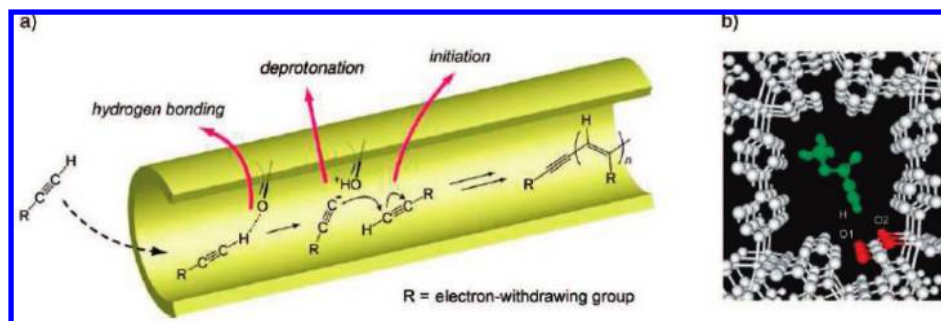
In a recently published review⁷⁷ Kitagawa and co-workers summarized their results of several elegant studies on the use of microporous coordination polymers as a nanosize reactor or heterogeneous catalyst for olefin or alkyne polymerization reactions. They demonstrated that olefin polymerization can advantageously be performed within the regulated and tunable nanochannels of an appropriate porous coordination polymer, which may allow for multilevel control (tacticity and molecular weight, substrate specificity, etc.) in the reaction. The first example of radical polymerization within tunnels of porous coordination polymers was reported in 2005 by Kitagawa and co-workers,⁷⁸ who successfully carried out a styrene polymerization in $[\text{M}_2(1,4\text{-benzenedicarboxylate})_2(\text{triethylenediamine})]_n$ ($\text{M} = \text{Zn}^{2+}$ and Cu^{2+}) (**38a** and **39a**) (Scheme 28) with 2,2'-azobis(isobutyronitrile) (AIBN) as the radical initiator. Previous structural studies by X-ray crystallography indicated that the host coordination polymers **38a** and **39a** are isomorphous and have regular and continuous one-dimensional nanochannels with cross-sections slightly larger than the size of styrene (7.5×7.5 and $8.2 \times 6.0 \text{ \AA}^2$, respectively). The overall three-dimensional networks of **38a** and **39a** can be viewed as being constructed by pillaring the 2D layers of metal dicarboxylates (based on the well-known "paddle-wheel" units) with the rigid linear DABCO ligands. The radical polymerization of styrene inside **38a** and **39a** led to formation of polystyrene (PSt) composite (**38a**- or **39a**⊃PSt) with the resultant PSt chain being encapsulated in the nanochannels. The accommodated PSts were released from the hosts by treatment with aqueous NaOH and found by GPC measurements to have similar molecular weights and distributions. It was noted that

Scheme 28. Radical Polymerization of Vinyl Monomers (styrene, methyl methacrylate, and vinyl acetate) Inside the Tunnels of Porous Coordination Polymers **38 and **39****


the polydispersities (M_w/M_n ca. 1.6) are significantly narrower than that of the bulk PSt synthesized under comparable conditions (M_w/M_n ca. 4.7), presumably as a result of a favorable confinement effect induced by the nanochannels. Interestingly, the ESR spectrum of **38a** collected during polymerization showed an intense signal persistent over 3 weeks at 70 °C, which was assigned to the propagating living radical of polystyrene. The remarkable stabilization effect for the propagating radical in this system was ascribed by the authors to suppression of termination reaction and radical transfer in the nanochannel, which can be viewed as another manifestation of the beneficial confinement effect of host frameworks. Very recently, Kitagawa and co-workers reported the successful extension of the strategy to the radical inclusion polymerization of several vinyl monomers (styrene, methyl methacrylate, and vinyl acetate) within the nanochannels of $[\text{M}_2(\text{dicarboxylate})_2(\text{triethylenediamine})]_n$ ($\text{M} = \text{Zn}^{2+}$ or Cu^{2+}) (**38** and **39**) (Scheme 28),⁷⁹ a family of porous coordination polymers with analogous structural features. The poly(vinyl)s were obtained with relatively a narrow molecular weight distribution and an increased stereoregularity, which are difficult to control in conventional bulk and solution polymerizations.

Apart from the radical polymerization of olefins with porous coordination polymers as the hosts Kitagawa and co-workers also demonstrated that properly functionalized nanochannels in porous coordination polymers can effectively be used to promote the anionic polymerization of acetylene derivatives (Scheme 29).⁸⁰ The research was inspired by the observation that acetylene molecules can be selectively adsorbed into the one-dimensional nanochannels of microporous coordination polymer $[\text{Cu}_2(\text{pzdc})_2(\text{pyrazine})]_n$ (pzdc = pyrazine-2,3-dicarboxylate) and are held there at a periodic distance from one another by hydrogen bonding with two noncoordinated carboxylate oxygen atoms on the pore wall.⁸¹ By taking advantage of the potential catalytic activity of basic carboxylate oxygen atoms inside the channels and the possible confinement effect of the narrow nanochannels

Scheme 29. Schematic Representation of the Mechanism for the Nanochannel-Promoted Polymerization of Acidic Acetylenes in Porous Coordination Polymers 40 (a), and Optimized Structure of Methyl Propiolate (MP) (green) Incorporated in a Nanochannel of 40b Showing the Hydrogen-Bonding Interaction between MP and the Channel Surface (b)^a



^a Reproduced with permission from ref 80. Copyright Wiley-VCH Verlag GmbH & Co. KGaA.

on the selectivity of the reaction Kitagawa and co-workers further carried out an anionic polymerization of more acidic acetylene derivatives bearing an electron-withdrawing group, such as methyl propiolate, in the channels of analogous porous coordination polymers $[\text{Cu}_2(\text{pzdc})_2(\text{L})]_n$ (**40a,b**) [$\text{L} = 4,4'$ -bipyridine, or 1,2-di(4-pyridyl)ethylene] (Scheme 29a). The authors proposed that strong interaction of the basic sites inside the channels with acetylenes might produce reactive acetylide species by C–H bond dissociation, which would subsequently initiate anionic polymerization. Indeed, polymerization of methyl propiolate in the nanochannel of $[\text{Cu}_2(\text{pzdc})_2(4,4'$ -bipyridine)]_n (**40a**) for 12 h at room temperature provided a composite material wherein the poly(methyl propiolate) was encapsulated in the channels of the coordination polymer. DMF extraction at elevated temperature releases the accommodated poly(methyl propiolate), which was found to be of predominant *trans* geometry with weight- and number-average molecular weights of 4800 and 850, respectively. The *trans* selectivity of the polymerization was rationalized by assuming an ordered array of the monomers in the channels, as inferred from IR measurements and a molecular-mechanics structural simulation. Further experiments using analogous porous coordination polymers in combination with different acetylene monomers indicated that the monomer recognizes precisely the channel size as well as the surface functionality of the coordination polymers, and the strong hydrogen-bonding interaction (acid–base) between the monomers and the channel surface (Scheme 29b) is a key factor to this unique spontaneous polymerization.

2.5. Ring Opening of Epoxides

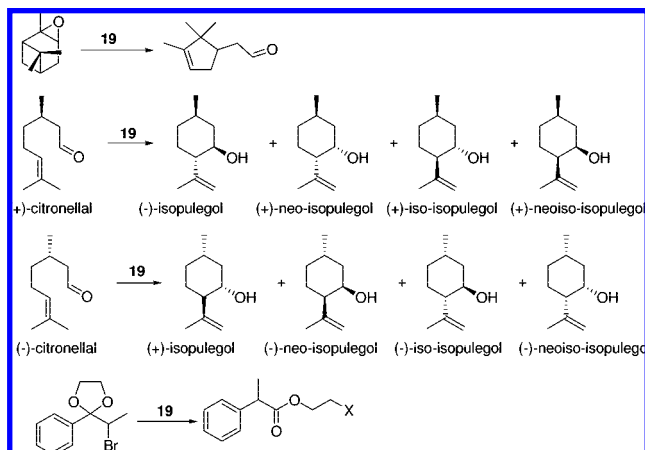
Some copper-containing coordination polymers of the Cu(II)–btp type [btp = 2,6-bis(*N'*-1,2,4-triazolyl)pyridine] were reported by Kim and co-workers to be effective for heterogeneous catalysis of the alcoholysis of selected epoxides by methanol.^{82–84} The polymer $[\text{Cu}_2(\text{btp})_3(\text{NO}_3)_4]_n$ was prepared by self-assembly as single crystals and shown to contain a btp-bridged tetranuclear Cu(II) unit connected by nitrate ions. Alcoholysis of several epoxides was carried out in a large excess of methanol in the presence of the copper polymer (2 mol %) as the catalyst with nearly quantitative conversions being achieved in 3–60 days at ambient temperature.⁸² The catalyst could be recovered by simple filtration and reused with some decrease in activity. However, the potential metal leaching and heterogeneity of catalysis may need to be checked since $\text{Cu}(\text{NO}_3)_2$ was also found to be catalytically active (albeit to a lesser degree) in the methanolysis of cyclohexene oxide under identical condi-

tions. Similar Cu(II)–btp polymer $[\text{Cu}(\text{btp})_2(\text{ClO}_4)_2]$ was also shown to catalyze the ring-opening reaction of cyclohexene epoxide with methanol at room temperature with quantitative conversion being attained in 8 days.⁸³ Control experiments showed that in this case the dominant reactive species is in the solid phase, accounting for ca. 90–95% of the total reactivity. The catalyst was recovered by filtration and reused at least once with a slight loss (ca. 5–10%) of activity.

Baiker and co-workers examined the catalytic properties of the copper coordination polymer **31a** mentioned above in the ring opening of epoxides with alcohols and aniline.⁸⁵ **31a** was remarkably active and selective in the methanolysis of several aliphatic and cyclo-aliphatic epoxides at ambient solvent-free conditions. For the reaction of styrene oxide with methanol in the presence of ca. 10 mol % of **31a** the ring-opening product 2-methoxy-2-phenylethanol was obtained with conversion and selectivity greater than 90% in only 2 h, wherein the reaction rate was almost comparable to that obtained using the reference homogeneous catalyst $\text{Cu}(\text{BF}_4)_2 \cdot \text{H}_2\text{O}$. However, methanolysis of the sterically bulkier epoxides *trans*- and *cis*-stilbene oxide was considerably more sluggish, even incomplete after several days. Furthermore, the **31a**-catalyzed alcoholysis of styrene oxide also exhibited a considerable steric effect toward the alcohol reactants. When bulkier alcohols such as *i*PrOH, *t*BuOH, and benzyl alcohol were used, conversions of less than 20% were observed in 24 h. These data supported the heterogeneous nature of catalysis using **31a**, further confirmed by the conventional filtration test in the methanolysis of styrene oxide. Furthermore, catalyst **31a** was shown to be reusable in the same reaction, maintaining an essentially constant reactivity for up to four recyclings. Apart from alcoholysis, **31a** was also effective for the aminolysis of cyclohexene oxide with aniline, albeit with a somewhat lower activity than that provided by the homogeneous catalyst $\text{Cu}(\text{BF}_4)_2 \cdot \text{H}_2\text{O}$. Finally, structural characterization of **31a** both before and after catalytic application indicated that some type of structural modification has occurred for **31a** during the reaction, presumably caused by partial replacement of the structural water by methanol.

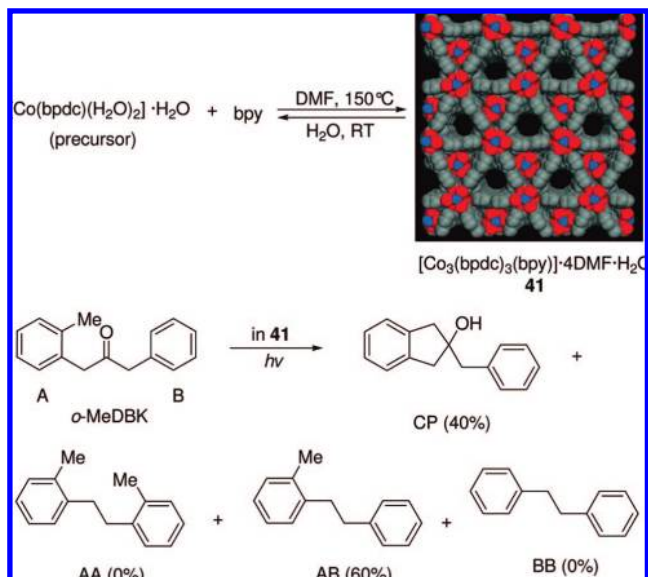
2.6. Miscellaneous

The aforementioned desolvated coordination polymer $[\text{Cu}_3(\text{BTC})_2]$ (**19**) was also demonstrated by De Vos et al. to be a selective and well-defined heterogeneous Lewis acid catalyst for isomerization of terpene derivatives, such as the rearrangement of α -pinene oxide to campholenic aldehyde and cyclization of citronellal to isopulegol (Scheme 30).⁸⁶

Scheme 30. Isomerization of Terpene Derivatives Catalyzed by 19


The active sites of **19** were shown to be hard Lewis acids using the ethylene ketal of 2-bromopropiophenone as a test substrate. Catalyst performance, reusability, and heterogeneity were critically assessed. Recycling experiments in isomerization of α -pinene oxide and cyclization of citronellal showed that selectivity remained constant for each consecutive run, whereas reaction rate decreased owing to formation of deposits in the pores. By applying suitable regeneration procedures, the catalytic activity of recovered **19** could be brought back close to its original value.

Recently, the potential application of metal–organic frameworks (MOF) in the fields of heterogeneous catalysis and gas processing has begun to arouse interest from some industry researchers. Mueller and co-workers from BASF reported their testing results using zinc-based coordination polymers with terephthalic acid (H_2BDC), $\text{Zn}(\text{BDC})_3 \cdot (\text{DMF})(\text{H}_2\text{O})$ (referred to as MOF-2), and $\text{Zn}_4\text{O}(\text{BDC})_3 \cdot (\text{DMF})_8(\text{C}_6\text{H}_5\text{Cl})$ (referred to as MOF-5) for catalytic activation of alkynes to prepare methoxypropene and vinyl ester.⁸⁷ Synthesis and characterization of crystalline MOF-2⁸⁸ and MOF-5⁸⁹ were first reported by Yaghi and co-workers. X-ray single-crystal analysis revealed that in the as-synthesized MOF-2, dimeric Zn clusters are linked to each other by the terephthalate ligands in a way that is reminiscent of the well-known paddle-wheel pattern to yield 2-D layers with a regular tiling topology. Stacking of the layers in the solid leads to formation of a microporous 3-D framework with 1-D channels of ca. 5 Å in diameter. MOF-5 exhibits excellent thermal stability and retains its single crystallinity even up to 300 °C. It is a highly porous solid with a 3-D channel system of 8 Å aperture and 12 Å cross-section. As a result, the guest molecules in the original as-synthesized MOF-5 have good mobility and can be fully exchanged with chloroform as evidenced by Yaghi et al. in a solvent sorption/desorption experiment.⁹⁰ Mueller and co-workers further demonstrated diffusion for both ethane and benzene in MOF-5 is orders of magnitude faster than in zeolite NaX, probably as a result of the difference between the diameters of the two large nanoporous cavities in the MOF-5 (1.1–1.3 nm²) over the smaller NaX supercage (1.2 nm) with an even lower entrance window size (0.7 nm) according to the authors.⁸⁷ Furthermore, Mueller and co-workers also showed that the effective self-diffusion coefficient of benzene in the MOF-5 structure is only slightly smaller than that in the neat liquids at the same temperature. This was considered to be a valuable feature from the prospect of catalysis since it

Scheme 31. Photolysis of *o*-Methyldibenzylketone in Microporous Coordination Polymer **41^a**


^a Reproduced with permission from ref 91. Copyright Wiley-VCH Verlag GmbH & Co. KGaA.

promises facile molecular diffusion when using MOF materials as the catalysts. In Mueller and co-workers' report MOF-2 and MOF-5 were readily prepared in relatively large laboratory scale (tens of grams) and tested as catalysts in the preparation of methoxypropene from propyne and vinyl ester from acetylene, respectively. The study demonstrated that the MOFs undoubtedly can act as heterogeneous catalysts with the selectivity depending on the detailed structure of the MOFs. In the esterification of 4-*tert*-butylbenzoic acid with acetylene MOF-2 was more selective than MOF-5 at similar acid conversions. However, a clear understanding of the underlying mechanism is not yet available. As concluded by the authors, more work needs to be done to pinpoint the origin of catalytic properties of MOFs and assess if MOFs can compete with well-known heterogeneous industrial catalysts in terms of not only activity and selectivity but also time-on-stream behavior and leaching stability.

Li and co-workers reported an interesting application of $[\text{Co}_3(\text{bpdc})_3(\text{bpy})] \cdot 4\text{DMF} \cdot \text{H}_2\text{O}$ (**41**) (bpdc = biphenyldicarboxylate) as a zeolite-like host in the photolysis of *o*-methyldibenzylketone (*o*-MeDBK) (Scheme 31).⁹¹ Complex **41** was synthesized as crystals by a solvothermal reaction from $[\text{Co}(\text{bpdc})(\text{H}_2\text{O})_2] \cdot \text{H}_2\text{O}$ and bpy. X-ray structural analysis indicated that **41** possesses a nanoporous structure with 1D channels, containing large supercavities (11 × 11 × 5 Å) with smaller windows (maximum dimension of about 8 Å). The desolvated **41** showed no sign of decomposition up to 400 °C and exhibited a high sorption capacity for hydrocarbons. **41** was examined as a host for the photochemical reaction of *o*-MeDBK. A cage effect was observed in the reaction, as reflected by the high shape selectivity (100%) to the α -cleavage products (Scheme 31). Remarkably, the photochemical products can be completely recovered simply by immersing the product containing **41** in water wherein the polymer was converted back to its nonporous synthetic precursor, $[\text{Co}(\text{bpdc})(\text{H}_2\text{O})_2] \cdot \text{H}_2\text{O}$. It is conceivable that the framework of **41** can in principle be rebuilt from its recovered precursor, and such a structural reversibility may allow for the recyclable use of **41** according to the authors.

Chen and co-workers reported the use of water-insoluble U–Ni–organic⁹² and Ag–U–organic⁹³ bimetallic hybrid polymers $[\text{Ni}_3(\text{H}_2\text{O})_2(\text{QA})_2(\text{bpy})_2\text{U}_5\text{O}_{14}(\text{H}_2\text{O})_2(\text{OAc})_2] \cdot 2\text{H}_2\text{O}$ (HOAc = acetic acid; H_2QA = quinolinic acid), $[\text{Ag}(\text{bipy})(\text{UO}_2)(\text{BDC})_{1.5}]$ (bipy = 2,2'-bipyridyl) and $[\text{Ag}_2(\text{phen})_2\text{UO}_2(\text{btec})]$ (phen = 1,10-phenanthroline, btec = 1,2,4,5-benzenetetracarboxylate), respectively, for photocatalytic degradation of methyl blue and rhodamine B (both as models of dye pollutants in water). Crystallographic analyses indicated that all these structures contain uranyl units that are connected in different ways by the bridging ligands. A mechanism was proposed for the photodegradation pathways of the rhodamine B substrate in the presence of uranium–silver–organic hybrid compounds involving a catalytic cycle of photoexcitation of the uranyl units, α -hydrogen abstraction of the rhodamine B, and regeneration of uranyl species by molecular oxygen dissolved in water.⁹³ For these heterogeneously catalyzed reactions, at least in the case of the uranium–nickel–organic hybrid compound, the reaction should be surface promoted since the pore size of this compound was not shown to be large enough to allow for penetration of N_2 molecules. The catalyst particles can be isolated from solution by filtration after reaction, but no catalyst reuse was reported. Natarajan reported that three-dimensional MOFs $[\text{Co}_2(\text{bpy})(\text{OBA})_2]$, $[\text{Ni}_2(\text{bpy})_2(\text{OBA})_2] \cdot \text{H}_2\text{O}$, and $[\text{Zn}_2(\text{bpy})(\text{OBA})_2]$ [OBA = 4,4'-oxybis(benzoate)] are active catalysts for photodegradation of orange G, rhodamine B, Remazol Brilliant Blue R, and methylene blue.⁹⁴

Granato and co-workers examined the use of $[\text{Cu}_3(\text{BTC})_2(\text{H}_2\text{O})_3]$ (**18**) for chemical pretreatment of olive oil mill wastewaters (OOMW),⁹⁵ which are not suitable for direct biological treatment owing to their high contents of nonbiodegradable and phytotoxic compounds (such as polyphenols). The wet hydrogen peroxide catalytic oxidation (WHPCO) process is useful for pretreatment of highly polluted OOMW containing polyphenols. Preliminary results showed that **18** is effective in catalysis of the WHPCO process, especially for decomposition of nonbiodegradable compounds. Under the test conditions the polyphenol content could be reduced significantly with an abatement of 96%. The main advantage of using **18** as a heterogeneous catalyst over that homogeneous Fenton reagent system (Fe^{2+} and H_2O_2), according to the authors, is the possibility to recover and reuse the catalyst.

Xu and co-workers investigated the catalytic activity of porous MOFs $\{[\text{Li}_{11}(\text{Ni}_8\text{L}_{12})(\text{H}_2\text{O})_{12}]\text{Li}_9(\text{H}_2\text{O})_{20}\}_n$ (H_3L = 4,5-imidazoledicarboxylic acid), $\{[\text{Na}_{20}(\text{Ni}_8\text{L}_{12})(\text{H}_2\text{O})_{28}](\text{H}_2\text{O})_{13}(\text{CH}_3\text{OH})_2\}_n$ (H_3L = 4,5-imidazoledicarboxylic acid), and $[\text{Cu}(\text{mipt})(\text{H}_2\text{O})](\text{H}_2\text{O})_2$ (H_2mipt = 5-methylisophthalic acid) for gas-phase oxidation of CO to CO_2 .^{96,97} All three compounds were structurally well-defined solids with the latter two being found active in catalysis. For the copper(II) coordination polymer $[\text{Cu}(\text{mipt})(\text{H}_2\text{O})](\text{H}_2\text{O})_2$ ⁹⁷ crystallographic analysis revealed a local coordination environment similar to that of **18** and an overall microporous framework structure with two types of open channels. Thermogravimetric analysis indicated that the complex loses all water molecules, both uncoordinated and coordinated ones, around 150 °C in vacuum. Remarkably, XRPD measurement revealed that the open framework of dehydrated copper polymer remains intact, thus leaving the Lewis-acidic copper sites inside the channel walls accessible for catalytic transformation of reactants with proper size and function-

alities. The tested CO oxidation was performed in a flow reactor over a fixed bed of the $[\text{Cu}(\text{mipt})]$ polymer. Prior to the reaction the catalyst was activated by heating in air at 250 °C for 3 h. For CO oxidation the activity of $[\text{Cu}(\text{mipt})]$ was found to be similar to or higher than that of CuO and $\text{CuO}/\text{Al}_2\text{O}_3$ along with an extra advantage of being stable when exposed to ambient air. Furthermore, the framework of $[\text{Cu}(\text{mipt})]$ remained intact after catalytic reaction as evidenced by the XRPD patterns, suggesting reusability of the catalyst. Finally, FT-IR spectra of CO (¹²CO and ¹³CO) adsorbed on $[\text{Cu}(\text{mipt})]$ were collected to probe the nature of the active sites in the solid with the results suggesting formation of mono-CO species on the Cu center inside the cavity of the desolvated coordination polymer.

Curini and co-workers reported a zirconium sulfophenyl phosphonate for heterogeneous catalysis of a variety of synthetic reactions.⁹⁸ The catalyst was prepared as an amorphous solid containing zirconium phosphate layers with acidic sulfonic groups pointing to the interlayer spaces. The solid proved quite versatile as a heterogeneous Brønsted acid catalyst in several reactions, including preparation of cyclic ketals and thioketals,⁹⁹ pyrroles,^{100,101} and β -amino alcohols¹⁰² as well as protection of alcohols and phenols,^{103–105} etc.^{106–108} The protocols are generally attractive for the features of mild reaction conditions, simple workup, and recyclable nature of the catalysts.

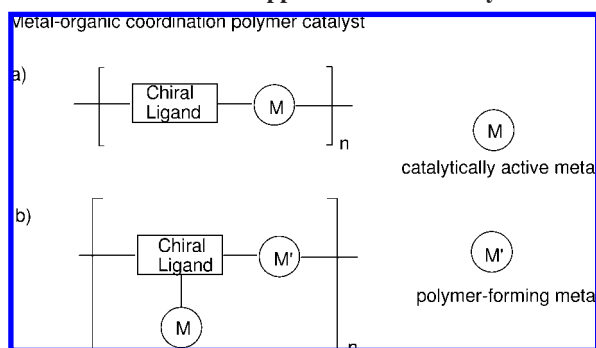
Kim and co-workers reported that the zinc(II) coordination polymer $[\text{Zn}(\text{Hdpa})(\text{H}_2\text{O})_2(\text{SO}_4)]$ (Hdpa = 2,2'-dipyridylamine) was effective as a heterogeneous catalyst for the transesterification reaction of esters by methanol.¹⁰⁹ Treatment of *p*-nitrophenyl acetate with methanol in the presence of the polymer (4 mol %) at room temperature produced quantitatively the corresponding product methyl acetate within 7 days. According to the report, the catalyst was recovered and reused 10 times without deterioration of the activity. Some metal and/or ligand leaching may have occurred during the reaction since the filtrate showed about 20% conversion within the same time interval.

Szeto, Bordiga, and co-workers reported the synthesis and characterization of two heterobimetallic Pt-containing MOFs with empirical formulas of $[(\text{BPDC})\text{PtCl}_2]_3[\text{M}(\text{H}_2\text{O})_3]_2 \cdot 5\text{H}_2\text{O}$ (BPDC = 2,2'-bipyridine-5,5'-dicarboxylate, M = Gd or Y).^{110–112} Both coordination polymers have been well characterized and were thermally rather stable (up to 400 or 350 °C for the MOF containing Y or Gd, respectively). X-ray single-crystallographic analyses indicated that the compounds share a notable structural feature in that the Pt centers are coordinated to Cl and the N atoms of the BPDC unit, giving a local environment that is reminiscent of that found in some molecular Pt complexes with catalytic activity toward C–H bond cleavage of alkanes. Such a feature led the authors to propose that these heterobimetallic coordination polymers can be viewed as heterogeneous counterparts to the corresponding homogeneous Pt complex catalyst and thus may serve as potential heterogeneous Pt catalysts. However, to our knowledge, the catalytic activities of these polymers have not been reported yet.

3. Self-Supported Chiral Catalysts

3.1. Background

Asymmetric catalysis to provide enantiomerically enriched chiral chemicals is of broad current interest to both academia and industry. Extensive research in this area over the past

Scheme 32. Schematic Representation of the Two Methods for Construction of Self-Supported Chiral Catalysts


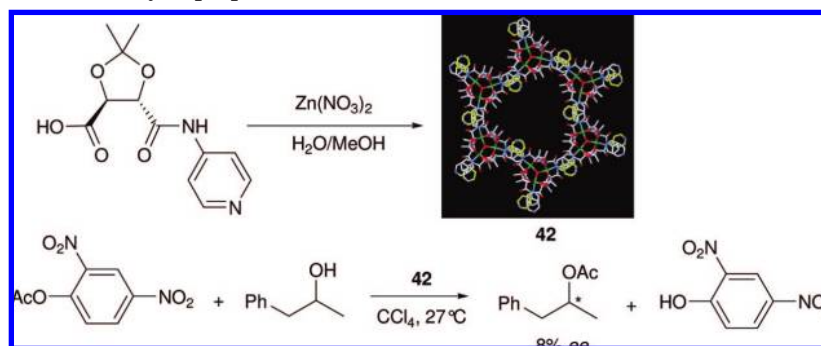
several decades has led to the successful development of numerous efficient chiral catalysts, which have demonstrated high enantioselectivity in a broad range of homogeneous asymmetric catalytic reactions.^{113–117} Despite this fact, however, further development of the asymmetric catalytic reactions into practical industrial processes still remains a challenging task.^{7,118} A major reason is that both the chiral ligands and the metal for making the chiral catalysts are very expensive; therefore, systems that allow for their easy recovery and efficient recycling would be highly desirable. This is especially true and important for large-scale industrial production but unfortunately is usually difficult to achieve in a homogeneous catalytic process. Furthermore, potential contamination of the products by metal leaching in a homogeneous reaction is particularly unacceptable for pharmaceutical production. For these reasons, a number of approaches to immobilize homogeneous asymmetric catalysts for heterogeneous enantioselective reactions have been developed, most frequently by anchoring the chiral catalyst to a support which can be either an inorganic solid or an organic polymer.^{5,119–123}

Within the past decade, some homochiral metal–organic coordination polymers (or oligomers) have been examined as a new type of immobilized chiral catalysts, which demonstrated high enantioselectivities in several types of heterogeneous asymmetric catalytic reactions. These catalysts are typically produced via self-assembly of the chiral bridging ligands with metal ions by coordination bonds to afford homochiral solids which may provide the chiral environment necessary for asymmetric induction. While the basic concept is to transform a homogeneous molecular catalyst into a polymeric one by taking advantage of the cross-linking property of the bridging ligand, there are two variations to incorporate the active sites into the polymeric scaffold. One variation is to incorporate the catalytically active metal centers directly into the main backbone of the homochiral solid (Scheme 32a), which can be obtained by direct alternating copolymerization of the enantiopure bridging ligands and the catalytic metals. In such a case the metal plays the dual role as both the structural binders and the active sites in the resulting solid. For a catalytic application without an extensive breakdown of the polymer the metal should be capable of bonding simultaneously with at least two bridging ligand moieties and still with vacant or labile sites available for substrate coordination. From this perspective, the method might be more suitable for reactions with transition states containing two or more ligands. By tailoring the spacer and chiral units in the self-supported chiral catalysts, enantioselectivity and other useful properties can be fine tuned for the targeted reactions.

The other variation also uses chiral polyfunctional ligand as the linker and metal ion or cluster as the node to construct a homochiral metal–organic polymer with the exception in that the active sites are located as pendant auxiliaries on the backbone of the resulting solid (Scheme 32b). Two distinct types of metals are generally employed: one being responsible for structure assembly and the other for catalytic activity. The chiral bridging ligand should contain at least two types of orthogonal functional groups: one for network formation by interaction with the structural metal ions and the other for attachment of the catalytic centers. This type of catalyst is generally obtained by stepwise generation of the network and subsequent uploading of catalytically active metals (or vice versa). In some cases, porous homochiral metal–organic assemblies with uniform active sites can be obtained.

Despite the conceptual simplicity, the first demonstration of using homochiral metal–organic polymers for enantioselective catalysis was not reported until in 2000 by Kim and co-workers.¹²⁴ The study was initiated by a motivation to develop chiral porous materials and explore their applications. It is noteworthy that in spite of the tremendous efforts over the past decades little progress has been made in the development of chiral zeolites, presumably as a result of some inherent limitations in zeolite synthesis (e.g., harsh conditions). New strategies are therefore needed to prepare chiral zeolitic materials, employing relatively mild synthetic conditions in order to retain the subtle chiral information throughout the process. From this point of view, metal–organic coordination polymers seem to be a viable option for making chiral porous solids.¹²⁵ Compared to inorganic zeolites, the metal–organic polymers are generally synthesized under much milder conditions. This would in principle allow for faithful incorporation of chiral properties into the solid simply by use of an appropriately designed chiral polytopic ligand. To demonstrate the validity of this idea, Kim and co-workers designed an enantiopure chiral bridging ligand which is derived from tartaric acid and contains both carboxylic and pyridyl groups as the coordination sites (Scheme 33). Treatment of the ditopic ligand with $\text{Zn}(\text{NO}_3)_2$ in $\text{H}_2\text{O}/\text{MeOH}$ led to isolation of a crystalline homochiral coordination polymer, $\{[\text{Zn}_3\text{O}(\text{L})_6] \cdot 2\text{H}_3\text{O} \cdot 12\text{H}_2\text{O}\}_n$ (**42**) ($\text{L} = 4$ -aminopyridine amide derivative of tartaric acid, see Scheme 33). X-ray single-crystal structural analysis revealed that large triangular-shaped chiral 1D channels with a side length of approximately 13.4 Å are present in the homochiral porous solid **42**. Remarkably, some uncoordinated pyridyl groups are found dangling toward the interiors of the channel walls and thus might be usable for Lewis-base catalysis. **42** was tested as a heterogeneous catalyst in the transesterification, and a kinetic resolution effect was observed in the reaction of racemic 1-phenyl-2-propanol (Scheme 33). Although the resulting ee value of the corresponding ester is only modest (~8%), the work demonstrated for the first time the feasibility of using a homochiral metal–organic polymer for enantioselective heterogeneous catalysis.

This proof-of-concept work of Kim has triggered some further research activities in using a homochiral metal–organic hybrid solid constructed from molecular building blocks as a heterogeneous catalyst in asymmetric synthesis. The work published before 2006 has been partially covered in recent reviews by Lin,^{126–128} Ding,^{129,130} and Sasaki¹³¹ and highlighted by Dai.¹³² Beyond catalysis, porous homochiral coordination polymers have also begun to show potential in enantioselective

Scheme 33. Synthesis of Homochiral Coordination Polymer 42 and Its Catalytic Application in Enantioselective Transesterification of Racemic 1-Phenyl-2-propanol^a


^a Figure of **42** was reprinted with permission from ref 124. Copyright 2000 Macmillan Publishers Ltd.

lective separation of racemic organic molecules.^{133,134} The ensuing discussions are focused on the enantioselective catalytic performance using such a solid with case studies being categorized according to reaction types.

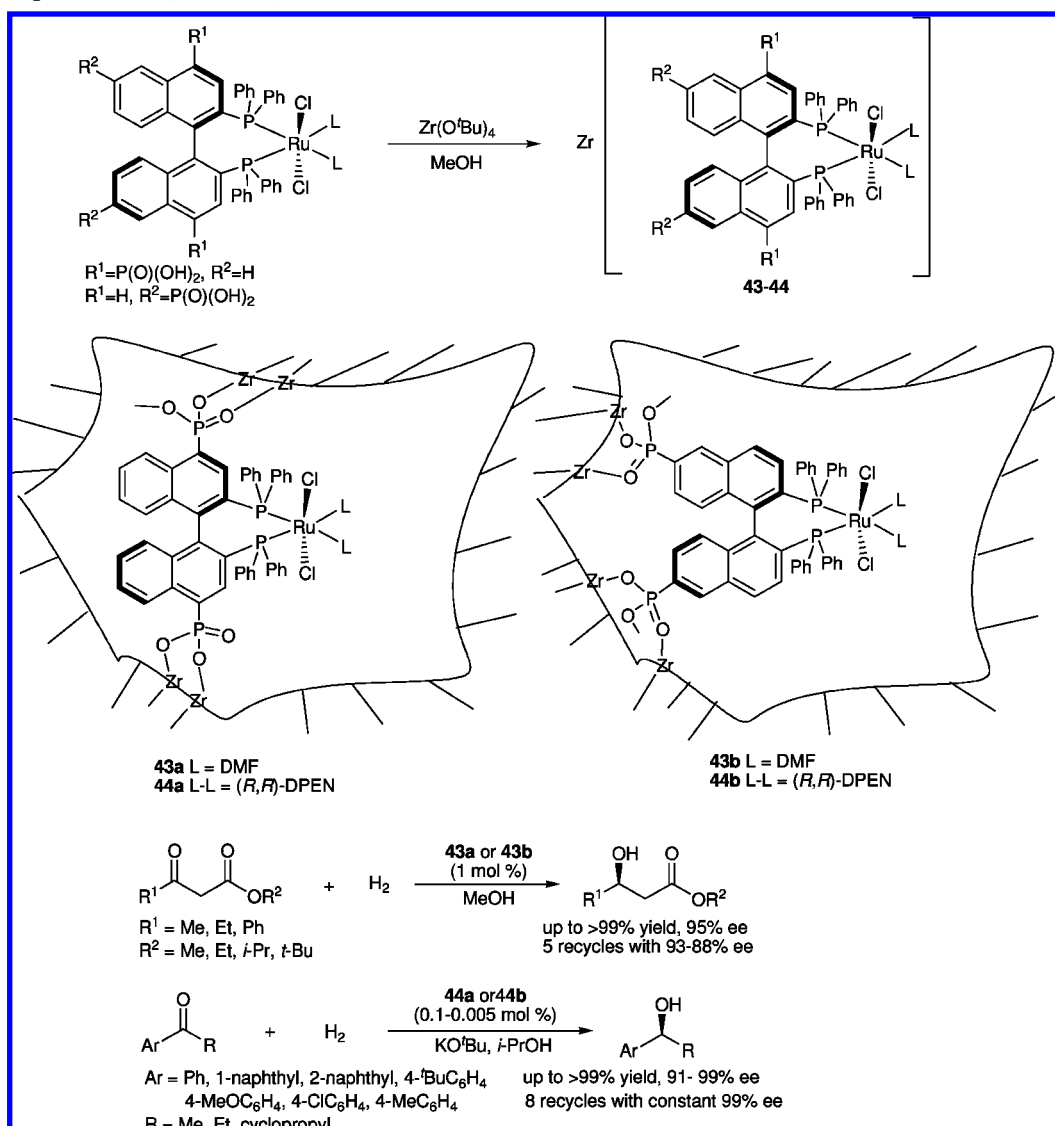
3.2. Enantioselective Hydrogenation

Lin and co-workers reported the use of chiral porous zirconium phosphonates containing Ru–BINAP¹³⁵ [BINAP = 2,2'-bis(diphenylphosphino)-1,1'-binaphthyl] moieties as highly enantioselective heterogeneous catalysts for hydrogenation of β -keto esters.¹³⁶ The molecular version of Ru–BINAP has been developed by Noyori as an extremely successful and versatile chiral catalyst¹³⁷ and is one of the most privileged targets for chiral catalyst immobilization.¹²² Therefore, in Lin's work Ru–BINAP was considered appropriate to highlight the potential of chiral hybrid solids containing catalytic units immobilized using a molecular building-block approach in heterogeneous asymmetric catalysis. Furthermore, the authors envisaged that metal phosphonates containing pendant chiral chelating bisphosphanes can be designed, which may combine the robustness of a metal phosphonate framework with enantioselectivity of the metal complex, to obtain a highly enantioselective heterogeneous catalyst. The chiral zirconium phosphonates **43a,b** were obtained as amorphous solids by refluxing the Ru(II)-containing bisphosphonic acid species with $\text{Zr}(\text{O}^i\text{Bu})_4$ in methanol (Scheme 34). Although the amorphous nature precludes an exact structure elucidation, the solids have been characterized by microanalysis, thermogravimetric analysis, XRPD, SEM, and IR spectroscopy. In addition, nitrogen adsorption measurements indicated that both solids are highly porous with wide pore size distributions. **43b** was shown to be a highly enantioselective catalyst in the asymmetric hydrogenation of the β -keto esters (Scheme 34) with enantioselectivity (ca. 70–95% ee) comparable to that of its homogeneous counterpart Ru–BINAP. However, **43b** was found to be somewhat less reactive than its homogeneous analogue, a common phenomenon often observed for an immobilized catalyst. **43a** displayed much inferior enantioselectivity (ca. 16–79% ee) for hydrogenation of same substrates, suggesting that the catalytic performance of such kinds of hybrid solids should in principle be tunable. **43b** was reused for five runs with only slight deterioration of enantioselectivity (ca. 93–88% ee) in the hydrogenation of methyl acetoacetate, and less than 0.01% ruthenium leaching was detected for each run. The heterogeneous nature of catalysis was further confirmed by the inactivity of the supernatants from the reaction system. Finally, it is note-

worthy that the two metals function differently in these hybrid catalysts with zirconium being responsible for network formation and ruthenium for catalysis, respectively.

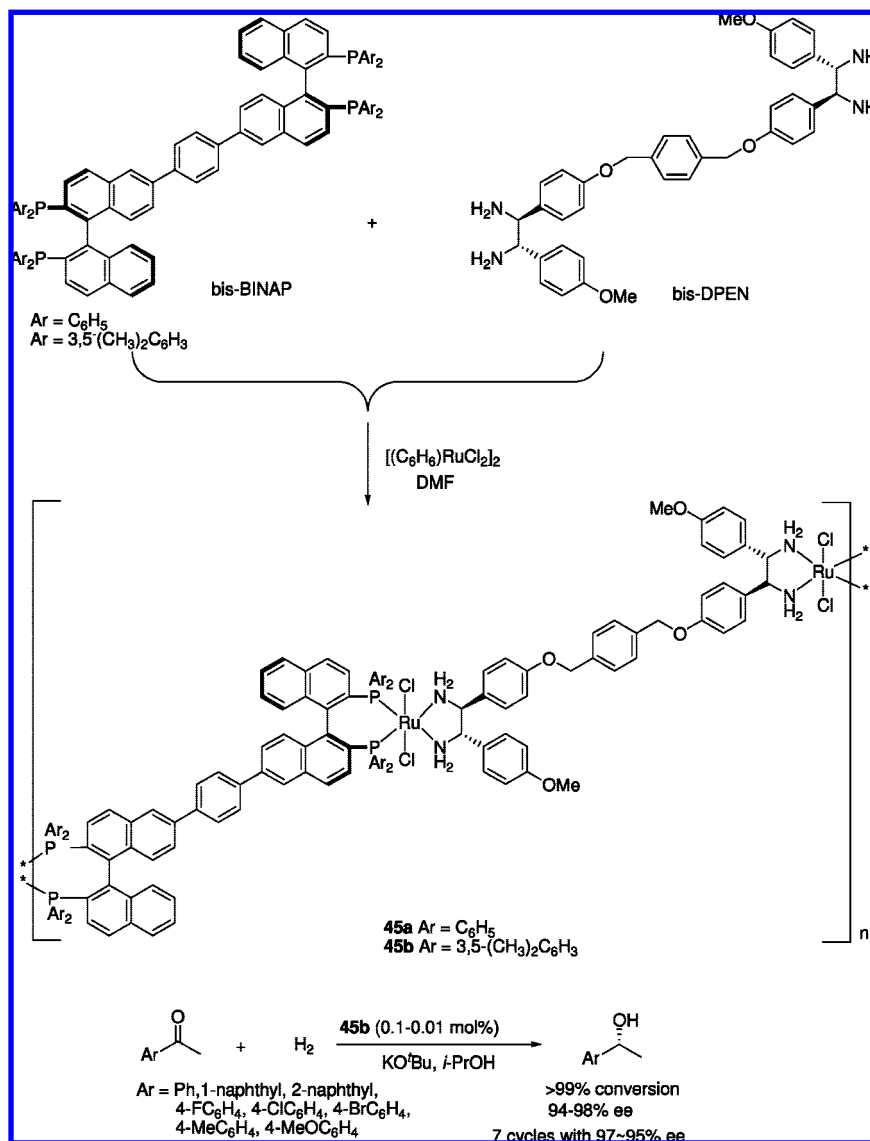
Lin and co-workers further extended the strategy to the preparation of similar chiral porous Zr phosphonates (**44a,b**) with the built-in Ru–BINAP–DPEN^{138,139} (DPEN = 1,2-diphenylethylenediamine) entities as active sites in the hybrid solids (Scheme 34).¹⁴⁰ **44a,b** were prepared and characterized in a way similar to that of **43a,b** and were also found to be amorphous porous solids with relatively high BET surface areas. Catalyst **44a** exhibited excellent performance in the asymmetric hydrogenation of aromatic ketones (Scheme 34), affording the corresponding secondary alcohols in high enantioselectivity (90.6–99.2% ee) with 0.1 mol % catalyst loading. In particular, in the hydrogenation of acetophenone catalyst **44a** afforded 1-phenylethanol with an ee (96%) superior to that obtained with its parent homogeneous complex Ru–BINAP–DPEN (ca. 80%) under the testing conditions. Moreover, catalyst **44a** was remarkably active in the hydrogenation of 1-acetonaphthone, attaining a TOF value of 500 h^{-1} at full conversion with a product ee of 98.6%. Although catalyst **44b** was also highly active, it generally gave lower ee values than those of **44a** in the same reactions. Both **44a** and **44b** were shown to be reusable in the asymmetric hydrogenation of 1-acetonaphthone. Especially noteworthy is that catalyst **44a** was reused up to eight times without any loss of enantioselectivity (all 99% ee), albeit with some loss of activity in the last two runs, presumably owing to poisoning of the ruthenium hydride species by oxygen in air during the catalyst recovery process.

Ding and co-workers demonstrated that self-supported chiral catalysts **45a,b**, which contain repeating units featuring Noyori's Ru–BINAP–DPEN catalyst, were highly enantioselective in the heterogeneous asymmetric hydrogenation of aromatic ketones (Scheme 35).¹⁴¹ A programmed assembly of two enantiopure ditopic bridging ligands, the bis-BINAP and bis-DPEN, with ruthenium ions of $[(\text{C}_6\text{H}_6)\text{RuCl}_2]_2$ led to formation of **45a,b**. Both solid products were characterized by a variety of analytical techniques including elemental C/H/N/Cl/P and Ru analyses, FT-IR, ³¹P CP/MAS NMR, XRPD, and SEM. However, the amorphous nature of **45a,b** prevents a further detailed elucidation of their exact microstructures. **45a,b** were tested as self-supported chiral catalysts for asymmetric hydrogenation of aromatic ketones with excellent enantioselectivity (94–98% ee) being attained for reactions with catalyst **45b** (Scheme 35). **45a** performed less impressively, affording a product ee of 78.2% in the hydrogenation of acetophenone, comparable to that obtained with molecular

Scheme 34. Enantioselective Hydrogenation of β -Keto Esters and Aromatic Ketones Catalyzed by Ru-Bearing Chiral Porous Zirconium Phosphonates 43a,b and 44a,b


Ru-BINAP-DPEN catalyst under similar conditions. The heterogeneous nature of catalysis was confirmed in the hydrogenation of acetophenone with catalyst **45b**, as the supernatant of the catalyst in 2-propanol did not show any further reactivity. Moreover, Ru leaching to the organic phase was not detected (<0.1 ppm). Finally, catalyst **45b** was reusable in the hydrogenation of acetophenone. After completion of the reaction, the catalyst was recovered by simple filtration under argon and reused for up to seven runs without significant loss in enantioselectivity or activity. Although impressive in terms of the catalytic performance, the procedure is still plagued by the somewhat tedious preparation of the ditopic ligands both in enantiopure forms. In a subsequent paper, Ding and co-workers reported a modification of the strategy using achiral bridged bis-BIPHEP-type ligands [BIPHEP = 2,2'-bis(diphenylphosphino)-1,1'-biphenyl] together with enantiopure bis-DPEN for assembly of heterogenized Noyori-type catalysts.¹⁴² Moderate to good ee values were obtained in the asymmetric hydrogenation of aromatic ketones with the resulting chiral solids as the catalysts, implying that subtle variation in the structural component of a self-supported catalyst may significantly affect its chiral induction capability.

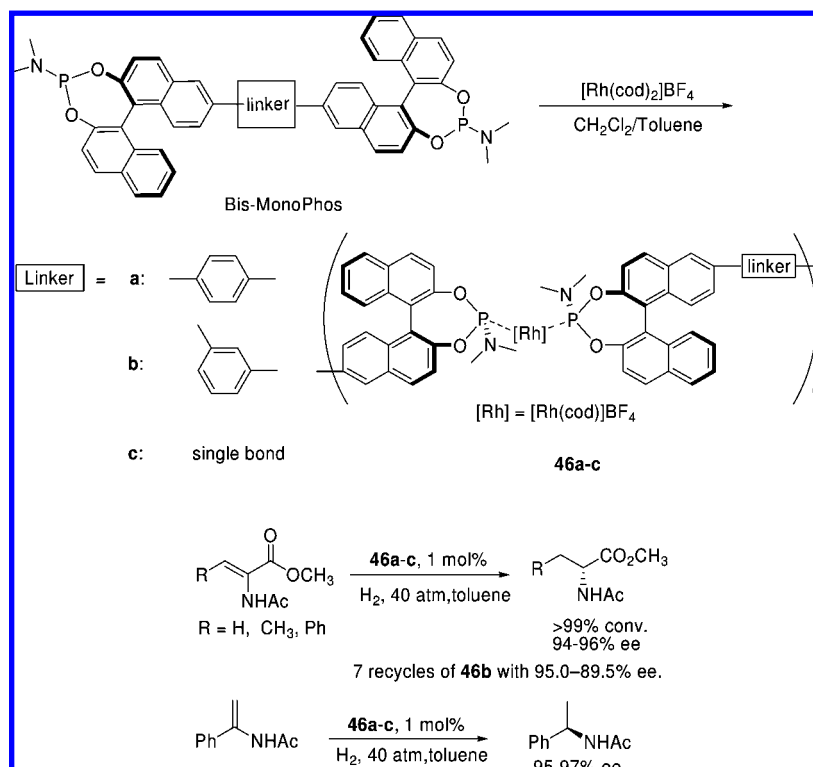
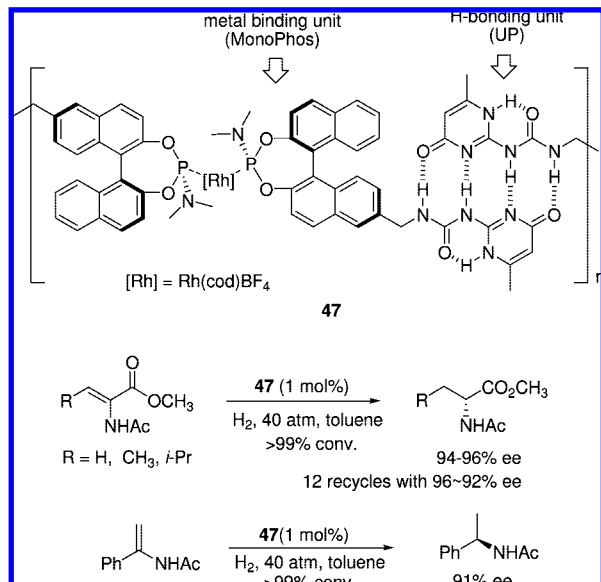
Ding and co-worker demonstrated a successful immobilization of Feringa's MonoPhos/Rh catalyst^{143,144} via a self-supporting strategy for heterogeneous enantioselective hydrogenation of prochiral olefins such as dehydro- α -amino acid esters and enamides.¹⁴⁵ On the basis of the mechanistic understanding that two monodentate phosphorus ligands can be involved in bonding with Rh in the active species, Ding designed ditopic bis-phosphoramidites (Bis-MonoPhos) with the expectation that on coordination with a Rh(I) precursor the catalytically active P-Rh-P units could be spontaneously incorporated into the resulting insoluble polymeric (or oligomeric) assemblies. Treatment of the ditopic bis-phosphoramidites (Bis-MonoPhos) in toluene with a solution of [Rh(cod)]BF₄ in dichloromethane resulted in immediate precipitation of Bis-MonoPhos/Rh-containing solids **46a-c** (Scheme 36). XRPD indicated that these solids are amorphous, thus precluding a detailed analysis of their precise structures. Data from microanalysis were consistent with the proposed structures, while SEM images showed that these solids are composed of micrometer particles. Asymmetric hydrogenation of several representative prochiral olefins was carried out in toluene, wherein the chiral self-supported catalysts **46a-c** were found to be insoluble (Scheme 36).

Scheme 35. Programmed Assembly of Heterogenized Noyori-Type Catalysts 45a,b for Enantioselective Hydrogenations of Aromatic Ketones


Consistently excellent ee values (around 95%) were obtained with each catalyst for hydrogenation of all examined olefinic substrates, including β -aryl- or alkyl-substituted dehydro- α -amino acid and enamide derivatives (Scheme 36). In particular, in the asymmetric hydrogenation of the enamide all three catalysts gave ee values (95–97%) higher than that of their homogeneous counterpart (89% ee). Catalysis was confirmed to be heterogeneous in nature as the supernatant of the catalyst **46b** was shown to be inactive for catalysis of hydrogenation of methyl 2-acetamidoacrylate ($\text{R} = \text{H}$, Scheme 36). Furthermore, the rhodium leaching and phosphorus concentration in organic phase were both determined to be negligible after reaction. In the hydrogenation of methyl 2-acetamidoacrylate catalyst **46b** was recovered by filtration under argon and reused for seven runs with full conversion and a slight decrease in enantioselectivity (95–89.5% ee). These data have undoubtedly substantiated the validity of the “bottom-up” design strategy; however, little information is available so far with regard to the exact distribution of the active sites in the self-supported catalysts. Interestingly, Wong and co-workers also reported the catalytic activity of the Rh(I) complex with a chiral ditopic bis-phosphoramidite ligand bearing the tetraphenylene core in the asymmetric

hydrogenation of some acetamidocinnamate derivatives.¹⁴⁶ With 1 mol % loading of catalyst, up to 99.0% ee and 100% conversion could be achieved for reactions performed in dichloromethane. However, it seems that the reaction proceeds in a homogeneous manner.

For construction of homochiral metal–organic polymers covalent linkers are usually used to incorporate the coordinating chiral subunits into the bridging ligand. Ding and co-workers demonstrated that noncovalent interactions such as hydrogen bonding can be employed as an alternative way to generate the polytopic ligand and furthermore construct chiral supramolecular metal–organic catalyst effective for asymmetric hydrogenation of some prochiral olefins.¹⁴⁷ By taking advantage of the well-known self-complementary property of the hydrogen-bonding unit Ureido-4[1*H*]-ureidopyrimidone (UP), a bis-MonoPhos ligand with H bonding as the linkage was obtained which upon treatment with $[\text{Rh}(\text{cod})_2]\text{BF}_4$ afforded the supramolecular metal–organic polymer **47** as a precipitate in toluene (Scheme 37). It is worth noting that in this case the hydrogen-bonding and ligand-to-metal coordination interactions are orthogonal to each other as evidenced by ^1H NMR studies, thus ensuring an ordered alternating self-assembly and proper function of

Scheme 36. Heterogeneous Catalysis of Enantioselective Hydrogenation of Prochiral Olefins with Self-Supported MonoPhos/Rh Catalysts 46a–c**Scheme 37. Supramolecular Metal–Organic Polymer 47 for the Heterogeneous Catalysis of Asymmetric Hydrogenation of Prochiral Olefins**

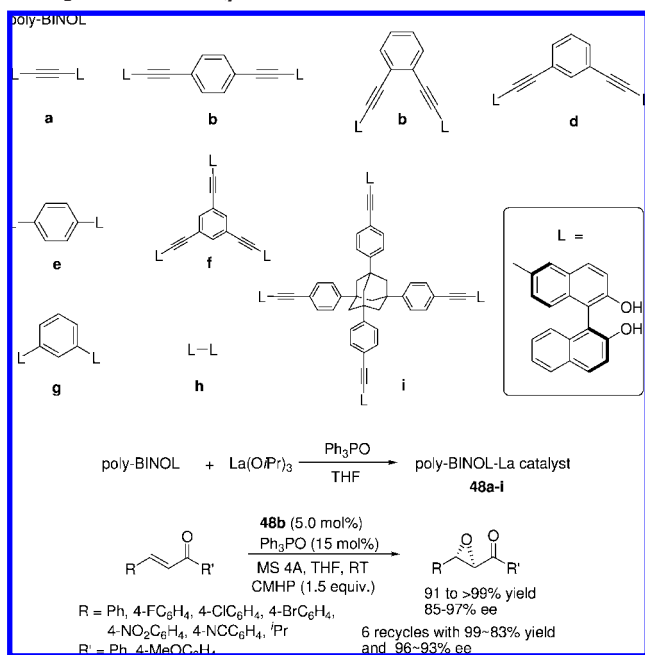
the resulting supramolecular polymer. Microanalysis (C, H, N, P) indicated that the composition of **47** is consistent with its expected structure, while XRPD showed it is an amorphous solid. Solid-state ³¹P CP-MAS NMR studies illustrated a similar coordination pattern in **47** as that of its parent MonoPhos/Rh(I) complex. FTIR revealed the UP functionalities are dimerized in the keto tautomer in **47**. The chiral supramolecular metal–organic polymer **47** demonstrated excellent asymmetric induction in the heterogeneous hydrogenation of dehydro- α -amino acid derivatives and *N*-(1-phenylvinyl)acetamide in toluene, affording the corresponding products in enantioselectivity (91–96% ee) comparable

to that of its homogeneous counterpart. The supernatant of **47** did not result in further hydrogenation of the substrate under otherwise identical experimental conditions, unambiguously confirming the heterogeneous nature of the present catalytic system. Furthermore, no metal leaching into the organic phases was detected (<1 ppm) by inductively coupled plasma (ICP) spectroscopic analysis. The filtration-recovered catalyst was reusable in the hydrogenation of (*Z*)-methyl 2-acetamidobut-2-enoate, affording full conversion and nearly constant enantioselectivity (96–92% ee) for 10 reaction cycles within a standard reaction period of 20 h. However, reaction profile measurements showed that catalyst reactivity declined with consecutive runs, presumably as a result of partial catalyst decomposition during catalyst recovery.

3.3. Enantioselective Oxidations

3.3.1. Enantioselective Epoxidation

In the immobilization of chiral catalysts with metal–organic coordination polymers the stereochemical properties of the bridging ligand can exhibit a profound influence on the enantioselectivity and activity of the targeted catalytic reaction. Such an effect has been studied by Ding and co-workers in the heterogenization of Shibasaki's BINOL/La^{148,149} (BINOL = 1,1'-bi-2-naphthol) catalyst for enantioselective catalysis of epoxidation of α,β -unsaturated ketones.¹⁵⁰ A collection of poly-BINOL ligands with various linker geometries, including linear, bent, trigonal-planar, as well as tetrahedral spacers, were treated with La(O^{*i*}Pr)₃ in THF to afford the poly-BINOL/La assemblies (**48a–i**) as amorphous precipitates, which were subsequently tested as self-supported chiral catalysts in the enantioselective epoxidation of α,β -unsaturated ketones in THF with cumene hydroperoxide (CMHP) as the oxidant (Scheme 38). In the reaction

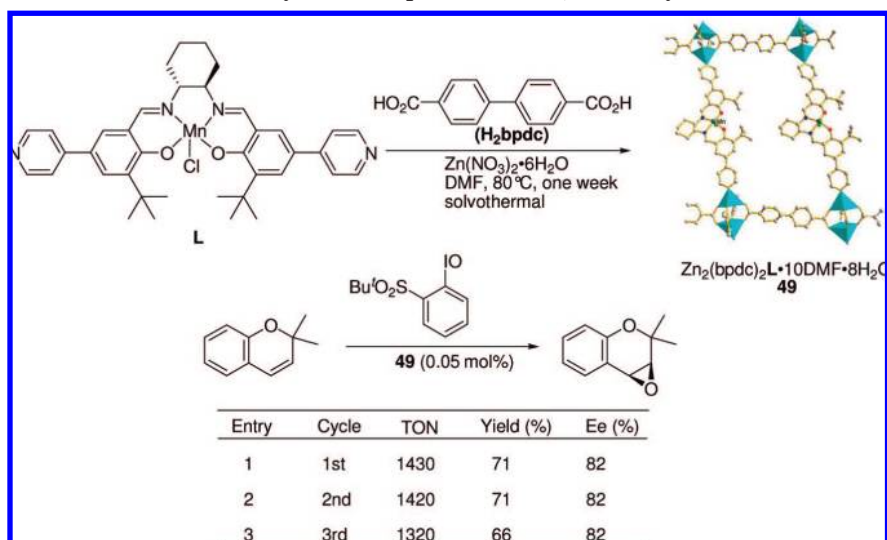
Scheme 38. Self-Supported Shibasaki's BINOL/La Catalysts for Epoxidation of α,β -Unsaturated Ketones


of chalcone ($R = R' = \text{Ph}$) catalyzed with **48a-i** the enantioselectivity exhibited a significant dependence on the length or angle of the spacer in the poly-BINOL ligands (82–95% ee). The data suggested that polytopic ligands with similar bonding units but different linker geometries may give rise to coordination assemblies with distinct microenvironments, which in turn can exert some impact on their catalytic behavior, such as the chiral induction capability. Therefore, the spacer in the polytopic ligand should also be considered as an important element to tune the catalytic properties of coordination polymers. Screening coordination polymers **48a-i** for catalysis revealed that **48b** was optimal, which was further examined in the epoxidation of a variety of α,β -unsaturated ketones (Scheme 38). The corresponding α,β -epoxy ketones were obtained in excellent yields (91–99%) with a high level of enantioselectivity (84–97% ee) comparable to their homogeneous counterpart under the testing conditions. Catalysis was demonstrated to be heterogeneous in nature since the supernatant of **48b** in THF was found to be completely inactive for catalysis of epoxidation of the chalcone ($R = R' = \text{Ph}$). ICP spectroscopic analysis of the above-mentioned supernatant indicated that the concentration of La(III) is negligible (0.093 ppm), supporting the heterogeneous nature of this catalyst system. In the epoxidation of the chalcone catalyst **48b** was readily recovered by simple filtration under argon after completion of the reaction. The recovered catalyst was reused for five cycles without significant loss of enantioselectivity (93–96% ee), albeit at a cost of slightly reduced activity in the last two runs. Lanthanum leaching in each cycle during catalyst reuse was determined to be less than 0.4 ppm, suggesting the catalyst is quite robust under the testing conditions.

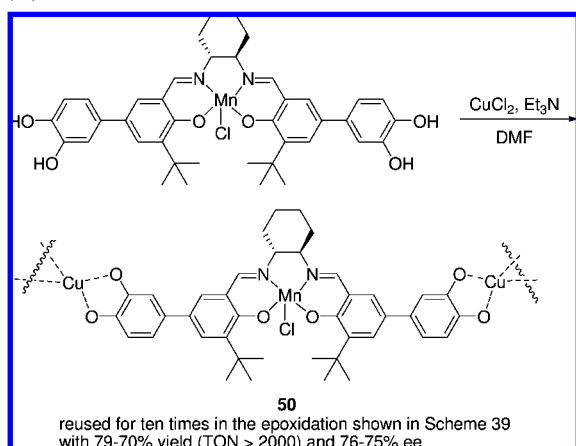
Nguyen, Hupp, and co-workers reported an interesting example of using a microporous MOF compound for heterogeneous catalysis of asymmetric olefin epoxidation (Scheme 39).¹⁵¹ In this case, a metalloligand with the chiral Salen-Mn moiety as a spacer and two terminal pyridyl groups as ligating units was used as the ditopic bridging ligand. Treatment of this functionalized metalloligand with zinc salt and biphenyldicarboxylic acid (H_2bpdC) in DMF

under solvothermal conditions afforded a crystalline solid with the formula of $\text{Zn}_2(\text{bpdC})_2\text{L} \cdot 10\text{DMF} \cdot 8\text{H}_2\text{O}$ (**49**, Scheme 39). Single-crystal X-ray structural analysis revealed that **49** contains a pair of interpenetrating networks, constructed by pillaring the dimeric zinc tetracarboxylate paddlewheels by the zinc–pyridine bonding with the metalloligand. As a result, two types of channels with dimensions of 6.2×15.7 and $6.2 \times 6.2 \text{ \AA}^2$, respectively, were occupied by the solvent molecules in the crystal. Remarkably, all Mn^{III} sites are accessible to the guest molecules that can be accommodated in the channels of **49**. The catalytic activity of **49** was tested in the enantioselective epoxidation of 2,2-dimethyl-2H-chromene using 2-(tertbutylsulfonyl) iodosylbenzene as the oxidant with the homogeneous counterpart L as the reference catalyst for comparison. Remarkably, reaction profile measurements revealed that the framework-immobilized catalyst **49** retained nearly constant reactivity during a 3 h reaction period, attaining a total turnover number of more than 3500. In contrast, the homogeneous analogue (L) of **49** lost much of its activity after the first few minutes in the epoxidation. Such a marked stability enhancement of the immobilized catalyst was ascribed to the confinement effect of the framework, which would suppress catalyst degradation by preventing deactivating encounters of active species. Beyond catalytic activity, the enantioselectivity of **49** was also remarkable, affording the corresponding epoxide with an ee value (82%) only slightly lower than that of its homogeneous counterpart (88%). Catalyst **49** recovered by centrifugation after reaction was shown to be reusable, giving the product in constant ee values for three cycles with some decrease in the yield of the third run. Although some manganese was found to leach into the solution during recycles (4–7% per cycle), either as molecular species or as fine particles, reaction profile measurements of the supernatant of **49** showed that the dissolved manganese did not catalyze the reaction. Finally, notable substrate size selectivity was observed in a competitive reaction of two olefins, indicating epoxidation occurred predominantly inside the channels.

Nguyen and Hupp et al. reasoned that fragmentation of MOF particles and loss of catalyst during recycle of **49** in the epoxidation could be caused by the relative weakness of the Zn(II)–N(pyridine) single bond and stronger chelate-type metal–ligand linkages might be used to overcome this problem. Therefore, [bis(catechol)salen]Mn(III) (Scheme 40), a chiral metalloligand capable of forming chelate-type metal–ligand linkages, was used as a building unit in construction of a series of coordination polymers that can be used as catalysts.¹⁵² Reaction of [bis(catechol)salen]Mn(III) with several di- and trivalent metal ions [Cu(II), Cr(III), Mn(II), Fe(III), Co(II), Ni(II), Zn(II), Cd(II), or Mg(II)] resulted in immediate precipitation of the corresponding metal-linked (salen)Mn coordination polymers as amorphous powders. Subsequently, the polymers were examined as self-supported catalysts for catalytic asymmetric epoxidation of 2,2-dimethyl-2H-chromene, affording the product in varying yields (22–89%) and ee values (20–76%). Especially noteworthy is the catalysis with the Cu-linked Salen–Mn polymer **50** (Scheme 40), which was reused up to 10 times with a slight decrease in activity (79–70% yield) and no loss in enantioselectivity (75–76% ee). Comparison of the reaction profiles of insoluble catalyst **50** and its homogeneous counterpart revealed a slower initial rate for the former; however, the total turnover number (2000 within 3 h) with catalyst **50** is considerably larger than that with the homo-

Scheme 39. Homochiral salen–Mn MOF for Asymmetric Epoxidation of 2,2-Dimethyl-2H-chromene^a

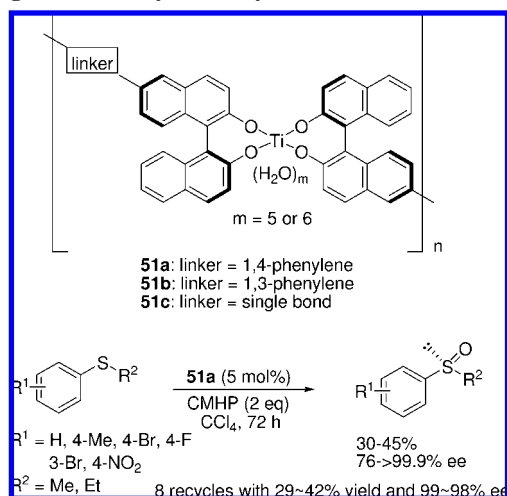
^a The cyan polyhedra in **49** represent the pyramidal coordination geometry around each Zn(II) ion.

Scheme 40. Generation of Self-Supported salen–Mn Catalyst **50** by Coordination of the Bidentate Catechol with Cu(II)

geneous one, which quickly lost much of its activity after the first few minutes. The authors noted that although **50** is highly stable under laboratory synthetic scale, it is not immortal and can eventually be degraded under highly oxidative environments. Additionally, a noticeable amount of Cu/Mn leaching (4.7% and 3.1%) was detected during the first two recycles, presumably caused by the Cu(II) ions and the metalloligand that were weakly bound or entrapped in the polymer matrix of **50**.

3.3.2. Enantioselective Sulfoxidation

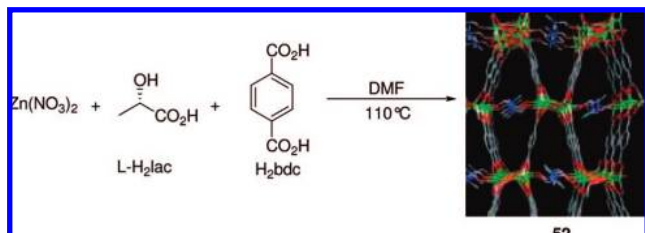
Some variants of the homochiral Ti–bis-BINOL coordination polymers have also been extended to the heterogeneous catalysis of asymmetric sulfoxidation reaction by Ding and co-workers (Scheme 41).¹⁵³ Treatment of the bis-BINOL ligands with an equimolar amount of Ti(OⁱPr)₄ and 40 equiv of water in CCl₄ resulted in precipitation of homochiral Ti–bis-BINOL coordination polymers **51a–c** as amorphous powders, which were examined as self-supported catalysts in the enantioselective oxidation of a variety of aryl alkyl sulfides in CCl₄ with CMHP as the oxidant. The corresponding chiral sulfoxides were obtained with extremely high ee values (96.4 to >99.9%), albeit in moderate yields (ca. 40%),

Scheme 41. Self-Supported BINOL–Ti Catalysts **51** for Heterogeneous Catalysis of Asymmetric Sulfoxidations

presumably as a result of overoxidation (Scheme 41). Remarkably, upon completion of the sulfoxidation reaction of thioanisole catalyst **51a** was readily isolated from the reaction mixture by filtration in open air. The recovered catalyst **51a** was reused for eight cycles that covered a period of more than 1 month with almost no loss of enantioselectivity (99% ee) or obvious decrease in sulfoxide yields being observed during the recycles.

Fedin, Kim, and co-workers investigated the catalytic activity of a homochiral metal–organic polymer of zinc for asymmetric oxidation of thioethers to sulfoxides.¹⁵⁴ The homochiral polymeric material, formulated as [Zn₂(BDC)(L-lac)(DMF)]·(DMF) (**52**), was obtained as crystals from a one-pot solvothermal reaction of Zn(NO₃)₂, L-lactic acid (L-H₂lac), and 1,4-benzenedicarboxylic acid (H₂BDC) in DMF (Scheme 42). Crystallographic analysis of **52** revealed a 3D metal–organic open framework structure that is neutral in charge with chiral channels of roughly 5 Å in diameter interconnected in three directions. By heating the as-synthesized material at 90 °C for 3 h some of the guest DMF molecules can be removed from the pores to give a partially evacuated **52** with permanent porosity and a somewhat sustained crystallinity. A notable size selectivity was ob-

Scheme 42. Homochiral Zn–MOF (**52**) for Catalysis of Sulfoxidation and Chromatographic Enantioselective Resolution of Sulfoxides^a



^a Reproduced with permission from ref 154. Copyright 2006 Wiley-VCH Verlag GmbH & Co. KGaA.

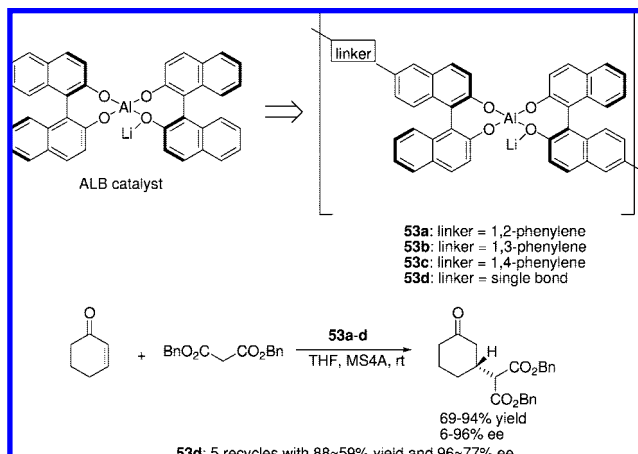
served in the oxidation of several thioethers by urea hydroperoxide (UHP) catalyzed with partially evacuated **52** (4 mol %), suggesting the reaction primarily occurs inside the micropores of the framework. Although chemoselectivity toward the sulfoxides was good to excellent, surprisingly, no asymmetric induction was observed in the catalytic sulfoxidations despite the homochiral nature of the solid catalyst. Nevertheless, aside from the size selectivity, **52** was also shown to have enantioselective sorption capability toward some racemic sulfoxides, allowing for selective enrichment of one enantiomer from the racemic mixture in the solid phase. Such an observation inspired the authors to further combine the catalytic oxidation of sulfides together with the chromatographic enantioselective resolution of the resulting sulfoxides in a one-pot process using **52** as both the heterogeneous catalyst for the reaction and the chiral stationary phase for chromatography.¹⁵⁵ The chiral chromatographic column was prepared by loading a glass tube with a suspension of **52** in 10% solution of DMF in CH₂Cl₂, and a mixture of the sulfide (PhSMe) and H₂O₂ was charged directly onto the top of the column. Using CH₂Cl₂/CH₃CN mixture as the eluent, (*R*)- or (*S*)-enantiomers of the sulfoxide (PhSOMe) could be collected separately in enantiopure form at the other end of the column. However, the mechanism with regard to the catalytic sulfoxidation using **52** is still unclear.

3.4. Asymmetric C–C Bond-Formation Reactions

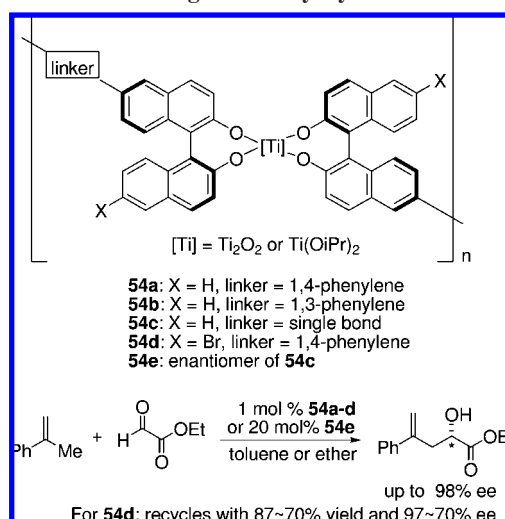
3.4.1. Michael Addition

Al–Li–bis(binaphthoxide) (ALB), a chiral heterobimetallic complex with Al and Li centers supported by two BINOLate units, can catalyze some asymmetric reactions in high efficiency and enantioselectivity.¹⁵⁶ Studies indicated that synergistic cooperation between the two types of active sites are required for the reactivity of this bifunctional catalyst; therefore, it is important to maintain the structural integrity of the active motif during immobilization of this catalyst. This is difficult to realize using a conventional immobilization approach, which usually involves random introduction of ligand onto a sterically irregular polymer backbone. On the basis of these considerations, Sasai and co-workers employed some bis-BINOL ligands in combination with LiAlH₄ and BuLi to generate insoluble aluminum-bridged homochiral polymers **53a–d** and examined their catalytic properties in the Michael reaction between 2-cyclohexenone and dibenzyl malonate (Scheme 43).¹⁵⁷ The Michael adduct was obtained in good yields and up to 96% ee (for **53d**), which is comparable to that attained with homogeneous ALB catalyst (97% ee). In contrast, an ALB

Scheme 43. Enantioselective Michael Addition Catalyzed by Al-Bridged Hybrid Polymers **53**



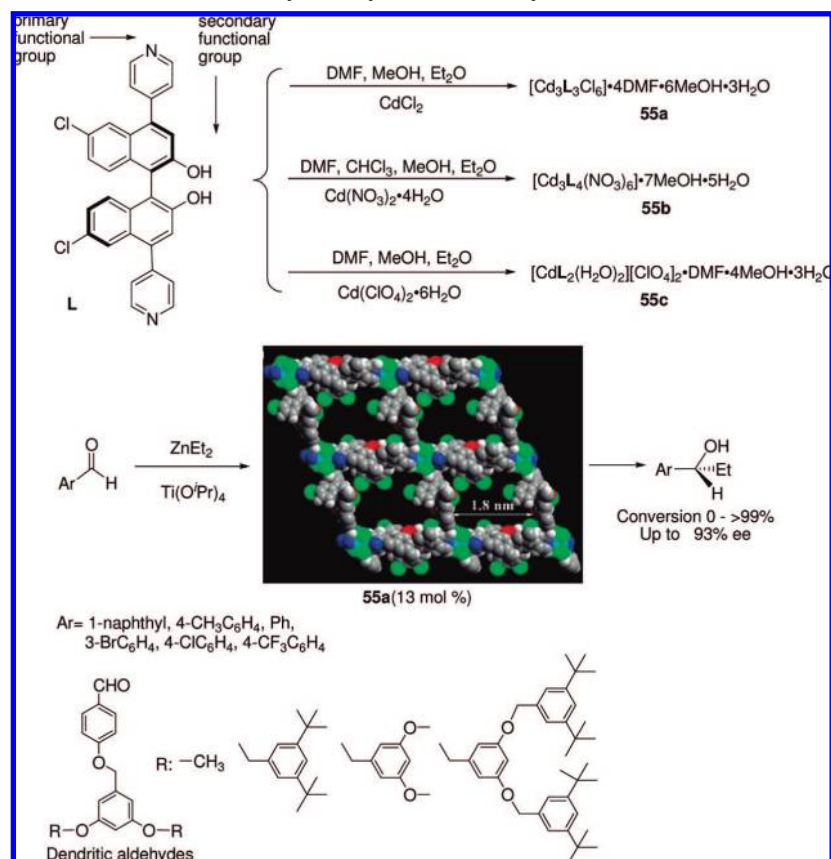
Scheme 44. Self-Supported BINOL–Ti Catalysts (**54**) for Enantioselective Heterogeneous Glyoxylate–Ene Reaction



catalyst supported on polystyrene gave the same Michael adduct in essentially racemic form. Obviously, the self-supporting strategy might be advantageous for immobilization of multicomponent asymmetric catalysts. Catalyst **53d** was recovered by syringe removal of the supernatant and reused for 5 cycles with a gradual decrease of product yields (88–59%) and ee values (96–77%).

3.4.2. Carbonyl–Ene Reaction

The research groups of Sasai¹⁵⁷ and Ding^{153,158} independently reported several homochiral bis-BINOL Ti polymers as self-supported catalysts for the asymmetric carbonyl–ene reaction. Self-assembly of bridged bis-BINOLs with Ti(O-*i*Pr)₄ in chlorinated solvents led to precipitation of chiral titanium–bis-BINOL polymers **54a–e** as amorphous precipitates, which were subsequently tested as immobilized catalysts for the carbonyl–ene reaction of α -methylstyrene with ethyl glyoxylate (Scheme 44). High yield and excellent enantioselectivity in the α -hydroxyester could be obtained for certain catalysts. Remarkably, the nature of linkers between the two BINOL units in the bis-BINOL ligands was found to profoundly influence the enantioselectivity of the catalysis, probably caused by the difference in the supramolecular structure of the assemblies. Catalyst **54d** could be recovered by simple filtration and reused up to five consecu-

Scheme 45. Homochiral MOFs **55** for Ti(IV)-Catalyzed Asymmetric Diethylzinc Addition to Aromatic Aldehydes^a

^a Figure of **55a** was reprinted from ref 159. Copyright 2005 American Chemical Society.

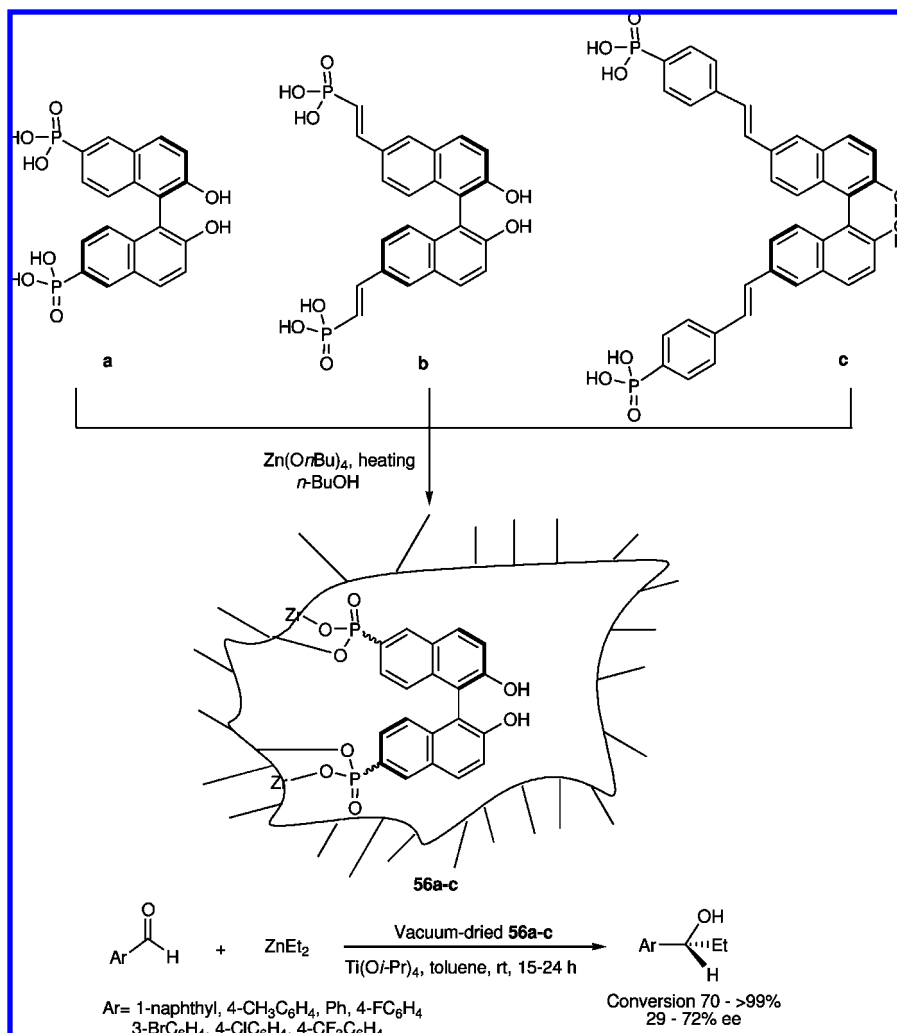
tive runs in diethyl ether. However, deterioration in yields and ee values was observed during catalyst recycling.

3.4.3. Addition of Diethylzinc to Aldehydes

Owing to the amorphous nature of most heterogeneous catalysts, a detailed elucidation of their structures is often a formidable task. Such a lack of structural understanding can severely hamper the mechanistic study of the corresponding heterogeneous catalytic process. In this respect, MOF catalyst with a high crystallinity would be advantageous not only for structure elucidation but also for the “single-site” nature of the active species in the solid. The uniformly distributed active sites in an identical microenvironment would help to understand the catalytic events in the solid phase from the molecular level and may facilitate the structure–activity relationship (SAR) study in the development of a catalyst.

Lin and co-workers investigated the synthesis and characterization of several BINOL-bearing crystalline homochiral MOF compounds **55a–c**, which in combination with excessive Ti(OⁱPr)₄ exhibited network-structure-dependent catalytic activities in the enantioselective diethylzinc addition to a range of aldehydes (Scheme 45).^{159,160} As shown in Scheme 45, the chiral bridging ligand L was designed to contain two orthogonal functionalities with the primary bipyridyl functionality being responsible for network formation and the secondary chiral BINOL functionality for attaching the active Ti(IV) unit. Interestingly, treatment of this ligand with three different Cd(II) salts afforded three crystalline coordination polymers (**55a–c**) (Scheme 45) with distinct compositions and structural features of the networks. Single-crystal X-ray diffraction studies indicated all the MOFs **55a–c** contain

chiral channels in nanometer dimensions (from 1.2 × 1.5 nm to 1.6 × 1.8 nm) with the free dihydroxy group of L ligands in the solids exposed to the open channel. After removal of the guest solvent molecules, the evacuated samples still maintained their permanent porosity as determined by CO₂ adsorption measurements. However, on uploading the evacuated **55a–c** with Ti(OⁱPr)₄ and testing the resultant solids in the asymmetric addition of diethylzinc to aldehydes, a drastic difference in their catalytic behavior was observed. While both catalysts **55a–Ti**(OⁱPr)₄¹⁵⁹ and **55b–Ti**(OⁱPr)₄¹⁶⁰ catalyzed addition of diethylzinc to a range of aromatic aldehydes with high activities and good to excellent enantioselectivities, **55c–Ti**(OⁱPr)₄¹⁶⁰ did not show any activity at all under the otherwise identical conditions. A closer re-examination of the structure of **55c** suggested that the steric crowdedness around the chiral dihydroxy groups in this compound might be held responsible for the inactivity, which was believed to prevent substitution of two isopropoxide groups in Ti(OⁱPr)₄ by the BINOL functionality on the channel walls. Although the exact reason for the reactivity difference is not yet very clear, the studies did show that the structure-dependent activity study for heterogeneous catalysis is feasible by using well-defined MOF catalysts. In the case of catalysis using **55a–Ti**(OⁱPr)₄,¹⁵⁹ the enantioselectivity was shown to be excellent and comparable to that achieved with its homogeneous counterpart BINOL–Ti(OⁱPr)₄. Besides, a remarkable substrate size-dependent reactivity was also observed in reactions of the tested aldehydes. For example, in reactions involving a series of homologous aromatic aldehydes containing Fréchet-type dendrons catalyzed by **55a–Ti**(OⁱPr)₄ the yields of addition

Scheme 46. Chiral Zirconium Phosphonate Hybrids 56-Ti(OⁱPr)₄ Catalyzed Enantioselective Diethylzinc Addition to Aromatic Aldehydes


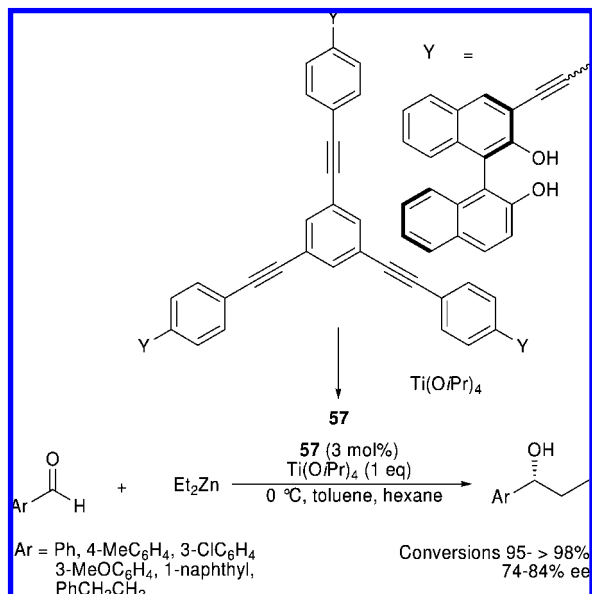
products decreased steadily with the increase of the dendron size. The data highlighted that catalysis can occur inside the chiral channels of this type of zeolite-like solids, whereby a simultaneous control of both size and stereoselectivities is possible. Although the nature of the catalysis with **55a**-Ti(OⁱPr)₄ was undoubtedly heterogeneous, no recovery/reuse of the catalyst or the framework itself was reported. Since aqueous hydrochloric acid was used for product isolation immediately after completion of the reaction, the solid catalyst probably cannot survive the hydrolytic workup.

Lin and co-workers also reported the synthesis of several chiral BINOL-bearing porous Zr phosphonates using a molecular building block approach and studied their uses in combination with Ti(OⁱPr)₄ for the heterogeneous catalysis of asymmetric additions of diethylzinc to aromatic aldehydes (Scheme 46).¹⁶¹ The zirconium phosphonates **56a-c** were obtained by refluxing the BINOL-derived bisphosphonic acids **a-c** with Zr(OⁱBu)₄ in butanol and characterized as homochiral amorphous porous solids by powder X-ray diffraction, solid-state ³¹P CP-MAS NMR, IR, TGA, adsorption measurements, and circular dichroism spectroscopy. After removal of the guest solvents by drying at 80 °C in vacuo, the evacuated hybrid polymers were treated with Ti(OⁱPr)₄ to generate active catalysts for additions of diethylzinc to aromatic aldehydes. Under relatively high solid loading (20–50 mol %), the aldehyde conversions were good to excellent but the enantioselectivity (up to 72% ee) for the

chiral secondary alcohols was significantly inferior to that of their homogeneous counterpart Ti-BINOL system. The authors believed that background reactions induced by the achiral active sites, e.g., the residual phosphonic acid protons in the Zr phosphonate solids, could be responsible for the relatively lower ee values of the adducts.

Using the molecular assembly approach, Harada and Nakatsugawa immobilized a BINOLate/Ti(OⁱPr)₄ catalyst for asymmetric addition of diethylzinc to aldehydes.¹⁶² Treatment of the chiral tris-BINOL ligand with 3 equiv of Ti(OⁱPr)₄ in CH₂Cl₂/toluene gave an insoluble amorphous aggregate solid **57**. It was proposed that such an aggregate might undergo partial dissociation in a reversible manner to generate active sites, thus exhibiting an activity similar to that of its parent homogeneous catalyst while maintaining a heterogeneous state. **57** was tested as a catalyst in combination with a large excess of Ti(OⁱPr)₄ for the diethylzinc addition to several aldehydes to give the corresponding alcoholic products in good enantioselectivity (74–84% ee) (Scheme 47). However, control experiments indicated the catalytic reaction of benzaldehyde is only partially heterogeneous since the supernatant of the reaction mixture also exhibited a significant level of reactivity, albeit with a somewhat reduced reaction rate and ee value. This observation suggests that some kinds of soluble catalytic species, generated by decomposition of the aggregate under the testing conditions, may have been leached into the solution phase. Nevertheless, catalyst **57** was

Scheme 47. Enantioselective Diethylzinc Addition to Aldehydes Catalyzed by a tris-BINOL–Ti Aggregate Solid 57



shown to be reusable for ethylation of benzaldehyde and 1-naphthaldehyde. For the reaction of benzaldehyde the catalyst recovered by filtration maintained its activity (>98% conversion in 18 h) even after six cycles without lowering of the enantioselectivity (72–75% ee). However, the potential catalyst leaching into the organic phase during the recycles may need to be investigated.

Cotton and co-workers reported an interesting example of using chiral dinuclear Rh₂-containing triangular organometallic supramolecules for enantioselective catalysis of cyclopropanation of styrene with ethyl diazoacetate.¹⁶³ In some cases, the triangular supramolecules were practically insoluble in the nonpolar reaction medium (pentane). They exhibited remarkable catalytic activity with a moderate enantiocontrol in this reaction and can be separated from the reaction products by filtration. No reuse of the catalysts was reported.

3.5. Asymmetric Ring Opening of Epoxide

Tanaka and co-workers studied the catalytic activity of a chiral metal–organic framework, [Cu₂(5,5′-BDA)₂] (**58**) (5,5′-H₂BDA = 2,2′-dihydroxy-1,10-binaphthalene-5,5′-dicarboxylic acid), in the asymmetric ring-opening reaction of some meso epoxides with aromatic amines (Scheme 48).¹⁶⁴ Treatment of the BINOL-derived enantiopure dicarboxylic ligand 5,5′-H₂BDA with copper nitrate in aqueous/methanol solution afforded [Cu₂(5,5′-BDA)₂(H₂O)₂]·MeOH·2H₂O (the as-synthesized **58**) as needle-like crystals. Single-crystal X-ray diffraction analysis indicated that the as-synthesized **58** adopts a 2D square grid coordination network structure with the paddle-wheel dinuclear copper carboxylate clusters as nodes (Scheme 48). The layers are stacked alternately to form a 3D structure with the void space being filled by one MeOH and two H₂O guest molecules. The evacuated **58** was examined for asymmetric catalysis of ring-opening reactions of epoxides with aromatic amines. The reactions were performed at room temperature in toluene under a catalyst loading of 5 mol %, giving the corresponding optically active β-amino alcohols in low to moderate yields (up to 54% in 1 or 2 days) and ee values (up to 50% ee). Upon completion

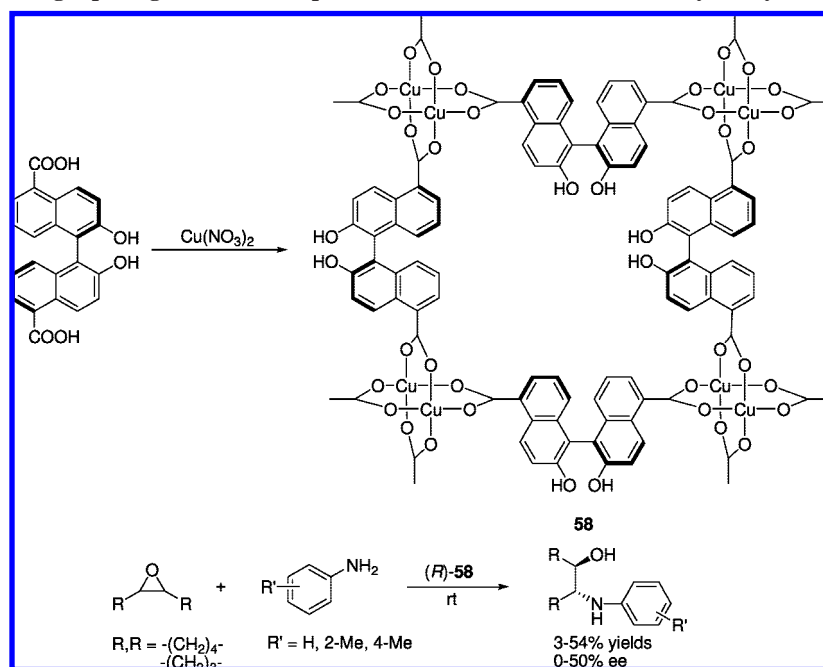
of the reaction, the catalyst was recovered by simple filtration and reported to be reusable in the next cycles of the reaction without appreciable loss of reactivity and enantioselectivity. Significant improvement in both reactivity and enantioselectivity was observed when the reactions were carried out under solvent-free conditions. The control experiment showed that under the test conditions BINOL alone cannot act as an effective catalyst for the reaction. Thus, the observed catalytic activity of **58** might be attributable to either the Lewis acidity of Cu(II) sites exposed on the external surface of the solid or the double hydrogen-bonding activation via synergistic cooperation of two adjacent BINOL units of square grids in the solid. This point remained to be clarified for a deeper understanding of the catalysis.

Rosseinsky and co-workers reported an elegant study on the use of Brønsted-acid-functionalized porous homochiral MOF solids for heterogeneous catalysis of the asymmetric ring-opening reaction of *cis*-2,3-epoxybutane with methanol.¹⁶⁵ Protonation of the amino acid–based open frameworks [Ni(L-asp)bpy_{0.5}]_n (L-asp = L-aspartate) and Cu(L-asp)(bpe)_{0.5}–(guests) using HCl in Et₂O led to formation of [Ni(L-asp)bpy_{0.5}(HCl)_{0.9}(MeOH)_{0.5}] (**59**) and Cu(L-asp)bpe_{0.5}(HCl)(H₂O) (**60**), respectively. The site of protonation was identified to be on the carboxylate group(s) of the aspartate ligands by infrared spectroscopic studies, leading to formation of COOH groups as Brønsted-acidic sites in the solids. The protonated solids **59** and **60** gave similar XRPD patterns to their unprotonated forms, respectively, indicating comparable framework connectivities were retained during the protonation process. Both protonated solids **59** and **60** were shown to be catalytically active in the methanolysis of *rac*-propylene oxide (PO) with the former being less active probably due to its nonporous nature. On the other hand, **60** was porous and capable of uptaking both the reactant molecules of methanol and propylene oxide. Therefore, **60** exhibited a significant improved reactivity in the methanolysis of PO. Catalysis was demonstrated to be heterogeneous as the filtered supernatant of **60** was inactive, which precludes possible catalysis by leached HCl. Catalysis also exhibited shape selectivity toward the epoxides as evidenced by the nearly zero turnover for the reaction involving bulkier 2,3-epoxypropyl benzene, suggesting that the reaction should have taken place not only on the surface but also within the pores of the solid **60**. Furthermore, the framework structure of **60** remains intact after catalysis. Despite its homochiral framework structure, however, the chiral induction ability of **60** was modest in the methanolysis of several tested epoxides. **60** was effective to catalyze the enantioselective methanolysis of the meso epoxide, *cis*-2,3-epoxybutane, affording 3-methoxybutan-2-ol with modest ee values (≤17%). For the methanolysis of racemic PO and *trans*-2,3-epoxybutane, only racemic products were obtained.

3.6. Miscellaneous

Lin and co-worker reported the synthesis, structures, and catalytic properties of a series of homochiral porous lamellar lanthanide bisphosphonates **61a–g** (Scheme 49).¹⁶⁶ The solids are isomorphous in structure as judged from their similar XRPD patterns. Single-crystal X-ray diffraction study on **61f** (Ln = Gd) revealed a 2D lamellar structure of lanthanide phosphonates with nanometer-sized channels being present as a result of crystal packing. Apart from the phosphonate oxygens from the bisphosphonate ligands, the Gd center is also coordinated with four water molecules,

Scheme 48. Asymmetric Ring-Opening Reaction of Epoxides with Aromatic Amines Catalyzed by Chiral MOF 58



which can be removed by evacuation to generate a Lewis-acidic site. Besides, among the four phosphonate groups that are coordinated to the Gd, three are monodeprotonated while the fourth remain protonated. Thus, there are both Lewis- and Brønsted-acid sites present in **61f** (also **61a–e** and **61g**), rendering them usable in catalyzing organic reactions. **61e** ($\text{Ln} = \text{Sm}$) was tested for catalysis of asymmetric cyanosilylation of several aldehydes, asymmetric methanolysis of *meso*-2,3-dimethylsuccinic anhydride, and Diels–Alder reaction between methyl acrylate and cyclopentadiene. Good reactivities were observed in all tested reactions. For the cyanosilylation and ring-opening reactions, catalysis was confirmed to be heterogeneous and the recovered catalyst **61e** was reported to be reusable without loss of activity. Unfortunately, only modest ee values ($<5\%$) were obtained in these reactions despite the homochirality of the framework in **61e**.

4. General Considerations in Self-Supported Catalyst Design

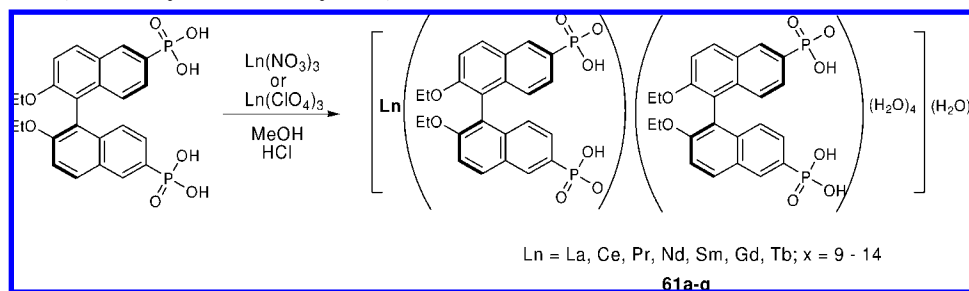
The discussions in previous sections have clearly shown that the self-supported catalysts, constructed from molecular organic and inorganic building blocks, can exhibit heterogeneous catalytic activity and selectivity in a range of organic reactions. Although successful examples of synthetic applications are still scarce so far, the potential for future development is expected to be great given the wide chemical and structural diversity of the catalysts. Such a diversity would imply the possibility to incorporate into the catalyst a large variety of active sites, such as Brønsted/Lewis-acid/base or redox-active metal centers, radical species, etc., and thus may hold promise for a wide range of organic transformations. By virtue of the modular nature of the catalyst synthesis, both the structure and the catalytic properties of the self-supported catalysts are in principle tunable by tailoring the corresponding molecular synthons. Under certain circumstances, the self-supported catalysts can exhibit an efficiency and/or selectivity rivaling those of their homogeneous counterparts with extra advantages of simpli-

fied catalyst/product separation and possible catalyst recycling. The following aspects are recommended to be considered in the design, synthesis, and application of self-supported catalysts for heterogeneous catalysis.

Despite these attractive features, however, formidable challenges still remain in the context of catalyst development. Apart from the catalyst network construction, consideration must also be given to incorporation of the potentially active sites into the solid without deactivation. The modular approach to a self-supported catalyst has provided a possibility to use the molecular building blocks, i.e., the organic bridging ligand and/or the metal ion, as both the structural units and the catalytic sites in the material. Such a way for direct introduction of catalytically active sites has been demonstrated very successfully in many cases, which can sometimes replicate the key features of a homogeneous molecular counterpart and thus exhibit a somewhat predictable catalytic behavior. On the other hand, successful implementation of this strategy would necessitate a compatible chemistry, i.e., catalyst framework construction without destruction of the catalytic functionality. This can be problematic in some cases since the framework construction may be accompanied with the loss of Lewis acidity at all metal centers (coordinative saturation) and Lewis-basic sites on the ligands. In such a case, uploading the active site after construction of the framework, called postsynthetic modification, would be feasible.

Over the last two decades impressive success has been achieved in the rational synthesis of various coordination networks for specific applications. However, considering the numerous coordination polymers and hybrid materials developed so far and great interest in their catalytic applications it is surprising that only relatively few studies have demonstrated such activities. A reason for this phenomenon is often ascribed to the coordinative saturation of the metal centers. Usually for a metal-catalyzed reaction prior coordination of a substrate for its activation is necessary, which requires that one or more free coordination sites or at least some labile ligands should be available on the metal. Unfortunately this

Scheme 49. Homochiral Porous Lanthanide Bisphosphonates 61a–g for the Catalytic Cyanosilylation of Aldehydes, Methanolysis of *meso*-2,3-Dimethylsuccinic Anhydride, and Diels–Alder Reactions



is not the case with most coordination polymers since frequently all coordination sites are used in polymer formation for the sake of structural stability. However, this problem does not necessarily preclude their involvement in catalytic transformation. Several approaches for direct introduction or creation of coordinatively unsaturated metal centers in a coordination polymer, which should also be in principle applicable to catalysis, have been described in an excellent recent review by Kitagawa et al.,¹⁶⁷ typically including use of proper metal ions with large coordination numbers (e.g., lanthanides), metal clusters with labile terminal ligands, or metallogligands containing a prefabricated catalytic unit. Many metal ions have a rather flexible coordination mode and geometry, which may allow for creation of free coordination sites by removal of some ancillary ligands without damaging the matrix structure. Examples in this regard can be found, for instance, in the previously discussed work by Kaskel et al.⁴⁷ and De Vos et al.,⁸⁶ wherein the coordinated water ligand on the copper sites of the paddle-wheel cluster in the as-synthesized Cu–BTC material can be removed without collapse of the structure, thus leaving free copper coordination sites available for substrate activation in the dehydrated catalyst. Alternatively, using a different type of metal for polymer formation may result in a change in the catalytic properties as, for instance, in Aoyama's report with La⁴¹ in anthracene bisresorcinol coordination polymer formation, creating a catalytically active La–OH group reminiscent of the silanol groups in zeolite chemistry. Furthermore, it is noteworthy that the active sites do not necessarily locate on the metal nodes of the self-supported catalyst; there are many options to incorporate the active sites into the bridging ligand building unit. As an illustration of the potential versatility, one can cite examples discussed in this review, such as use of an elegant design strategy with orthogonal multifunctional ligands by Lin et al.,¹⁵⁹ application of metallogligands in the preparation of polymeric catalyst as illustrated by Hupp's work,^{151,152} using the basic functionality on the linker as by Kitagawa³⁷ or the basic groups in the solids as in the transesterification by Kim,¹²⁴ and polymerization of acetylene derivatives by Kitagawa,⁸⁰ Brønsted-acidic sites as in zirconium phosphonate by Curini,⁹⁸ and the lanthanide phosphonates by Lin.¹⁶⁶ Alternatively, preparation of a functionalized MOF solid with targeted catalytic property may also be achieved by postsynthetic modification as exemplified in Rosseinsky's study.¹⁶⁵ Given the surge of current interest in organocatalysis,¹⁶⁸ use of functional groups on the bridging ligands for organocatalysis might also be an attractive approach. An interesting variation was use of peptides as bridging ligands in hybrid solid formation, reported very recently by Manton and Taubert and co-workers.¹⁶⁹ With

many functionalities integrated in the solids, one can expect some interesting catalytic applications to be discovered in the future.

Despite such versatility in active site incorporation, however, it is worth noting that successful examples of a tailor-made self-supported catalyst for specifically targeted reactions are still very rare. In many reported cases the catalytic properties of a coordination polymer were tested and discovered on a trial-and-error basis and in the conceptual level. Although the self-supported catalysts are modularly constructed from tailorable molecular building units, the exact structures of the resulting solids are generally hard to predict. This is not surprising given the inherently flexible ligating mode of most metals and typically moderate strength in coordination bonding. Furthermore, sometimes the coexistence of multiple inorganic species (building blocks) under the synthetic conditions may also complicate the structural prediction of the solid product. In this respect, some rational approaches recently developed for engineering the structure of a coordination polymer or an organic–inorganic hybrid could be of great reference value. For example, Yaghi and O'Keeffe and co-workers illustrated their elegant reticular chemistry concept in the design of the IRMOF series.⁴⁴ They demonstrated convincingly that by identifying formation of well-defined and rigid inorganic and organic building blocks in solution predetermined ordered structures with various pore sizes and functional groups (e.g., bromo, amino, *n*-propoxy) can be synthesized with some rational design. Férey and co-workers developed a new method for predicting the structures of MOFs based on identification of inorganic secondary building units (SBU) in solvothermal medium and a computer simulation approach.¹⁷⁰

The accessibility of substrate molecules to the active sites in the solid matrix of a self-supported catalyst is also an important issue in the context of heterogeneous catalysis. The high metal loading in a self-supported catalyst alone is not a guarantee for its good catalytic activity since space accessibility for reactants to the active sites is also a prerequisite to minimize diffusion problems and allow efficient catalytic turnovers. It is conceivable that especially for some self-supported catalysts with dense structures many of the would-be active sites are embedded in the matrix and thus will not be freely accessible to reagent molecules. Fortunately, porosity in the nanometer range is one of the most often observed features for such a class of catalysts, and chiral pores can also be obtained using homochiral bridging ligands under relatively mild conditions. Regularly distributed pores with uniformly dispersed and well-exposed active sites are obviously desirable for a self-supported catalyst since they not only allow for ready access to the reactants but also impart size and/or shape selectivity and/

or exhibit favorable confinement effects such as stabilization of reactive intermediates.

A general concern for a self-supported catalyst is that it should be stable enough during the reaction process. Although the thermal stability of a self-supported hybrid catalyst might be not as good as the conventional inorganic solid catalysts such as zeolites, this will not prevent their catalytic applications in many organic transformations that are performed under relatively mild conditions. Another primary concern in the self-supported hybrid catalysts is the chemical stability, which is important for their recovery and reuse as well as elimination of metal/ligand leaching. The catalysts maintain their structural integrity by various metal–ligand coordination bonds, which can encompass a broad spectrum of strengths depending on the metal-binding motifs. Factors such as the strength of ligation, ligand denticity, and coordination number, etc., can be synergistically tuned to enhance the metal–ligand interaction and thus improve the catalyst stability. As summarized in a review by Bielawski et al.,¹⁷¹ this can usually be accomplished by two ways, i.e., using donor ligands with exceptionally high metal affinity (high binding constants) and/or increasing the number of donor atoms that are bonding to the metal using multidentate ligands. The strong monodentate phosphine–Rh bonding motifs and multidentate binding arrays such as BINOL–Ti(IV) that was discussed in the previous section exemplified these approaches.

Since most catalytic applications of organic reactions are performed in solution, therefore the solubility of a self-supported catalyst is of special interest in terms of catalyst recovery and reuse. Although the solubility of a self-supported catalyst in a given solvent is hard to predict owing to the diversity in organic/inorganic composition and degree of cross-linking, solvents of low polarity are generally preferable since the solubility of an extended coordination polymer is usually low in such solvents. Sometimes use of strongly coordinating solvents was found to be deleterious since they may compete with the substrate for coordination on catalytic sites of the metal. In some cases they may even cause depolymerization/decomposition of a self-supported catalyst, leading to metal/ligand leaching during catalyst recycling or a loss of selectivity in reactions. With these considerations in mind, it is clear that reaction conditions which do not cause an extensive decomposition of the catalysts are a prerequisite for successful applications. Furthermore, care should be taken in the interpretation of catalytic results. Similar to the test using other types of immobilized catalysts, a meaningful catalytic study using such a self-supported catalyst should always include investigation of the liquid-phase supernatant over the solid-state catalyst after a catalytic cycle. This is to ensure that the self-supported catalyst does not partly dissolve or decompose in solution so as to exclude that it is its components which act as a homogeneous catalyst in the reaction system.

5. Concluding Remarks and Outlook

Application of functionalized coordination polymers as self-supported catalysts in heterogeneous catalytic reactions is an emerging area of research and has met with some notable success. The molecular building units of the catalysts are tailorable in nature, allowing for systematic engineering of the catalytic performance. The catalysts have demonstrated high efficiency and/or excellent selectivity in a variety of reactions and can be separated from the product by simple

filtration and even reused in multiple cycles without loss of activity or selectivity. In some cases, all active sites in the self-supported catalyst can be identical because of the high crystallinity of the solid. This would not only facilitate the structural elucidation of the catalyst and further mechanistic studies in relevant reactions but also may lead to development of new heterogeneous single-site catalysts for highly selective synthesis. These remarkable features coupled with the enormous diversity of the chemical compositions and structures suggest more catalytic applications of these materials can be expected in the future.

However, much still remains to be done to further explore the strength, limitations, and application potential of the self-supported catalysts. For rational synthesis of the catalysts toward targeted reactions, systematic studies that show the capability in design of catalytically functionalized molecular building blocks would be desirable. More materials need to be tested for their potential activities in the catalysis of chemically interesting and industrially useful reactions. Development of new analytical techniques that can be applied for characterization of the microstructure of an amorphous self-supported catalyst (for example, to ascertain how many active units are actually incorporated into the catalyst) still remains a great challenge. In addition, chiral porous self-supported catalysts with larger cavities and more functionalities are obviously desirable for asymmetric transformation of useful and bulky molecules. Finally, more studies remain to be done to evaluate if these catalysts can compete with other types of well-known heterogeneous catalysts in specified applications. Clearly the challenges are interdisciplinary and multifarious, which call for collaborative research efforts from both catalysis- and materials-orientated groups.

6. Abbreviations

AIBN	2,2'-azobis(isobutyronitrile)
ALB	Al–Li-bis(binaphthoxide)
L-asp	L-aspartate
BDC	benzene-1,4-dicarboxylate
BINAP	2,2'-bis(diphenylphosphino)-1,1'-binaphthyl
BINOL	1,1'-bi-2-naphthol
BIPHEP	2,2'-bis(diphenylphosphino)-1,1'-biphenyl
bipy	2,2'-bipyridyl
Bis-MonoPhos	bis-phosphoramidites
BPDC	2,2'-bipyridine-5,5'-dicarboxylate
bpdo	4,4'-bipyridyl- <i>N,N'</i> -dioxide
bpy	4,4'-bipyridine
4-btapa	1,3,5-benzene tricarboxylic acid tris[<i>N</i> -(4-pyridyl)-amide]
BTC	benzene-1,3,5-tricarboxylate
btcc	1,2,4,5-benzenetetracarboxylate
btpp	2,6-bis(<i>N'</i> -1,2,4-triazolyl)pyridine
DABCO	1,4-diazabicyclo[2,2,2]octane
DMF	<i>N,N'</i> -dimethylformamide
DPEN	1,2-diphenylethylenediamine
EG	ethylene glycol
fcz	1-(2,4-difluorophenyl)-1,1-bis[(1 <i>H</i> -1,2,4-triazol-1-yl)methyl]ethanol
5,5'-H ₂ BDA	2,2'-dihydroxy-1,10-binaphthalene-5,5'-dicarboxylic acid
H-BEA	acidic form of beta zeolite
H ₂ BDC	1,4-benzenedicarboxylic acid
H ₂ bpdc	biphenyldicarboxylic acid
H ₂ -BPDS	biphenyl-4,4'-disulfonic acid
L-H ₂ lac	L-lactic acid
H ₂ mipt	5-methylisophthalic acid
H ₂ QA	quinolinic acid

H ₂ TCP	4,4',4'',4'''-(21 <i>H</i> ,23 <i>H</i> -porphine-5,10,15,20-tetra- yl)tetrakis benzoic acid
H ₃ BTT	1,3,5-benzenetristetrazol-5-yl
Hdpa	2,2'-dipyridylamine
HOAc	acetic acid
Im	imidazole
IRMOF	isoreticular metal-organic framework
MAO	methylalumoxane
<i>o</i> -MeDBK	<i>o</i> -methyl dibenzylketone
MOF	metal-organic framework
NDC	2,6-naphthalenedicarboxylate
NDS	1,5-naphthalenedisulfonate
OBA	4,4'-oxybis(benzoate)
PA-TAP-Pd	poly(acrylamide)triarylphosphine palladium
phen	1,10-phenanthroline
Ph ²⁻	dianion of <i>o</i> -phthalic acid
PPA	polyphenylacetylene
2-pymo	2-hydroxypyrimidinolate
pzdc	pyrazine-2,3-dicarboxylate
RCM	ring-closing metathesis
UP	ureido-4[1 <i>H</i>]-ureidopyrimidone
WHPCO	wet hydrogen peroxide catalytic oxidation
XRPD	X-ray powder diffraction

7. Acknowledgments

Thanks are expressed to the National Natural Science Foundation of China (nos. 20532050, 20632060), the Chinese Academy of Sciences, the Major Basic Research Development Program of China (grant no. 2006CB806106), the Science and Technology Commission of Shanghai Municipality, and Merck Research Laboratories for financial support. We are indebted to all our co-workers who have contributed to the developments presented in this review. This paper is dedicated to Prof. Zhitang Huang on the occasion of his 80th birthday.

8. References

- (1) *Catalysis from A To Z: A Concise Encyclopedia*; Cornils, B., Herrmann, W. A., Muhler, M., Wong, C.-H., Eds.; Wiley-VCH Verlag GmbH & Co. KGaA: Weinheim, 2007; Vols. 1–3.
- (2) Sheldon, R.; Arends, I.; Hanefeld, U. *Green Chemistry and Catalysis*; Wiley-VCH: Weinheim, 2007.
- (3) van Leeuwen, P. W. N. M. *Homogeneous Catalysis-Understanding the Art*; Kluwer Academic Publishers: Dordrecht, 2004.
- (4) *Handbook of Heterogeneous Catalysis*, 2nd ed.; Ertl, G., Knözinger, H., Schüth, F., Weitkamp, J., Eds.; Wiley-VCH: Weinheim, 2008; Vols. 1–8.
- (5) *Handbook of Asymmetric Heterogeneous Catalysis*; Ding, K., Uozumi, Y., Eds.; Wiley-VCH: Weinheim, 2008.
- (6) *Multiphase Homogeneous Catalysis*; Cornils, B., Herrmann, W. A., Horváth, I. T., Leitner, W., Mecking, S., Olivier-Bourbigou, H., Vogt, D., Eds.; Wiley-VCH: Weinheim, 2005.
- (7) *Asymmetric Catalysis on Industrial Scale: Challenges, Approaches and Solutions*; Blaser, H. U., Schmidt, E., Eds.; Wiley-VCH: Weinheim, 2004.
- (8) *Catalyst Separation, Recovery and Recycling: Chemistry and Process Design*; Cole-Hamilton, D. J., Tooze, R. P., Eds.; Springer: Berlin 2006.
- (9) For a thematic issue on recoverable catalysts and reagents, see: Gladysz, J. A. *Chem. Rev.* **2002**, *102*, 3215.
- (10) Rowsell, J. L. C.; Yaghi, O. M. *Microporous Mesoporous Mater.* **2004**, *73*, 3.
- (11) Cheetham, A. K.; Rao, C. N. R.; Feller, R. K. *Chem. Commun.* **2006**, 4780.
- (12) Férey, G. *Chem. Soc. Rev.* **2008**, *37*, 191.
- (13) Efraty, A.; Feinstein, I. *Inorg. Chem.* **1982**, *21*, 3115.
- (14) Jaffe, I.; Segal, M.; Efraty, A. *J. Organomet. Chem.* **1985**, *294*, c17.
- (15) Feinstein-Jaffe, I.; Efraty, A. *J. Mol. Catal.* **1986**, *35*, 285.
- (16) Feinstein-Jaffe, I.; Efraty, A. *J. Mol. Catal.* **1987**, *40*, 1.
- (17) Batten, S. R. *Curr. Opin. Solid State Mater. Sci.* **2001**, *5*, 107.
- (18) James, S. L. *Chem. Soc. Rev.* **2003**, *32*, 276.
- (19) Kitagawa, S.; Kitaura, R.; Noro, S. *Angew. Chem., Int. Ed.* **2004**, *43*, 2334.
- (20) Rosseinsky, M. J. *Microporous Mesoporous Mater.* **2004**, *73*, 15.

- (21) Forster, P. M.; Cheetham, A. K. *Top. Catal.* **2003**, *24*, 79.
- (22) Janiak, C. *Dalton Trans.* **2003**, 2781.
- (23) Schuth, F. *Annu. Rev. Mater. Res.* **2005**, *35*, 209.
- (24) Lawrence, S. A.; Sermon, P. A.; Feinstein-Jaffe, I. *J. Mol. Catal.* **1989**, *51*, 117.
- (25) Tannenbaum, R. *Chem. Mater.* **1994**, *6*, 550.
- (26) Tannenbaum, R. *J. Mol. Catal. A: Chem.* **1996**, *107*, 207.
- (27) Naito, S.; Tanibe, T.; Saito, E.; Miyao, T.; Mori, W. *Chem. Lett.* **2001**, 1178.
- (28) Ohmura, T.; Mori, W.; Hiraga, H.; Ono, M.; Nishimoto, Y. *Chem. Lett.* **2003**, *32*, 468.
- (29) Sato, T.; Mori, W.; Kato, C. N.; Ohmura, T.; Sato, T.; Yokoyama, K.; Takamizawa, S.; Naito, S. *Chem. Lett.* **2003**, *32*, 854.
- (30) Mori, W.; Takamizawa, S.; Kato, C. N.; Ohmura, T.; Sato, T. *Microporous Mesoporous Mater.* **2004**, *73*, 31.
- (31) Sato, T.; Mori, W.; Kato, C. N.; Yanoaka, E.; Kuribayashi, T.; Ohtera, R.; Shiraishi, Y. *J. Catal.* **2005**, *232*, 186.
- (32) Mori, W.; Sato, T.; Ohmura, T.; Kato, C. N.; Takei, T. *J. Solid State Chem.* **2005**, *178*, 2555.
- (33) Fujita, M.; Kwon, Y. J.; Washizu, S.; Ogura, K. *J. Am. Chem. Soc.* **1994**, *116*, 1151.
- (34) Aoyagi, M.; Biradha, K.; Fujita, M. *Bull. Chem. Soc. Jpn.* **2000**, *73*, 1369.
- (35) Ohmori, O.; Fujita, M. *Chem. Commun.* **2004**, 1586.
- (36) Horike, S.; Dinka, M.; Tamaki, K.; Long, J. R. *J. Am. Chem. Soc.* **2008**, *130*, 5854.
- (37) Hasegawa, S.; Horike, S.; Matsuda, R.; Furukawa, S.; Mochizuki, K.; Kinoshita, Y.; Kitagawa, S. *J. Am. Chem. Soc.* **2007**, *129*, 2607.
- (38) Sawaki, T.; Aoyama, Y. *J. Am. Chem. Soc.* **1999**, *121*, 4793.
- (39) Sawaki, T.; Dewa, T.; Aoyama, Y. *J. Am. Chem. Soc.* **1998**, *120*, 8539.
- (40) Dewa, T.; Aoyama, Y. *J. Mol. Catal. A: Chem.* **2000**, *152*, 257.
- (41) Saiki, T.; Aoyama, Y. *Chem. Lett.* **1999**, 797.
- (42) Dewa, T.; Saiki, T.; Aoyama, Y. *J. Am. Chem. Soc.* **2001**, *123*, 502.
- (43) Saito, S.; Murase, M.; Yamamoto, H. *Synlett* **1999**, 57.
- (44) Yaghi, O. M.; O'Keeffe, M.; Ockwig, N. W.; Chae, H. K.; Eddaoudi, M.; Kim, J. *Nature (London)* **2003**, *423*, 705.
- (45) Perles, J.; Iglesias, M.; Ruiz-Valero, C.; Snejko, N. *Chem. Commun.* **2003**, 346.
- (46) Perles, J.; Iglesias, M.; Ruiz-Valero, C.; Snejko, N. *J. Mater. Chem.* **2004**, *14*, 2683.
- (47) Schlichte, K.; Kratzke, T.; Kaskel, S. *Microporous Mesoporous Mater.* **2004**, *73*, 81.
- (48) Chui, S. S. Y.; Lo, S. M. F.; Charmant, J. P. H.; Orpen, A. G.; Williams, I. D. *Science* **1999**, *283*, 1148.
- (49) Henschel, A.; Gedrich, K.; Kraehnert, R.; Kaskel, S. *Chem. Commun.* **2008**, 4192.
- (50) Férey, G.; Mellot-Draznieks, C.; Serre, C.; Millange, F.; Dutour, J.; Surble, S.; Margiolaki, I. *Science* **2005**, *309*, 2040.
- (51) Horecjad, P.; Surble, S.; Serre, C.; Hong, D. Y.; Seo, Y. K.; Chang, J. S.; Grenèche, J. M.; Margiolaki, I.; Férey, G. *Chem. Commun.* **2007**, 2820.
- (52) Eddaoudi, M.; Kim, J.; Rosi, N.; Vodak, D.; Wachter, J.; O'Keeffe, M.; Yaghi, O. M. *Science* **2002**, *295*, 469.
- (53) Ravon, U.; Domine, M. E.; Gaudillère, C.; Desmartin-Chomel, A.; Farrusseng, D. *New J. Chem.* **2008**, *32*, 937.
- (54) Ishida, S.; Hayano, T.; Furuno, H.; Inanaga, J. *Heterocycles* **2005**, *66*, 645.
- (55) Liu, Q. P.; Chen, Y. C.; Wu, Y.; Zhu, J.; Deng, J. G. *Synlett* **2006**, 1503.
- (56) Chen, W.; Li, R.; Wu, Y.; Ding, L. S.; Chen, Y. C. *Synthesis* **2006**, 3058.
- (57) Yamada, Y. M. A.; Maeda, Y.; Uozumi, Y. *Org. Lett.* **2006**, *8*, 4259.
- (58) Uozumi, Y.; Yamada, Y. M. A.; Beppu, T.; Fukuyama, N.; Ueno, M.; Kitamori, T. *J. Am. Chem. Soc.* **2006**, *128*, 15994.
- (59) Xamena, F. X. L. I.; Abad, A.; Corma, A.; Garcia, H. *J. Catal.* **2007**, *250*, 294.
- (60) Navarro, J. A. R.; Barea, E.; Salas, J. M.; Masciocchi, N.; Galli, S.; Sironi, A.; Ania, C. O.; Parra, J. B. *Inorg. Chem.* **2006**, *45*, 2397.
- (61) Chen, S. W.; Kim, J. H.; Song, C. E.; Lee, S. G. *Org. Lett.* **2007**, *9*, 3845.
- (62) Xing, B. G.; Choi, M. F.; Xu, B. *Chem. Eur. J.* **2002**, *8*, 5028.
- (63) Han, H.; Zhang, S.; Hou, H.; Fan, Y.; Zhu, Y. *Eur. J. Inorg. Chem.* **2006**, 1594.
- (64) Arai, T.; Takasugi, H.; Sato, T.; Noguchi, H.; Kanoh, H.; Kaneko, K.; Yanagisawa, A. *Chem. Lett.* **2005**, *34*, 1590.
- (65) Arai, T.; Sato, T.; Kanoh, H.; Kaneko, K.; Oguma, K.; Yanagisawa, A. *Chem. Eur. J.* **2008**, *14*, 882.
- (66) Arai, T.; Sato, T.; Noguchi, H.; Kanoh, H.; Kaneko, K.; Yanagisawa, A. *Chem. Lett.* **2006**, *35*, 1094.
- (67) Gomez-Lor, B.; Gutierrez-Puebla, E.; Iglesias, M.; Monge, M. A.; Ruiz-Valero, C.; Snejko, N. *Inorg. Chem.* **2002**, *41*, 2429.

- (68) Perles, J.; Iglesias, M.; Martin-Luengo, M. A.; Monge, M. A.; Ruiz-Valero, C.; Snejko, N. *Chem. Mater.* **2005**, *17*, 5837.
- (69) Kato, C. N.; Hasegawa, M.; Sato, T.; Yoshizawa, A.; Inoue, T.; Mori, W. *J. Catal.* **2005**, *230*, 226.
- (70) Kato, C. N.; Mori, W. *C. R. Chim.* **2007**, *10*, 284.
- (71) Kato, C. N.; Ono, M.; Hino, T.; Ohmura, T.; Mori, W. *Catal. Commun.* **2006**, *7*, 673.
- (72) Han, J. W.; Hill, C. L. *J. Am. Chem. Soc.* **2007**, *129*, 15094.
- (73) Baca, S. G.; Reetz, M. T.; Goddard, R.; Filippova, I. G.; Simonov, Y. A.; Gdaniec, M.; Gerbeleu, N. *Polyhedron* **2006**, *25*, 1215.
- (74) Snejko, N.; Cascales, C.; Gomez-Lor, B.; Gutierrez-Puebla, E.; Iglesias, M.; Ruiz-Valero, C.; Monge, M. A. *Chem. Commun.* **2002**, 1366.
- (75) Tanski, J. M.; Wolczanski, P. T. *Inorg. Chem.* **2001**, *40*, 2026.
- (76) Park, K. H.; Jang, K.; Son, S. U.; Sweigart, D. A. *J. Am. Chem. Soc.* **2006**, *128*, 8740.
- (77) Uemura, T.; Horike, S.; Kitagawa, S. *Chem. Asian J.* **2006**, *1*, 36.
- (78) Uemura, T.; Kitagawa, K.; Horike, S.; Kawamura, T.; Kitagawa, S.; Mizuno, M.; Endo, K. *Chem. Commun.* **2005**, 5968.
- (79) Uemura, T.; Ono, Y.; Kitagawa, K.; Kitagawa, S. *Macromolecules* **2008**, *41*, 87.
- (80) Uemura, T.; Kitaura, R.; Ohta, Y.; Nagaoka, M.; Kitagawa, S. *Angew. Chem., Int. Ed.* **2006**, *45*, 4112.
- (81) Matsuda, R.; Kitaura, R.; Kitagawa, S.; Kubota, Y.; Belosludov, R. V.; Kobayashi, T. C.; Sakamoto, H.; Chiba, T.; Takata, M.; Kawazoe, Y.; Mita, Y. *Nature* **2005**, *436*, 238.
- (82) Yoo, S. K.; Ryu, J. Y.; Lee, J. Y.; Kim, C.; Kim, S. J.; Kim, Y. *Dalton Trans.* **2003**, 1454.
- (83) Hong, S. J.; Ryu, J. Y.; Lee, J. Y.; Kim, C.; Kim, S. J.; Kim, Y. *Dalton Trans.* **2004**, 2697.
- (84) Hong, S. J.; Seo, J. S.; Ryu, J. Y.; Lee, J. H.; Kim, C.; Kim, S. J.; Kim, Y.; Lough, A. J. *J. Mol. Struct.* **2005**, *751*, 22.
- (85) Jiang, D.; Mallat, T.; Krumeich, F.; Baiker, A. *J. Catal.* **2008**, *257*, 390.
- (86) Alaerts, L.; Seguin, E.; Poelman, H.; Thibault-Starzyk, F.; Jacobs, P. A.; De Vos, D. E. *Chem. Eur. J.* **2006**, *12*, 7353.
- (87) Mueller, U.; Schubert, M.; Teich, F.; Puetter, H.; Schierle-Arndt, K.; Pastre, J. *J. Mater. Chem.* **2006**, *16*, 626.
- (88) Li, H.; Eddaoudi, M.; Groy, T. L.; Yaghi, O. M. *J. Am. Chem. Soc.* **1998**, *120*, 8571.
- (89) Li, H.; Eddaoudi, M.; O'Keeffe, M.; Yaghi, O. M. *Nature* **1999**, *402*, 276.
- (90) Eddaoudi, M.; Li, H. L.; Yaghi, O. M. *J. Am. Chem. Soc.* **2000**, *122*, 1391.
- (91) Pan, L.; Liu, H.; Lei, X.; Huang, X.; Olson, D. H.; Turro, N. J.; Li, J. *Angew. Chem., Int. Ed.* **2003**, *42*, 542.
- (92) Yu, Z. T.; Liao, Z. L.; Jiang, Y. S.; Li, G. H.; Li, G. D.; Chen, J. S. *Chem. Commun.* **2004**, 1814.
- (93) Yu, Z. T.; Liao, Z. L.; Jiang, Y. S.; Li, G. H.; Chen, J. S. *Chem. Eur. J.* **2005**, *11*, 2642.
- (94) Mahata, P.; Madras, G.; Natarajan, S. *J. Phys. Chem. B* **2006**, *110*, 13759.
- (95) De Rosa, S.; Giordano, G.; Granato, T.; Katovic, A.; Siciliano, A.; Tripicchio, F. *J. Agric. Food. Chem.* **2005**, *53*, 8306.
- (96) Zou, R. Q.; Sakurai, H.; Xu, Q. *Angew. Chem., Int. Ed.* **2006**, *45*, 2542.
- (97) Zou, R. Q.; Sakurai, H.; Han, S.; Zhong, R. Q.; Xu, Q. *J. Am. Chem. Soc.* **2007**, *129*, 8402.
- (98) Curini, M.; Rosati, O.; Costantino, U. *Curr. Org. Chem.* **2004**, *8*, 591.
- (99) Curini, M.; Epifano, F.; Marcotullio, M. C.; Rosati, O. *Synlett* **2001**, 1182.
- (100) Curini, M.; Montanari, F.; Rosati, O.; Liyo, E.; Margarita, R. *Tetrahedron Lett.* **2003**, *44*, 3923.
- (101) Curini, M.; Rosati, O.; Campagna, V.; Montanari, F.; Cravotto, G.; Bocalini, M. *Synlett* **2005**, 2927.
- (102) Curini, M.; Epifano, F.; Marcotullio, M. C.; Rosati, O. *Eur. J. Org. Chem.* **2001**, 4149.
- (103) Curini, M.; Epifano, F.; Marcotullio, M. C.; Rosati, O.; Costantino, U. *Tetrahedron Lett.* **1998**, *39*, 8159.
- (104) Curini, M.; Epifano, F.; Marcotullio, M. C.; Rosati, O.; Costantino, U. *Synth. Commun.* **1999**, *29*, 541.
- (105) Curini, M.; Epifano, F.; Marcotullio, M. C.; Rosati, O.; Rossi, M. *Synth. Commun.* **2000**, *30*, 1319.
- (106) Curini, M.; Epifano, F.; Marcotullio, M. C.; Rosati, O.; Nocchetti, M. *Tetrahedron Lett.* **2002**, *43*, 2709.
- (107) Curini, M.; Marcotullio, M. C.; Pisani, E.; Rosati, O. *Synlett* **1997**, 769.
- (108) Curini, M.; Rosati, O.; Pisani, E. *Synlett* **1996**, 333.
- (109) Lee, Y. M.; Hong, S. J.; Kim, H. J.; Lee, S. H.; Kwak, H.; Kim, C.; Kim, S. J.; Kim, Y. *Inorg. Chem. Commun.* **2007**, *10*, 287.
- (110) Szeto, K. C.; Lillerud, K. P.; Tilset, M.; Bjorgen, M.; Prestipino, C.; Zecchina, A.; Lamberti, C.; Bordiga, S. *J. Phys. Chem. B* **2006**, *110*, 21509.
- (111) Szeto, K. C.; Prestipino, C.; Lamberti, C.; Zecchina, A.; Bordiga, S.; Bjorgen, M.; Tilset, M.; Lillerud, K. P. *Chem. Mater.* **2007**, *19*, 211.
- (112) Szeto, K. C.; Kongshaug, K. O.; Jakobsen, S.; Tilset, M.; Lillerud, K. P. *Dalton Trans.* **2008**, 2054.
- (113) Noyori, R. *Asymmetric Catalysis in Organic Synthesis*; Wiley-Interscience: New York, 1994.
- (114) *Catalytic Asymmetric Synthesis*, 2nd ed.; Ojima, I., Ed.; Wiley-VCH: New York, 2000.
- (115) *Comprehensive Asymmetric Catalysis*; Jacobsen, E. N., Pfaltz, A., Yamamoto, H., Eds.; Springer: Berlin, 1999; Vols. I–III.
- (116) *Acid Catalysis in Modern Organic Synthesis*; Yamamoto, H., Ishihara, K., Eds.; Wiley-VCH: Weinheim, 2008; Vols. I–2.
- (117) *Phosphorus Ligands in Asymmetric Catalysis: Synthesis and Application*; Börner, A., Ed.; Wiley-VCH: Weinheim, 2008; Vols. I–3.
- (118) Sheldon, R. A. *Chirotechnology: Industrial Synthesis of Optically Active Compounds*; Dekker: New York, 1993.
- (119) *Chiral Catalyst Immobilization and Recycling*; De Vos, D. E., Vankelecom, I. F. J., Jacobs, P. A., Eds.; Wiley-VCH: Weinheim, 2000.
- (120) Bergbreiter, D. E. *Chem. Rev.* **2002**, *102*, 3345.
- (121) Fan, Q. H.; Li, Y. M.; Chan, A. S. C. *Chem. Rev.* **2002**, *102*, 3385.
- (122) Heitbaum, M.; Glorius, F.; Escher, I. *Angew. Chem., Int. Ed.* **2006**, *45*, 4732.
- (123) Dicos, B. M. L.; Vankelecom, I. F. J.; Jacobs, P. A. *Adv. Synth. Catal.* **2006**, *348*, 1413.
- (124) Seo, J. S.; Whang, D.; Lee, H.; Jun, S. I.; Oh, J.; Jeon, Y. J.; Kim, K. *Nature (London)* **2000**, *404*, 982.
- (125) Bradshaw, D.; Claridge, J. B.; Cussen, E. J.; Prior, T. J.; Rosseinsky, M. J. *Acc. Chem. Res.* **2005**, *38*, 273.
- (126) Kesanli, B.; Lin, W. *Coord. Chem. Rev.* **2003**, *246*, 305.
- (127) Lin, W. *J. Solid State Chem.* **2005**, *178*, 2486.
- (128) Ngo, H. L.; Lin, W. *Top. Catal.* **2005**, *34*, 85.
- (129) Ding, K.; Wang, Z.; Wang, X.; Liang, Y.; Wang, X. *Chem. Eur. J.* **2006**, *12*, 5188.
- (130) Ding, K. *Pure Appl. Chem.* **2006**, *78*, 293.
- (131) Jayaprakash, D.; Takizawa, S.; Arai, T.; Sasai, H. *J. Exp. Nanosci.* **2006**, *1*, 477.
- (132) Dai, L. X. *Angew. Chem., Int. Ed.* **2004**, *43*, 5726.
- (133) Xiong, R. G.; You, X. Z.; Abrahams, B. F.; Xue, Z. L.; Che, C. M. *Angew. Chem., Int. Ed.* **2001**, *40*, 4422.
- (134) Li, G.; Yu, W. B.; Ni, J.; Liu, T. F.; Liu, Y.; Sheng, E. H.; Cui, Y. *Angew. Chem., Int. Ed.* **2008**, *47*, 1245.
- (135) Noyori, R.; Ohkuma, T.; Kitamura, M.; Takaya, H.; Sayo, N.; Kumabayashi, H.; Akutagawa, S. *J. Am. Chem. Soc.* **1987**, *109*, 5856.
- (136) Hu, A.; Ngo, H. L.; Lin, W. *Angew. Chem., Int. Ed.* **2003**, *42*, 6000.
- (137) Noyori, R. *Angew. Chem., Int. Ed.* **2002**, *41*, 2008.
- (138) Ohkuma, T.; Ooka, H.; Hashiguchi, S.; Ikariya, T.; Noyori, R. *J. Am. Chem. Soc.* **1995**, *117*, 2675.
- (139) Ohkuma, T.; Ooka, H.; Ikariya, T.; Noyori, R. *J. Am. Chem. Soc.* **1995**, *117*, 10417.
- (140) Hu, A.; Ngo, H. L.; Lin, W. *J. Am. Chem. Soc.* **2003**, *125*, 11490.
- (141) Liang, Y.; Jing, Q.; Li, X.; Shi, L.; Ding, K. *J. Am. Chem. Soc.* **2005**, *127*, 7694.
- (142) Liang, Y.; Wang, Z.; Ding, K. *Adv. Synth. Catal.* **2006**, *348*, 1533.
- (143) van den Berg, M.; Minnaard, A. J.; Schudde, E. P.; van Esch, J.; de Vries, A. H. M.; de Vries, J. G.; Feringa, B. L. *J. Am. Chem. Soc.* **2000**, *122*, 11539.
- (144) Pena, D.; Minnaard, A. J.; de Vries, J. G.; Feringa, B. L. *J. Am. Chem. Soc.* **2002**, *124*, 14552.
- (145) Wang, X.; Ding, K. *J. Am. Chem. Soc.* **2004**, *126*, 10524.
- (146) Peng, H. Y.; Lam, C. K.; Mak, T. C. W.; Cai, Z.; Ma, W. T.; Li, Y. X.; Wong, H. N. C. *J. Am. Chem. Soc.* **2005**, *127*, 9603.
- (147) Shi, L.; Wang, X.; Sandoval, C. A.; Li, M.; Qi, Q.; Li, Z.; Ding, K. *Angew. Chem., Int. Ed.* **2006**, *45*, 4108.
- (148) Bougauchi, M.; Watanabe, S.; Arai, T.; Sasai, H.; Shibasaki, M. *J. Am. Chem. Soc.* **1997**, *119*, 2329.
- (149) Watanabe, S.; Arai, T.; Sasai, H.; Bougauchi, M.; Shibasaki, M. *J. Org. Chem.* **1998**, *63*, 8090.
- (150) Wang, X.; Shi, L.; Li, M.; Ding, K. *Angew. Chem., Int. Ed.* **2005**, *44*, 6362.
- (151) Cho, S. H.; Ma, B.; Nguyen, S. T.; Hupp, J. T.; Albrecht-Schmitt, T. E. *Chem. Commun.* **2006**, 2563.
- (152) Cho, S. H.; Gadzikwa, T.; Afshari, M.; Nguyen, S. T.; Hupp, J. T. *Eur. J. Inorg. Chem.* **2007**, 4863.
- (153) Wang, X.; Wang, X.; Guo, H.; Wang, Z.; Ding, K. *Chem. Eur. J.* **2005**, *11*, 4078.
- (154) Dybtsev, D. N.; Nuzhdin, A. L.; Chun, H.; Bryliakov, K. P.; Talsi, E. P.; Fedin, V. P.; Kim, K. *Angew. Chem., Int. Ed.* **2006**, *45*, 916.

- (155) Nuzhdin, A. L.; Dybtsev, D. N.; Bryliakov, K. P.; Talsi, E. P.; Fedin, V. P. *J. Am. Chem. Soc.* **2007**, *129*, 12958.
- (156) Shibasaki, M.; Sasai, H.; Arai, T. *Angew. Chem., Int. Ed.* **1997**, *36*, 1237.
- (157) Takizawa, S.; Somei, H.; Jayaprakash, D.; Sasai, H. *Angew. Chem., Int. Ed.* **2003**, *42*, 5711.
- (158) Guo, H.; Wang, X.; Ding, K. *Tetrahedron Lett.* **2004**, *45*, 2009.
- (159) Wu, C. D.; Hu, A.; Zhang, L.; Lin, W. *J. Am. Chem. Soc.* **2005**, *127*, 8940.
- (160) Wu, C. D.; Lin, W. *Angew. Chem., Int. Ed.* **2007**, *46*, 1075.
- (161) Ngo, H. L.; Hu, A.; Lin, W. *J. Mol. Catal. A: Chem.* **2004**, *215*, 177.
- (162) Harada, T.; Nakatsugawa, M. *Synlett* **2006**, 321.
- (163) Cotton, F. A.; Murillo, C. A.; Střiriba, S. E.; Wang, X.; Yu, R. *Inorg. Chem.* **2005**, *44*, 8223.
- (164) Tanaka, K.; Oda, S.; Shiro, M. *Chem. Commun.* **2008**, 820.
- (165) Ingleson, M. J.; Barrio, J. P.; Bacsá, J.; Dickinson, C.; Park, H.; Rosseinsky, M. J. *Chem. Commun.* **2008**, 1287.
- (166) Evans, O. R.; Ngo, H. L.; Lin, W. *J. Am. Chem. Soc.* **2001**, *123*, 10395.
- (167) Kitagawa, S.; Noro, S.; Nakamura, T. *Chem. Commun.* **2006**, 701.
- (168) Dalko, P. I.; Moisan, L. *Angew. Chem., Int. Ed.* **2004**, *43*, 5138.
- (169) Manton, A.; Massuger, L.; Rabu, P.; Palivan, C.; McCusker, L. B.; Taubert, A. *J. Am. Chem. Soc.* **2008**, *130*, 2517.
- (170) Férey, G.; Mellot-Draznieks, C.; Serre, C.; Millange, F. *Acc. Chem. Res.* **2005**, *38*, 217.
- (171) Williams, K. A.; Boydston, A. J.; Bielawski, C. W. *Chem. Soc. Rev.* **2007**, *36*, 729.

CR800406U